



TUM School of Life Sciences

Chair of Forest Growth and Yield Science

**Modeling ecosystem services of urban trees to improve air quality  
and microclimate**

**Rocco Pace**

Vollständiger Abdruck der von der Fakultät TUM School of Life Sciences der Technischen Universität München zur Erlangung des akademischen Grades eines

Doktors der Naturwissenschaften (Dr. rer. nat.)

genehmigten Dissertation.

Vorsitzende/-r:

Prof. Dr. Michael Suda

Prüfende/-r der Dissertation:

1. Prof. Dr. Dr. h.c. Hans Pretzsch

2. Prof. Dr. Stephan Pauleit

Die Dissertation wurde am 19.06.2020 bei der Technischen Universität München eingereicht und durch die Fakultät TUM School of Life Sciences am 23.11.2020 angenommen.



*A mio nonno*

## Acknowledgments

First of all I would like to thank Dr. Rüdiger Grote for his valuable and constant support in these years: you are my master and your teachings will guide me in the future career.

Thanks to my supervisors and researchers from the Technical University of Munich, Prof. Pretzsch, Prof. Pauleit, Dr. Peter Biber, Dr. Thomas Rötzer, Dr. Mohammad Rahman, who accompanied me during this PhD providing important advices to improve the research.

Thanks to Prof. Stefan Emeis, Dr. Renate Forkel, and all colleagues from the Karlsruhe Institute of Technology IMK-IFU for welcoming me into their group and sharing these important years with me.

Thanks to the graduate schools GRACE, Micmor and Weihenstephan, especially to Dr. Schenk, Ms. Engelmann, Dr. Elija Bleher, Dr. Daniela Röder and Dr. Melanie Spornraft, for your kindness and availability.

Then I would like to thank Dr. David Nowak, Robbie Coville and the whole i-Tree team for your welcome and unforgettable days in the United States. Thanks to Dr. Carlo Calfapietra, Dr. Gregorio Sgrigna and Dr. Gabriele Guidolotti from CNR-IRET for your availability and precious advice: I'm happy to work with you in the coming year.

Thanks to Francesco De Fino for introducing me to the world of computer programming, Roland Stirnberg, Ivo Martone, Shade Amini and Levan Alpaidze for sharing parts of this path with me.

I would like also to thank Dr. Galina Churkina and Prof. Paolo De Angelis for opening me up with your passion to the world of scientific research. I met great people during these years at urban forest conferences, in my periods abroad, seminars, summer schools, and each of them has been fundamental for my personal and professional growth.

A heartfelt thanks to my father, my mother, my sister and all my family: you are the most important people in my life and every day I feel with me your love and encouragement in every choice I make.

Thanks to my dear friends Michele, Bruno, Aldo and Alessandro: the years go by but we are always together and though far away I feel your help and energy with me.

Last but not least thanks goes to you, my lovely Anna. These last years put us in front of unimaginable challenges that we were able to face only joined together in our true love. I thank you for all the great times we spent together, for your love and for supporting me in difficult moments. Because without you everything would be worthless. I will always be with you. Love you





# Contents

<b>Acknowledgments</b> .....	<b>4</b>
<b>Contents</b> .....	<b>6</b>
<b>List of Figures</b> .....	<b>8</b>
<b>List of Abbreviations</b> .....	<b>11</b>
<b>List of Species</b> .....	<b>12</b>
<b>Abstract</b> .....	<b>14</b>
<b>Zusammenfassung</b> .....	<b>15</b>
<b>I. Papers of the Cumulative Thesis</b> .....	<b>17</b>
Pace, R.; Biber, P.; Pretzsch, H.; Grote, R. (2018): Modeling Ecosystem Services for Park Trees: Sensitivity of i-Tree Eco Simulations to Light Exposure and Tree Species Classification. <i>Forests</i> 9 (2): 89-106, 10.3390/f9020089.....	17
Pace, R.; Grote, R. (2020): Deposition and resuspension mechanisms into and from tree canopies: A study modeling particle removal of conifers and broadleaves in different cities. <i>Frontiers in Forest and Global Change</i> 3 (26): 10.3389/ffgc.2020.00026. ....	18
Pace, R.; De Fino, F.; Rahman M. A.; Pauleit, S.; Nowak, D; Grote, R. (2020): A single tree model to consistently simulate cooling, shading, and pollution uptake of urban trees. <i>International Journal of Biometeorology</i> , submitted. ....	19
<b>II. Thesis: Modeling ecosystem services of urban trees to improve air quality and microclimate</b>	<b>21</b>
1) Introduction .....	21
2) Aims of the Study and Research Questions.....	27
3) Material and Methods.....	28
3.1. Study areas .....	28
3.2. Weather and pollution data.....	30
3.3. Model developments .....	34
3.3.1. Automated crown dimension and light exposure routine .....	34
3.3.2. A soil water balance module to affect stomatal conductance .....	39
3.3.3. Consideration of specific leaf properties to determine PM deposition.....	42
3.3.4. A new energy balance routine to calculate temperature changes .....	44
4) Results .....	46
4.1. Sensitivity of i-Tree Eco simulations to parameterization and competition determination	46
4.2. Particulate matter removal in dependence on plant-type specific deposition velocities ...	48
4.3. Gaseous pollutants uptake as a function of dynamic stomatal regulation .....	51
4.4. Temperature mitigation by cooling and shading .....	53
5) Discussion .....	55
5.1. i-Tree Eco model sensitivity to species composition and light exposure .....	55

5.2. Effect of tree species properties and weather conditions on PM removal.....	57
5.3. Physiological effects on temperature mitigation and pollution uptake .....	58
6) Conclusions and Prospects .....	60
<b>Literature .....</b>	<b>64</b>
<b>Contributions and other publications.....</b>	<b>75</b>
<b>Curriculum vitae .....</b>	<b>77</b>
<b>Eidesstattliche Erklärung .....</b>	<b>79</b>
<b>Appendix .....</b>	<b>80</b>
<b>Published Articles and Manuscripts.....</b>	<b>80</b>
<b>1. Paper I.....</b>	<b>80</b>
<b>2. Paper II.....</b>	<b>99</b>
<b>3. Paper III.....</b>	<b>112</b>

## List of Figures

<b>Figure 1.</b> Ecosystem services provided by urban trees. Source: (Pace 2019) .....	22
<b>Figure 2.</b> Dry deposition of gaseous and particles at canopy and leaf level. Source: (Lovett 1994)....	24
<b>Figure 3.</b> Input data and functions calculated by the i-Tree Eco model. Source: (i-Tree 2020).....	25
<b>Figure 4.</b> Cities analyzed with a focus on the study cases of Munich. ....	28
<b>Figure 5.</b> Bordeaux Platz (A) and Pariser Platz (B) in Munich. Source: (TUM 2016) – Google Maps	30
<b>Figure 6.</b> From top to bottom: temperature, PAR and precipitation of Munich in 2012. ....	31
<b>Figure 7.</b> Pollutants concentration of Munich in 2012. ....	31
<b>Figure 8.</b> Meteorological conditions at the two study sites. Source: (Pace et al.) .....	32
<b>Figure 9.</b> Crown light exposure (CLE) classification (A) and calculation of the competition index CCS (crown competition for sunlight) based on Pretzsch et al. (B). In the bottom right corner of (A), the conversion of CCS is indicated in CLE values. Source: (Pace et al. 2018).....	34
<b>Figure 10.</b> Relationship CCS-CLE and relative conversion classes determined from 100 sampled trees. ....	35
<b>Figure 11.</b> All trees in the south of Englischer Garten with relative crown light exposure (CLE) classes calculated by the CCS (crown competition for sunlight) competition index which is based on the algorithms provided in Pretzsch et al. (2002). In addition to competition between trees, shading by buildings has been considered as well. Source: (Pace et al. 2018).....	36
<b>Figure 12.</b> Deposition velocities (vd) of coniferous and broadleaved tree types in dependence on wind-speed (windSp). Red diamonds indicate the relationship as implemented in the original i-Tree model. Source: (Pace and Grote 2020).....	43
<b>Figure 13.</b> Leaf area (LA), leaf biomass, and carbon sequestration comparison between the “species- specific”, “genus-specific”, and “dominant species” simulations considering the crown light exposure (CLE) value for each tree (CLE individual) and the average CLE values (CLE average). Source: (Pace et al. 2018).....	46
<b>Figure 14.</b> Air pollution removal comparison between the “species-specific”, “genus-specific”, and “dominant species” simulations considering the crown light exposure (CLE) for each tree (CLE individual) and the average CLE values (CLE average). Source: (Pace et al. 2018) .....	47
<b>Figure 15.</b> Comparison of monoterpene and isoprene emissions between the “species-specific”, “genus-specific”, and “dominant species” simulations considering the crown light exposure (CLE) for each tree (CLE individual) and the average CLE values (CLE average). Source: (Pace et al. 2018) ...	48
<b>Figure 16.</b> Seasonal PM <sub>2.5</sub> deposition, removal, and resuspension for three cities, 2013–2015 [seasons: W, winter; SP, spring; S, summer; A, autumn]. Source: (Pace and Grote 2020).....	49
<b>Figure 17.</b> Sensitivity of deposition (blue lines), net removal (orange), and resuspension (green) to parameter changes of leaf area index (LAI, left), specific deposition velocity (vds, middle), and resuspension percentages (rr, right). All simulations were run with half, normal and double values	

relative to standard parameters and carried out for selected periods for Rome in 2014-2015. Source: (Pace and Grote 2020).....	50
<b>Figure 18.</b> Model resistances at the two sites. The quasi-laminar boundary layer is referred to as $O_3$ . Source: (Pace et al. submitted).....	51
<b>Figure 19.</b> Upper panels: Relative water content in each soil layer and measured soil moisture potential. Lower panels: Average daily temperature and rain events in the study period. Source: (Pace et al. submitted).....	52
<b>Figure 20.</b> Stomatal conductance ( $g_s$ ) at two sites. Source: (Pace et al. submitted).....	52
<b>Figure 21.</b> Dry deposition velocity ( $v_d$ ) of $O_3$ at the two sites. Missing values correspond to hours with precipitation. Source: (Pace et al. submitted).....	53
<b>Figure 22.</b> Comparison of modeled transpiration and values measured using the sap flow for the two sites. Source: (Pace et al. submitted).....	54
<b>Figure 23.</b> Energy reduction by concrete shading and cooling by transpiration at the two sites at midday. Source: (Pace et al. submitted).....	55

## List of Tables

<b>Table 1.</b> Species composition of the south part of Englischer Garten. Source: (Pace et al. 2018). .....	29
<b>Table 2.</b> Average morphological characteristics of trees at the two study sites. Source: (Pace et al.) .	30
<b>Table 3.</b> From top to bottom: precipitation, wind speed and PM <sub>2.5</sub> data in Berlin, Munich and Rome from 2013 to 2015. Source: (Pace and Grote 2020) .....	33
<b>Table 4.</b> Annual PM <sub>2.5</sub> removal by different tree types in three cities. Source: (Pace and Grote 2020). .....	48

## List of Abbreviations

BPM	Biological particulate matter
BVOC	Biogenic Volatile Organic Compound
CCS	Crown competition for sunlight
CLE	Crown light exposure
DBH	Diameter at breast height
EEA	European Environment Agency
EGCA	European Green Capital Award
ES	Ecosystem services
GIS	Geographic information system
LA	Leaf area
LAI	Leaf area index
NOAA	National Oceanic and Atmospheric Administration
PAR	Photosynthetically active radiation
PM	particulate matter
PM <sub>10</sub>	< 10 µm-diameter particulate-matter
PM <sub>2.5</sub>	< 2.5 µm-diameter particulate-matter
UHI	Urban heat island
VOC	Volatile Organic Compound

## List of Species

<i>Acer</i> spp.	Maples
<i>Acer campestre</i> L.	Field maple
<i>Acer platanoides</i> L.	Norway maple
<i>Acer pseudoplatanus</i> L.	Sycamore maple
<i>Aesculus hippocastanum</i> L.	Horse-chestnut
<i>Ailanthus altissima</i> (Mill.) Swingle	Tree of heaven
<i>Alnus incana</i> (L.) Moench	Grey alder
<i>Betula</i> spp.	Birches
<i>Carpinus betulus</i> L.	European hornbeam
<i>Cornus mas</i> L.	Cornelian cherry
<i>Corylus</i> spp.	Hazels
<i>Crataegus</i> spp.	Hawthorns
<i>Fagus</i> spp.	Beeches
<i>Fagus sylvatica</i> L.	European beech
<i>Fraxinus excelsior</i> L.	European ash
<i>Ginkgo biloba</i> L.	Ginkgo
<i>Gleditsia triacanthos</i> L.	Honey locust
<i>Juglans</i> spp.	Walnuts
<i>Liriodendron tulipifera</i> L.	Tulip tree
<i>Magnolia</i> spp.	Magnolia
<i>Picea abies</i> (L.) H. Karst.	Norway spruce
<i>Pinus</i> spp.	Pines
<i>Pinus pinea</i> L.	Stone pine
<i>Platanus × acerifolia</i> Aiton	London plane
<i>Populus</i> spp.	Poplars
<i>Prunus</i> spp.	Cherries
<i>Pterocarya fraxinifolia</i> (Lam.) Spach	Caucasian wingnut
<i>Pyrus communis</i> L.	Common pear
<i>Quercus</i> spp.	Oaks
<i>Quercus ilex</i> L.	Holly-holm oak
<i>Quercus robur</i> L.	English oak



<i>Robinia pseudoacacia</i> L.	Black locust
<i>Salix</i> spp.	Willows
<i>Salix alba</i> L.	White willow
<i>Sophora japonica</i> (L.) Schott	Japanese pagoda tree
<i>Sorbus</i> spp.	Whitebeams
<i>Taxus baccata</i> L.	Yew
<i>Tilia</i> spp.	Linden/lime trees
<i>Tilia cordata</i> Mill.	Small-leaved linden/lime
<i>Tilia x europaea</i> L.	Common lime
<i>Ulmus glabra</i> Huds.	Scotch elm

## Abstract

Cities host more than half of the world's population and are responsible for 70% of total energy and greenhouse gas emissions. Cities and their inhabitants are thus drivers of global environmental change and, simultaneously, they are strongly affected by it. The high concentration of air pollutants or the large percentage of soil sealing are worsening the environmental quality of cities causing serious health issues. Increasing green spaces within the urban fabric can improve the air quality and the microclimate providing important environmental benefits and contributing to the development of "green cities". The use of decision-making tools for urban greening such as models allows to maximize ecosystem services by selecting the suitable species and the most efficient tree density, based on current and future climate and emission scenarios. However, the reliability of such assessments is based on model accuracy which is seldom tested and validated.

The most commonly used tool to evaluate ecosystem services provided by urban trees and forests is the i-Tree Eco model. It calculates carbon sequestration, pollutant removal, and the emission of biogenic volatile compounds (BVOCs) that affect various air quality issues. In this thesis, the i-Tree Eco model has been evaluated and its sensitivity to the definition of crown light exposure has been investigated, also suggesting a new automated method to determine light competition of trees. Furthermore, the impact of uncertain tree species classification has been tested by comparing simulations that were based on different parameterizations, considering a decreasing level of detail (species-specific, genus-specific, dominant species). For the case study park "Englischer Garten" in Munich, it showed that in particular regarding BVOC emissions, a species-specific parameterization is indispensable. In a second step, the pollution removal functionality itself was addressed, discussing improvements for PM<sub>2.5</sub> deposition, resuspension, and removal. The study investigated the impacts of urban trees along a latitudinal gradient (Berlin, Munich, Rome) distinguishing deposition velocities between tree types (i.e. conifers and broadleaves). The different climatic conditions allowed to investigate the net removal capacity in dependence on the particular weather (wind speed, precipitation regimes), highlighting the importance of long-lasting dry spells. Finally, a new single-tree model has been developed and evaluated which uses the improved i-Tree Eco functionality and complements it with soil water balance and energy calculations. With this new development, it is possible to consistently quantify two major urban ecosystem services (temperature mitigation and gaseous pollutants uptake) in dependence on meteorology, site conditions, and tree properties. In combination, the thesis supplies considerable improvements for ecosystem service determination of urban trees and thus helps in the selection of resilient and suitable species to increase the environmental sustainability of cities.

## Zusammenfassung

Städte beherbergen mehr als die Hälfte der Weltbevölkerung und sind für 70% der gesamten Energie- und Treibhausgasemissionen verantwortlich. Städte und ihre Bewohner sind die treibenden Kräfte der globalen Umweltveränderungen und gleichzeitig sind sie stark von diesen Veränderungen betroffen. Die hohe Konzentration von Luftschadstoffen und der hohe Prozentsatz der Bodenversiegelung verschlechtern die Umweltqualität der Städte und verursachen ernsthafte Gesundheitsprobleme. Eine Vergrößerung der Grünflächen innerhalb des städtischen Gefüges kann die Luftqualität und das Mikroklima verbessern, was wichtige Umweltvorteile bietet und zur Entwicklung "grüner Städte" beiträgt. Der Einsatz von Entscheidungshilfen für die städtische Begrünung, wie z.B. Modellen, kann helfen, die Ökosystemleistungen durch die Auswahl von geeigneten Arten auf der Grundlage aktueller und zukünftiger Szenarien zu maximieren. Die Zuverlässigkeit solcher Bewertungen beruht jedoch auf der Modellgenauigkeit, die nur selten getestet und validiert wird.

Das am häufigsten verwendete Werkzeug zur Bewertung von Ökosystemdienstleistungen, die von städtischen Bäumen und Wäldern erbracht werden, ist das Modell i-Tree Eco. Es berechnet Kohlenstoffbindung, Luft-Schadstoffentfernung, und die Emission von biogenen flüchtigen Komponenten (BVOCs) die wiederum die Luftqualität beeinträchtigen können. In dieser Arbeit wurde zunächst die Sensitivität des i-Tree Eco Modells auf die Bestimmung der Konkurrenzsituation von Bäumen untersucht, wobei eine neue automatisierte Methode zur Ableitung der Lichtexposition vorgeschlagen wurde. Darüber hinaus wurde der Einfluss der Methode zur Baumartenklassifikation untersucht, indem die Parametrisierung mit abnehmendem Detaillierungsgrad (artenspezifisch, gattungsspezifisch, dominante Arten) durchgeführt wurde. Für das Beispiel des Englischen Gartens in München zeigte sich dabei, dass eine artspezifische Parametrisierung insbesondere für die Abbildung der BVOC Emission unverzichtbar ist. In einem zweiten Schritt wurde die Funktionalität der Modellprozesse selbst bearbeitet und Verbesserungen im Bereich Deposition und Resuspension von Partikeln (PM<sub>2.5</sub>) vorgeschlagen. Die Untersuchung umfasste Stadtbäume entlang eines Breitengradienten (Berlin, München, Rom), wobei die Depositionsgeschwindigkeiten zwischen Baumtypen (d.h. Nadel- und Laubbäume) unterschieden wurden. Die verschiedenen klimatischen Bedingungen in den Städten erlaubten es, die Auswirkungen des Wetters (Windgeschwindigkeit, Niederschlagsregime) auf die Feinstaubabscheidung zu untersuchen, wobei sich insbesondere längere Trockenphasen als besonders bedeutend für die Resuspension von Schadstoffen herausstellten. Schließlich wurde ein neues Einzelbaummodell entwickelt und evaluiert, das auf den verbesserten Prozessen des i-Tree Eco Modells beruht, diese aber mit Modulen zum Bodenwasserhaushalt zur Energiebilanz-Berechnung ergänzt. Mit dieser Neuentwicklung ist es möglich, zwei der wichtigsten Ökosystemleistungen von Stadtbäumen (Temperaturminderung und Aufnahme von gasförmigen Schadstoffen) in Abhängigkeit von Witterung, Standortbedingungen und Baumeigenschaften konsistent

zu quantifizieren. Damit liefert die Arbeit einen signifikanten Fortschritt bei der modell-gestützten Bewertung von Ökosystemleistungen und hilft so bei der Auswahl widerstandsfähiger und geeigneter Baumarten, um die ökologische Nachhaltigkeit von Städten zu erhöhen.

## I. Papers of the Cumulative Thesis

This dissertation is based on investigations that were published and submitted in the following four original articles:

**Pace, R.; Biber, P.; Pretzsch, H.; Grote, R. (2018): Modeling Ecosystem Services for Park Trees: Sensitivity of i-Tree Eco Simulations to Light Exposure and Tree Species Classification. *Forests* 9 (2): 89-106, 10.3390/f9020089.**

Summary:

Ecosystem modeling can help decision making regarding planting of urban trees for climate change mitigation and air pollution reduction. Algorithms and models that link the properties of plant functional types, species groups, or single species to their impact on specific ecosystem services have been developed. However, these models require a considerable effort for initialization that is inherently related to uncertainties originating from the high diversity of plant species in urban areas. We therefore suggest a new automated method to be used with the i-Tree Eco model to derive light competition for individual trees and investigate the importance of this property. Since competition depends also on the species, which is difficult to determine from increasingly used remote sensing methodologies, we also investigate the impact of uncertain tree species classification on the ecosystem services by comparing a species-specific inventory determined by field observation with a genus-specific categorization and a model initialization for the dominant deciduous and evergreen species only. Our results show how the simulation of competition affects the determination of carbon sequestration, leaf area, and related ecosystem services and that the proposed method provides a tool for improving estimations. Misclassifications of tree species can lead to large deviations in estimates of ecosystem impacts, particularly concerning biogenic volatile compound emissions. In our test case, monoterpene emissions almost doubled and isoprene emissions decreased to less than 10% when species were estimated to belong only to either two groups instead of being determined by species or genus. It is discussed that this uncertainty of emission estimates propagates further uncertainty in the estimation of potential ozone formation. Overall, we show the importance of using an individual light competition approach and explicitly parameterizing all ecosystem functions at the species-specific level.

**Pace, R.; Grote, R. (2020): Deposition and resuspension mechanisms into and from tree canopies: A study modeling particle removal of conifers and broadleaves in different cities. *Frontiers in Forest and Global Change* 3 (26): 10.3389/ffgc.2020.00026.**

Summary:

With increasing realization that particles in the air are a major health risk in urban areas, strengthening particle deposition is discussed as a means to air-pollution mitigation. Particles are deposited physically on leaves and thus the process depends on leaf area and surface properties, which change throughout the year. Current state-of-the-art modeling accounts for these changes only by altering leaf longevity, which may be selected by vegetation type and geographic location. Particle removal also depends on weather conditions, which determine deposition and resuspension but generally do not consider properties that are specific to species or plant type. In this study, we modeled  $< 2.5 \mu\text{m}$ -diameter particulate-matter ( $\text{PM}_{2.5}$ ) deposition, resuspension, and removal from urban trees along a latitudinal gradient (Berlin, Munich, Rome) while comparing coniferous with broadleaf (deciduous and evergreen) tree types. Accordingly, we re-implemented the removal functionality from the i-Tree Eco model, investigated the uncertainty connected with parameterizations, and evaluated the efficiency of pollution mitigation depending on city conditions. We found that distinguishing deposition velocities between conifers and broadleaves is important for model results, i.e., because the removal efficiency of conifers is larger. Because of the higher wind speed, modeled  $\text{PM}_{2.5}$  deposition from conifers is especially large in Berlin compared to Munich and Rome. Extended periods without significant precipitation decrease the amount of  $\text{PM}_{2.5}$  removal because particles that are not occasionally washed from the leaves or needles are increasingly resuspended into the air. The model predicted this effect particularly during the long summer periods in Rome with only very little precipitation and may be responsible for less-efficient net removal from urban trees under climate change. Our analysis shows that the range of uncertainty in particle removal is large and that parameters have to be adjusted at least for major tree types if not only the species level. Furthermore, evergreen trees (broadleaved as well as coniferous) are predicted to be more effective at particle removal in northern regions than in Mediterranean cities, which is unexpected given the higher number of evergreens in southern cities. We discuss to what degree the effect of current  $\text{PM}_{2.5}$  abundance can be mitigated by species selection and which model improvements are needed.

**Pace, R; De Fino, F.; Rahman M. A.; Pauleit, S; Nowak, D; Grote, R. (2020): A single tree model to consistently simulate cooling, shading, and pollution uptake of urban trees. International Journal of Biometeorology, submitted.**

Summary:

Extremely high temperatures, which negatively affect the human health and plant performances, are becoming more frequent in cities. Urban green infrastructure, particularly trees, can mitigate this issue through cooling due to transpiration, and shading. Temperature regulation by trees depends on feedbacks among the climate, water supply, and plant physiology. However, most current models still lack basic processes, such as the consideration of soil water limitation, or have not been evaluated sufficiently. In this study, we present a new model that couples the soil water balance with energy calculations to assess the physiological responses and microclimate effects of a common urban street-tree species (*Tilia cordata* Mill.) on temperature regulation. We contrast two urban sites in Munich, Germany with different degree of surface sealing at which micro-climate and transpiration had been measured. Simulations indicate that differences in wind speed and soil water supply can be made responsible for the differences in transpiration. Nevertheless, the calculation of the overall energy balance showed that the shading effect, which depends on the leaf area index and canopy cover, contribute the most to the temperature reduction at midday. Finally, we demonstrate that the consideration of soil water availability for stomatal conductance improves the calculation of gaseous pollutant uptake (e.g., ozone). In conclusion, the presented model has demonstrated its ability to quantify two major ecosystem services (temperature mitigation and air pollution removal) consistently in dependence on meteorological and site conditions.

**The above listed articles are attached in the appendix. Hereinafter, reference to the original articles is made by citation.**

**Authors contributions:**

For the above listed publications R. Pace designed and carried out the research, implemented the model code and wrote major parts of the text. For the publication I-II-III, R. Grote contributed significantly to the design, discussion and writing of the text and supervised the research. For the publication I, P. Biber and H. Pretzsch provided the competition algorithm, supported the implementation, and revised the text. For publication III, F. De Fino contributed to the implementation of the model, M. Rahman and S. Pauleit provided measurement data and revised the text, D. Nowak assisted simulations and revised the text.



## II. Thesis: Modeling ecosystem services of urban trees to improve air quality and microclimate

### 1) Introduction

Cities play a crucial role in the mitigation of the climate change as more than half of the world's population currently lives in cities and the share of urban population is expected to reach 75% by 2050 (United Nations 2014). They represent 80% of global economic outputs and are responsible for 70% of total energy and greenhouses gas emissions (UN-Habitat 2016). Cities and their inhabitants are the drivers of global environmental change and at the same time they are affected by it (Pace and Churkina submitted).

Indeed, the effects of climate change are particularly evident in cities where the high percentage of sealed surfaces contributes to the so-called heat island effect (Oke 2002; Wilby 2003). The increasing occurrence of heatwaves due to global warming (Perkins et al. 2012; Baldwin et al. 2019) presents a serious threat to human health (Watts et al. 2019). For example, the 2003 heatwave in Europe caused more than 70,000 deaths (Robine et al. 2008) and the heatwave-related premature mortality is expected to increase at the global scale (Guo et al. 2018).

Another relevant issue in urban areas is the high concentration of pollutants in the air (World Health Organization 2013). The major source of air pollution in cities is the combustion of fuels originated from fossil sources and biomass for domestic heating, power generation, and transportation (European Environment Agency 2018). Air pollutants are called “primary” if directly emitted to the atmosphere and “secondary” if formed in the atmosphere from precursor pollutants through chemical reactions and microphysical processes. Carbon monoxide (CO) and sulphur oxides (SO<sub>x</sub>) are examples of primary pollutants, while ozone (O<sub>3</sub>) is a secondary pollutant. Particulate matter (PM), nitrogen oxides (NO<sub>x</sub>), and several oxidized volatile organic compounds (VOCs) can be either emitted directly or formed in the atmosphere (European Environment Agency 2019). Because air pollution exposure may cause serious health effects – such as respiratory and cardiovascular diseases, leading to premature mortality and morbidity (World Health Organization 2016) – the European Union set concentration limits for different air pollutants.

The average annual concentration of particulate matter with a diameter of 10 (PM<sub>10</sub>) and nitrogen dioxide (NO<sub>2</sub>) should not exceed 40 µg m<sup>-3</sup> yr<sup>-1</sup>, while for particulate matter with a diameter of 2.5 (PM<sub>2.5</sub>) is 25 µg m<sup>-3</sup> yr<sup>-1</sup>. The limit value for CO and O<sub>3</sub> is 120 µg/m<sup>3</sup>, considering the maximum daily 8-hour mean, instead the concentration of sulphur dioxide (SO<sub>2</sub>) should be lower than 350 and 125 µg/m<sup>3</sup> for 1 or 24 hours, respectively (European Commission 2008). However, these values are often exceeded in many European cities, demanding considerable measures to improve air quality (European Environment Agency 2018).

The “Green City” concept was introduced as a model for the development of environmentally friendly cities which has its origin from the awareness in the late 1990s of reconciling economic development with the environmental conservation and social well-being, strengthened by the theory of sustainability and the emergence of a “sustainable city” vision (Brilhante and Klaas 2018). This concept suggests a responsible political and societal action of cities in order to achieve a high environmental quality, which contributes to enhanced human well-being (Pace et al. 2016). One of the environmental indicators to assess the degree of “greenness” of cities is the presence of green areas and their accessibility (Pace and Churkina submitted).

Among European cities with a population over 2 million, Berlin shows the highest percentage of green areas and forests (26.8%). Considering smaller cities, however, another virtuous example is Stockholm (1,6 million inhabitants) with more than half of the area (56%) covered by green areas and forests (Poelman 2018). On the other hand, the amount of total green areas does not reflect the accessibility for citizens because these areas can be located outside the urban fabric. Considering the median surface of accessible green urban areas (ha), among the cities with a population above 2 million, Madrid shows the highest value (30.2 ha) while Helsinki (1 million inhabitants) has the highest accessibility to green areas (78.8 ha) of all investigated European cities in a recent study (Poelman 2018).

Green areas and in particular trees provide many ecosystem services (ES) such as water purification, air quality improvement, space for recreation, and heat mitigation (Fig. 1). Recently, the European Commission has suggested the nature-based solutions concept, which includes preserving, managing, and restoring natural or modified ecosystems in order to respond to societal challenges and contribute to the human well-being and biodiversity (European Commission 2015). A recommendation for the practical implementation of nature based solutions is to design green infrastructures (Hansen et al. 2019), which are strategically planned networks of natural and semi-natural areas that are very efficient in providing ecosystem services for animals and people (Calfapietra and Cherubini 2019).

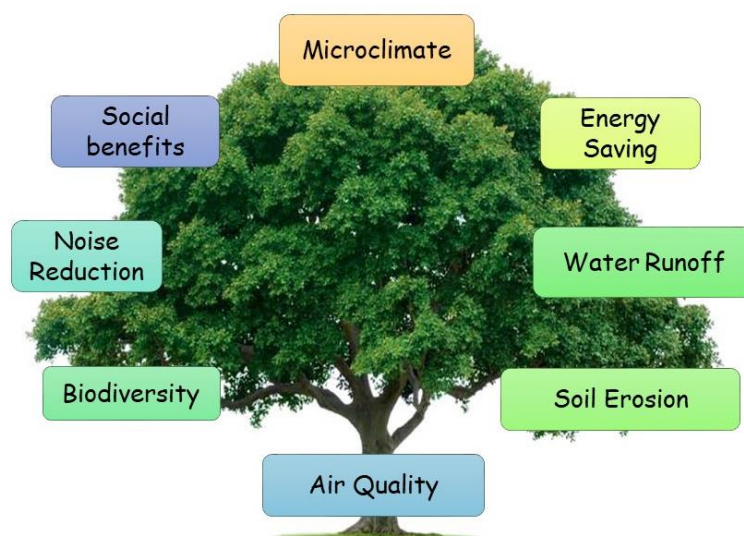


**Figure 1.** Ecosystem services provided by urban trees. Source: (Pace 2019)

Among all ecosystem services, air pollution removal and heat mitigation are two of the most investigated (Brink et al. 2016) and also of particular importance for people's health (Livesley et al. 2016). In fact, planting trees has a greater impact on temperature reduction than other types of green infrastructure (Zölch et al. 2016) and the pollution removal reduces the incidence of human mortality and acute respiratory symptoms (Nowak et al. 2014). Therefore, the nature and dependencies of these two functions will be further explained.

Trees reduce the air temperature in two ways: by preventing solar radiation from heating up surfaces below the canopy (shading) and by transpiring water through the stomata of leaves (cooling), which has previously been absorbed by roots in the soil (Rahman et al. 2020b). Both mechanisms are strongly related to climatic and soil conditions and depend on tree dimensions as well as on physiological processes (Rahman et al. 2018). LAI and crown width are the main tree traits affecting the tree shading, which is capable of reducing up to 20 °C the surface temperature at midday on sunny days (Speak et al. 2020). Transpiration demand is triggered by low relative humidity (or high vapor pressure deficit), which is often closely related to temperature, but it is nevertheless limited by soil water availability. The reason is that insufficient water supply causes stomata closure decreasing the water uptake and thus the cooling effect of evaporation (Rötzer et al. 2019). Other meteorological factors that are positively related to transpiration are solar radiation, because stomata tend to open if the radiation is high, and wind speed, which reduces the boundary layer thickness and thus the resistance to water transport from the canopy (Kramer 1983).

Air pollution can be removed by trees by two ways depending on the kind of pollution. Gaseous pollutants, such as ozone (O<sub>3</sub>), sulfur dioxide (SO<sub>2</sub>) or nitrogen dioxide (NO<sub>2</sub>), are taken up into the plant through the stomata (Hosker and Lindberg 1982). These molecules can be almost immediately metabolized as long as photosynthesis and membrane permeability are not severely damaged. In fact, leaves can activate defense mechanisms as the detoxification potential in the apoplast for O<sub>3</sub> and nitrogen oxides (NO<sub>x</sub>) or the transport resistances within cells and the ability to tolerate pH changes for SO<sub>2</sub> (Tiwari et al. 2016).

On the other hand, particulate matter is removed by physical deposition on plant surfaces such as leaf, bark, and branches and is later on washed off by rainfall or deposited on the ground with senescent tissue (Beckett et al. 1998; Janhäll 2015; Cai et al. 2017) (Fig. 2).

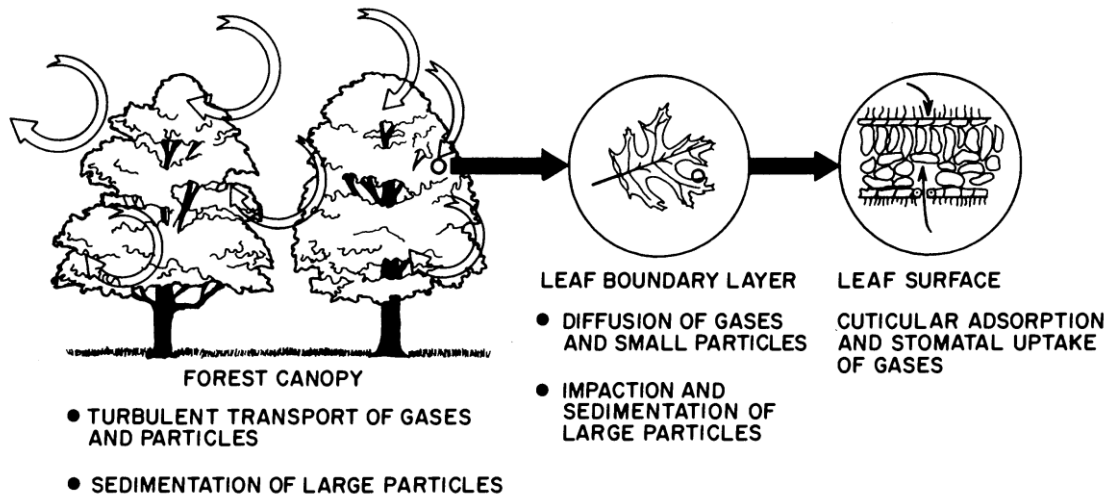


**Figure 2.** Dry deposition of gaseous and particles at canopy and leaf level. Source: (Lovett 1994)

The capacity to remove fine PM depends primarily on the leaf area since this is the usually the largest and most exposed surface of a tree. Thus, phenological transition phases (Wang et al. 2015) as well as leaf surface properties that are species-specific (Sæbø et al. 2012; Zhang et al. 2017; Shao et al. 2019) need to be considered. The actual deposition rate is then modified by weather conditions, such as wind speed or precipitation regime (Schaubroeck et al. 2014) as well as pollution concentration (Lu et al. 2018). Needles of conifers are considered more efficient than broadleaves in removing fine PM because of their shape, abundance of waxes on their surfaces, and their surface structure (Chen et al. 2017; Zhang et al. 2017; Muhammad et al. 2019). Species-specific foliage properties also determine how strongly deposited particles are stuck to the leaf and how easily they are resuspended into the air (Blanusa et al. 2015; Chen et al. 2017; Zhang et al. 2017).

However, trees can also worsen the air quality through the emission of pollen and BVOCs. Pollen, or more generally “airborne biological particulate matter” (BPM) is emitted by flowering plants and besides species-specific traits, the emission intensity is also related to temperature and wind (Grote et al. 2016). One of the important species-specific features is the allergenicity of pollen (Cariñanos et al. 2016), which can be modified by air pollutants increasing the amount of allergenic proteins or altering the lipid composition (Beck et al. 2013). The BVOC release is another highly species-specific trait which is controlled by environmental conditions such as sunlight, temperature, and water availability (Grote 2019). For example, poplar trees are high isoprene emitters and conifers generally emit monoterpenes but there are also genera such as *Quercus* which include species that are either isoprene, monoterpene or non-emitters (Loreto 2002). BVOCs reacting with anthropogenic emissions, especially nitrogen oxides (NO<sub>x</sub>), can contribute substantially to O<sub>3</sub> formation in the atmosphere (Calfapietra et al. 2013).

Since there are so many species-specific traits that influence ecosystem services, species selection is important to achieve optimal results of city greening (Churkina et al. 2015) and models that can be particularly useful as decision-support tools for city planning, need to consider the species level (Maes et al. 2012; Endreny et al. 2017). Urban forest-specific models represent a group of models, most prominent in urban ecosystem research, which focus on the physical and physiological properties and processes of trees. The most commonly used model types are the i-Tree toolset, ENVI-met and computational fluid dynamic models (Lin et al. 2019).

The i-Tree Eco model can be used to estimate a broad range of ecosystem functions such as the air pollution removal, carbon sequestration, as well as building energy conservation (Nowak et al. 2008a). The model needs a considerable effort for initialization: in addition to the species and the stem diameter at breast height (DBH) further input data are required, including land use criteria, total tree height, crown size (height to live top, height to the crown base, crown width, and percentage of crown missing), crown health (dieback or condition), and competition status. Also, meteorological data and pollution concentrations are used to calculate tree ecosystem services (Fig. 3).

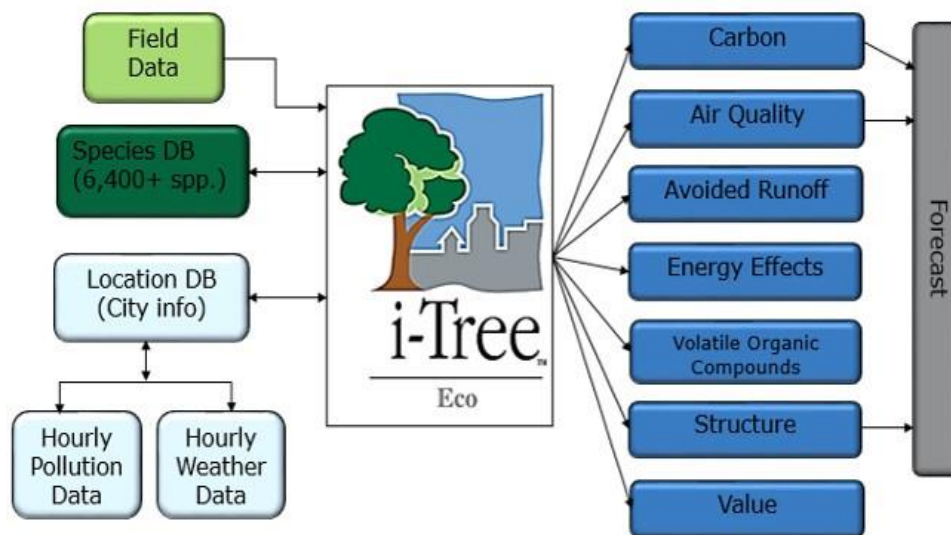


**Figure 3.** Input data and functions calculated by the i-Tree Eco model. Source: (i-Tree 2020)

The i-Tree Eco is applied extensively worldwide and particularly in Europe but only few studies tested and evaluated the underlying model functions (Hirabayashi et al. 2011; Morani et al. 2014; Russo et al. 2014). Since the model relies on a limited number of processes and is often parameterized on the genus level or coarser, results may be subjected to large uncertainties. The heterogeneity of urban areas characterized by a high number of tree species and different environmental conditions may be not appropriate to determine carbon sequestration, pollution removal, or the amount of BVOCs emitted by trees.

Also, the current version of the model does not allow to evaluate the temperature mitigation of urban trees and neglects drought stress on plant physiology by assuming always sufficient water availability. This is a crucial factor for the evaluation of the transpiration and deposition of the gaseous pollutants during the summer drought period which is particularly pronounced in the Mediterranean climate but also evident in Northern European cities (e.g. Brune 2016).

In order to approach these issues, this thesis investigated the current i-Tree Eco model approach and developed a more comprehensive framework that addresses some of the previously outlined major deficits. The new development is still based on core functions of the i-Tree Eco model and don't provide its extensive tool boxes and user guides. Also, climatic information is not provided automatically from the developer's databases but are needed to be explicitly given for a particular site – which, however, increases the flexibility.

First, I evaluated the sensitivity of the i-Tree Eco model processes to the crown light exposure (CLE), which is a means for characterizing the competition state of trees. A new automated method has been introduced to derive this variable. In addition, the impact that the kind of tree parameterization (either on the plant-type, genus or species level) has on the ecosystem services calculation has been evaluated, using the Englischer Garten park in Munich as an example.

Then, I developed and applied new model functions regarding deposition and resuspension to assess particulate matter removal of conifers and broadleaves under a range of climatic conditions (using the 3 European cities Berlin, Munich and Rome as case studies). Further model improvements consider dynamic stomatal conductance for estimating gaseous pollutant uptake and transpiration, as well as temperature mitigating effects (cooling and shading based on the calculation of the full energy balance). The development included the consideration of soil water availability using a newly implemented water balance model. The model has been evaluated with field measurements.

The range of locations that has been used in this thesis include a wide range of climate and pollution levels, which give reason to hope that the new model development could be applied generally to investigate pollution removal, cooling and shading of urban trees. The new single-tree model (Tree4City) can thus be seen as a research-support tool to study plant-atmosphere interactions and possibly employed to maximize ecosystem service benefits based on current and future climate and environmental scenarios.

## 2) Aims of the Study and Research Questions

The aim of the thesis was to analyze and develop a modeling approach for the evaluation of tree ecosystem services to improve air quality and microclimate in urban areas.

The first objective was to evaluate the impact of species classification and light exposure of urban trees on the assessment of carbon sequestration, pollution removal and biogenic emissions. To this purpose, the i-Tree Eco, a state of the art model for urban forestry analysis and benefits assessment, was initialized for the Englischer Garten park in Munich.

The second objective was to analyze which weather conditions promote the net removal of particulate matter and how its deposition differs between conifer and broadleaf trees. Therefore, the pollution removal functionality for PM<sub>2.5</sub> was tested in three European cities along a latitudinal gradient (Berlin, Munich, Rome) distinguishing deposition velocities between tree types (i.e. conifers and broadleaves).

Finally, the last objective was to introduce and validate with physiological measurements a new single-tree model able to quantify temperature mitigation and gaseous air pollution uptake consistently in dependence on meteorological and site conditions.

The following research questions were posed and investigated in detail:

- What is the current state of the art of modeling ecosystem services of urban trees?
- How does a more detailed tree inventory and a different crown light exposure affect the carbon sequestration, pollution removal and biogenic emissions?
- Which weather conditions promote particle removal? How does the deposition of particulate matter from conifers and broadleaf trees vary?
- How can a more comprehensive and physiological model be developed to assess temperature mitigation and gaseous pollution uptake based on weather (e.g. wind speed, drought) and site conditions (e.g. porous or paved surface)?

### 3) Material and Methods

#### 3.1. Study areas

In this thesis 3 European cities were investigated: Berlin, Munich and Rome (Fig. 4). These places are located on a latitudinal gradient and show different climate and environmental conditions (see paragraph below, Tab. 3). Also tree species diversity vary among these cities with evergreen trees more abundant in Rome, such as *Pinus pinea* L. and *Quercus ilex* L. (Caneva et al. 2020), compared to northern cities where deciduous trees as *Tilia* spp., *Acer* spp., and *Fagus* spp. are much more prominent (Tigges et al. 2017; Tab. 1).

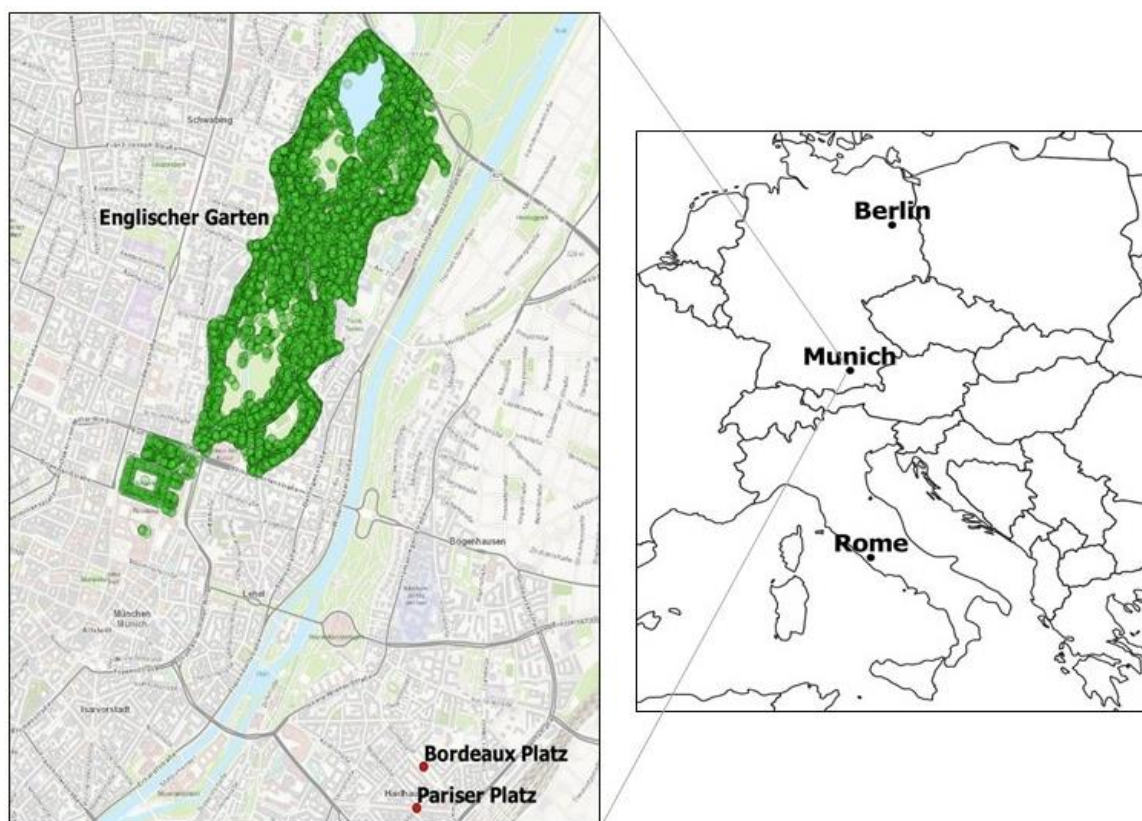


*Figure 4. Cities analyzed with a focus on the study cases of Munich.*

#### - Englischer Garten, Munich

For the first task, we analyzed the south of “Englischer Garten” in the simulation performed by the i-Tree Eco model, a 330-ha park located in Munich, Germany (Figure 4). The site is mainly comprised of a mix of deciduous trees dominated ( $\approx 77\%$ ) by the species Norway maple (*Acer platanoides* L.), European beech (*Fagus sylvatica* L.), small-leaved lime (*Tilia cordata* MILL.), sycamore maple (*Acer pseudoplatanus* L.), and European ash (*Fraxinus excelsior* L.). The park structure with large open spaces and areas with denser tree cover provides various degrees of light competition which have been considered in the model simulation.



Evergreen species contribute less than 1% to the total tree number (Tab. 1). The inventory comprises 9391 trees growing within the “Englischer Garten”, which have been measured by the Bavarian Administration of State-Owned Palaces, Gardens and Lakes. The respective tree data (species, tree height, DBH, crown diameter, and height to the crown base) were used as input parameters in the model to calculate the ecosystem services provided by the park.

**Table 1.** Species composition of the south part of Englischer Garten. Source: (Pace et al. 2018).

Species	Relative Number (%)	Basal Area (m <sup>2</sup> )
Norway maple ( <i>Acer platanoides</i> L.)	32.9	453.6
European beech ( <i>Fagus sylvatica</i> L.)	12.6	447.4
Small-leaved lime ( <i>Tilia cordata</i> Mill.)	11.2	160.1
Sycamore maple ( <i>Acer pseudoplatanus</i> L.)	10.4	122.8
European ash ( <i>Fraxinus excelsior</i> L.)	10.1	223.2
Field maple ( <i>Acer campestre</i> L.)	3.7	35.8
European hornbeam ( <i>Carpinus betulus</i> L.)	3.6	43.6
Horse-chestnut ( <i>Aesculus hippocastanum</i> L.)	2.6	70.1
English oak ( <i>Quercus robur</i> L.)	2	32.4
Scotch elm ( <i>Ulmus glabra</i> Huds.)	1.8	28.8
Black locust ( <i>Robinia pseudoacacia</i> L.)	1.6	21.7
London plane ( <i>Platanus × acerifolia</i> Aiton)	1.3	19.4
White willow ( <i>Salix alba</i> L.)	1.0	43.3
Willows ( <i>Salix</i> spp.), poplars ( <i>Populus</i> spp.), cherries ( <i>Prunus</i> spp.), Caucasian wingnut ( <i>Pterocarya fraxinifolia</i> ), birches ( <i>Betula</i> spp.), hazels ( <i>Corylus</i> spp.), walnuts ( <i>Juglans</i> spp.), common pear ( <i>Pyrus communis</i> ), honey locust <i>Gleditsia triacanthos</i> , tulip tree ( <i>Liriodendron tulipifera</i> ), hawthorns ( <i>Crataegus</i> spp.), ginkgo ( <i>Ginkgo biloba</i> ), whitebeams ( <i>Sorbus</i> spp.), grey alder ( <i>Alnus incana</i> ), tree of heaven ( <i>Ailanthus altissima</i> ), cornelian cherry ( <i>Cornus mas</i> ), Japanese pagoda tree ( <i>Sophora japonica</i> ), yew ( <i>Taxus baccata</i> ), pines ( <i>Pinus</i> spp.), and spruce ( <i>Picea abies</i> ), magnolia ( <i>Magnolia</i> spp.)	5.2 (evergreen species <1%)	82.6

### - Pariser Platz and Bordeaux Platz, Munich

The study sites which were used for simulations of temperature mitigation using the Tree4City model are located in Munich (Germany) (Fig. 4) and have different topographical features: *Bordeaux Platz* is an open green square and *Pariser Platz* is a circular paved square (Fig. 5).

The two sites share the same tree species *Tilia cordata* Mill. commonly present in European cities (Grote et al. 2016) and show contrasting features in terms of micro-meteorological conditions and surface cover. Furthermore, they are located close to the city center where UHI effect is more evident and thus the temperature reduction of urban trees is particularly demanded.

Apart from differences in sealing and wind speed, the trees at *Bordeaux Platz* were a bit smaller than those at *Pariser Platz* (Table 2).



**Figure 5.** Bordeaux Platz (A) and Pariser Platz (B) in Munich. Source: (TUM 2016) – Google Maps

**Table 2.** Average morphological characteristics of trees at the two study sites. Source: (Pace et al.)

Sites	DBH (cm)	Height (m)	Canopy cover (m <sup>2</sup> )	LAI
Bordeaux Platz	29.18 ± 0.52	15.12 ± 0.21	67.12 ± 3.37	2.41 ± 0.19
Pariser Platz	44.68 ± 1.27	16.78 ± 0.29	81.7 ± 3.97	2.54 ± 0.18

### 3.2. Weather and pollution data

i-Tree Eco simulations were conducted for the year 2012 using hourly meteorological data registered at the Munich Airport (about 40 km north of the Englischer Garten). These are provided by the National Oceanic and Atmospheric Administration (NOAA) and directly accessed by the model. These are supplemented by precipitation data from the weather station “München Theresienstrasse”, which is located about 1 km away from the *Englischer Garten* (Fig. 6). The average hourly concentration data for O<sub>3</sub>, SO<sub>2</sub>, NO<sub>2</sub>, CO, and PM<sub>2.5</sub> measured at the pollution stations of “München Stachus” and “Landshuter Allee” were provided from the Bavarian Environment Agency (LFU) (Fig. 7).

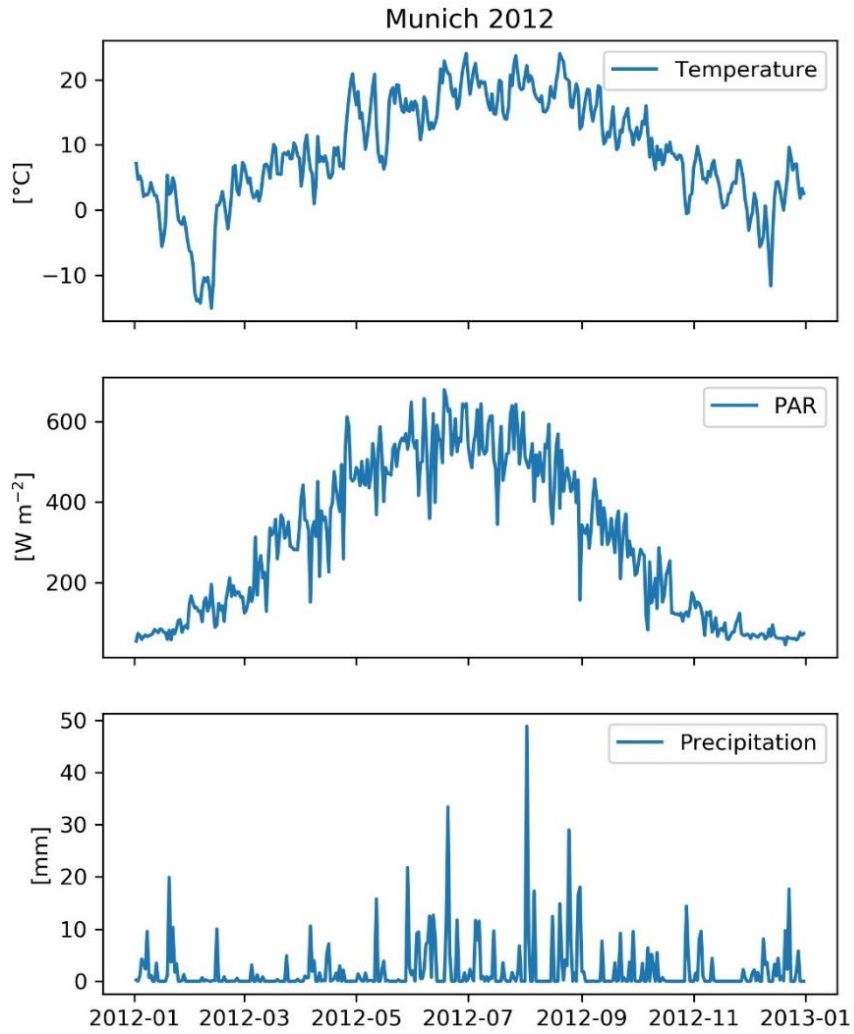


**Figure 6.** From top to bottom: temperature, PAR and precipitation of Munich in 2012.

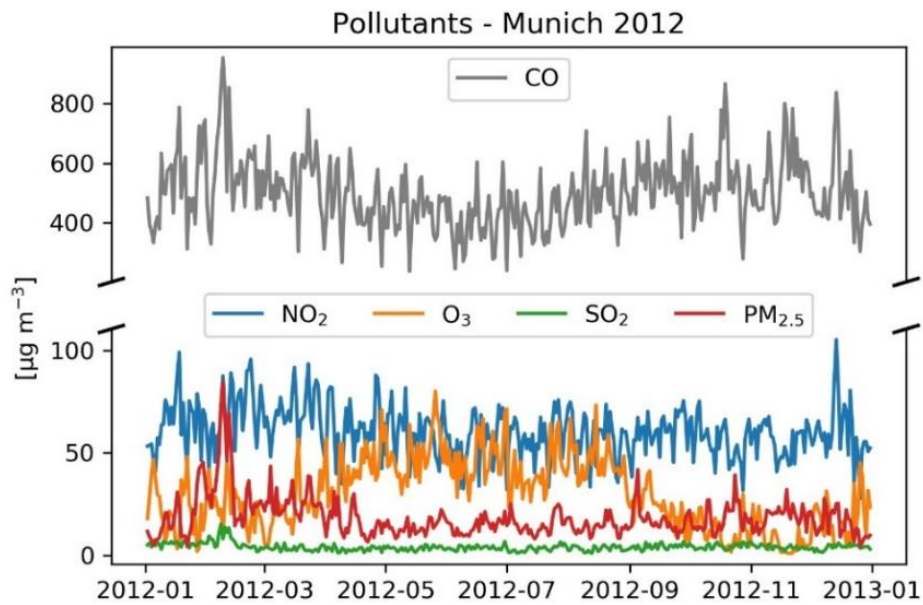


**Figure 7.** Pollutants concentration of Munich in 2012.

The simulations performed by the Tree4City model used air temperature, pressure, relative humidity, and wind speed data locally measured in August 2015 at the two study sites (*Bordeaux Platz* and *Pariser Platz*, in Munich; Fig. 8). Global radiation was measured at *Bordeaux Platz* and precipitation data were obtained from the *Theresienstrasse* weather station in Munich for the year 2015.

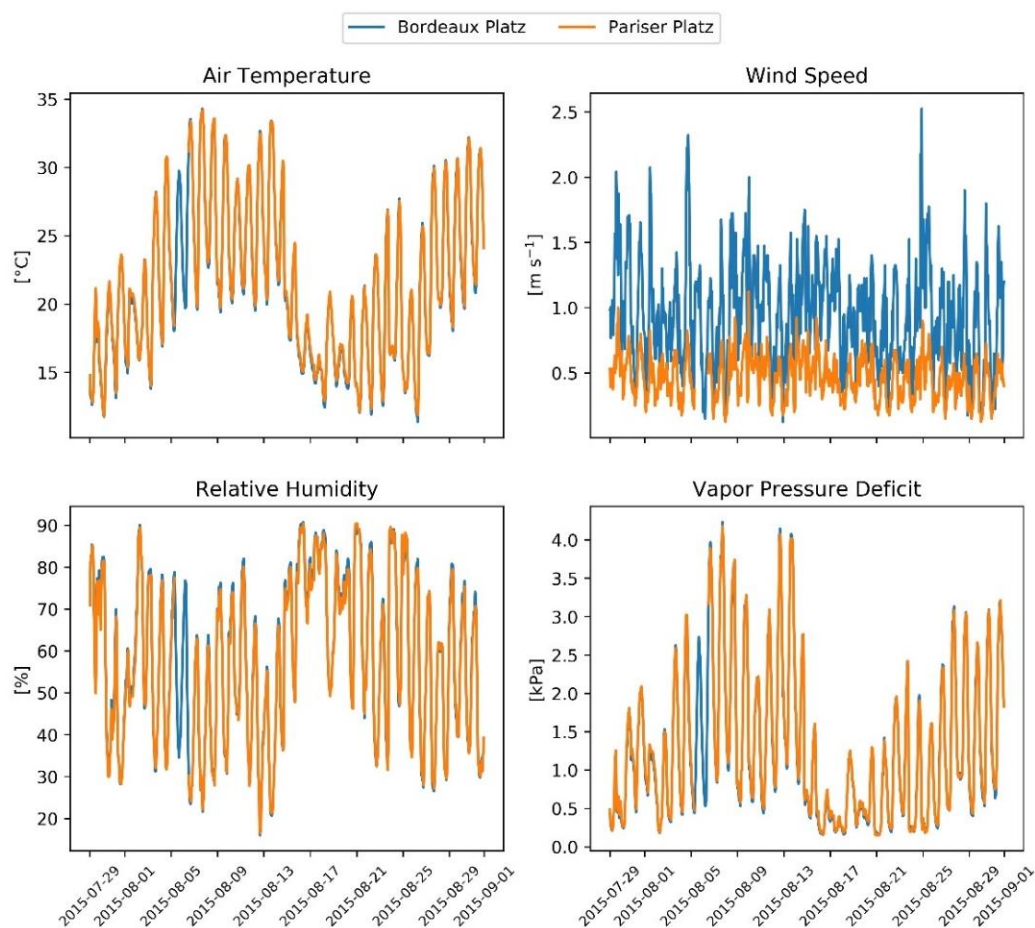


**Figure 8.** Meteorological conditions at the two study sites. Source: (Pace et al.)

For the comparison of PM pollution removal across a European gradient, hourly precipitation and wind-speed data were obtained from airport-station records in Berlin (Tegel) and Munich (München-Flughafen) and from the weather station in Castelporziano for Rome. These weather stations are all located at the city border, some distance from the city centers. Modeling simulations were performed for the years 2013–2015.

In Rome, spring, and summer precipitation is considerably lower than that in the winter and autumn, while the situation is almost the opposite in Munich, where the highest rainfalls occur in spring. The overall precipitation in Berlin is less by about a third than that at the other two sites (Tab. 3).

Also, there is a clear gradient in wind speed from Berlin to Munich and Rome, with the highest air movements mostly in the autumn and winter and the lowest in the summer. In Rome, there is hardly any seasonal variation, unlike at the German sites, which show some differences throughout the year (Tab. 3).

PM<sub>2.5</sub>-concentration data for all cities were taken from the i-Tree Eco database, which contains pollution data from the European Environment Agency (EEA). The pollution level is similar in all cases, with Berlin having slightly higher concentrations, particularly in 2014 (Tab. 3). Seasonality of PM<sub>2.5</sub> concentration is not very expressed in either of the sites, but the pollution minimum is in the summer, while the highest PM<sub>2.5</sub> concentrations occur in the winter (except in 2015 in Rome, which had the highest concentrations in autumn). The reason for the maximum in winter is the increased residential heating and the longer lifetime of PM precursors.

**Table 3.** From top to bottom: precipitation, wind speed and PM<sub>2.5</sub> data in Berlin, Munich and Rome from 2013 to 2015. Source: (Pace and Grote 2020)

Rain (mm)	2013					2014					2015				
	Winter	Spring	Summer	Autumn	Year	Winter	Spring	Summer	Autumn	Year	Winter	Spring	Summer	Autumn	Year
Berlin	98	154	168	143	564	54	137	158	69	418	88	81	132	158	458
Munich	114	276	213	134	737	59	158	306	164	688	88	319	119	136	662
Rome	285	123	27	270	706	343	108	128	315	893	212	110	86	154	562
Wind speed (m s <sup>-1</sup> )	2013					2014					2015				
	Winter	Spring	Summer	Autumn	Year	Winter	Spring	Summer	Autumn	Year	Winter	Spring	Summer	Autumn	Year
Berlin	3.4	3.2	2.9	3.5	3.3	3.8	3.1	2.9	3.4	3.3	4.0	3.6	3.6	3.7	3.7
Munich	3.1	2.9	2.4	2.6	2.7	2.6	2.7	2.6	2.9	2.7	3.5	3.1	2.5	3.1	3.1
Rome	2.6	2.3	2.0	2.0	2.2	2.3	2.1	2.1	2.0	2.1	2.2	2.1	1.9	1.8	2.0
PM <sub>2.5</sub> (µg m <sup>-3</sup> )	2013					2014					2015				
	Winter	Spring	Summer	Autumn	Year	Winter	Spring	Summer	Autumn	Year	Winter	Spring	Summer	Autumn	Year
Berlin	24.7	16.1	10.9	14.9	16.7	28.7	15.4	14.0	25.4	20.9	21.7	13.5	13.2	19.4	16.9
Munich	20.5	17.0	11.0	14.8	15.8	16.8	12.4	11.2	12.9	13.3	16.1	11.9	11.6	13.0	13.2
Rome	21.4	12.3	12.8	20.0	16.6	19.7	11.9	11.3	19.5	15.6	19.6	12.5	12.8	22.0	16.7

### 3.3. Model developments

#### 3.3.1. Automated crown dimension and light exposure routine

The i-Tree Eco model considers the average competition of a tree as the degree of crown exposure to sunlight, which is not supposed to change during the simulation. This competition is expressed as CLE (crown light exposure), which is an empirical index that reflects the number of sides of a tree receiving direct sunlight (Nowak et al. 2008a). Therefore, the tree crown is virtually divided into the four cardinal directions and an additional surface on top of the crown (Fig. 9) (Bechtold 2003). A classification can thus result in a CLE value between 0 (which would characterize a fully suppressed tree in the understorey of a closed canopy, only receiving diffuse light) and 5 (solitary tree not shaded by surrounding trees or other obstacles). CLE reflects broadly the capability for photosynthesis and is used to calculate LA and tree growth estimates. While growth directly determines carbon sequestration, LA influences various ecosystem services.

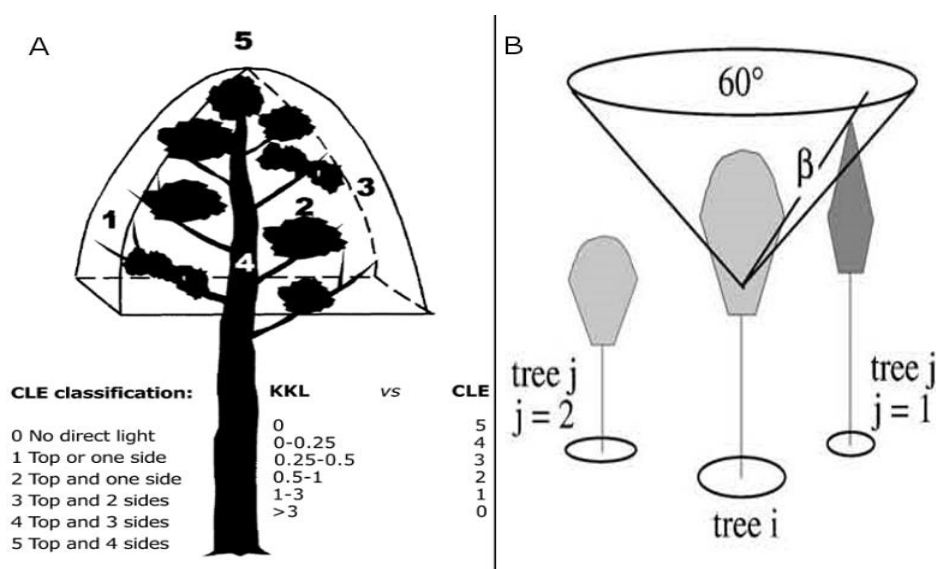


**Figure 9.** Crown light exposure (CLE) classification (A) and calculation of the competition index CCS (crown competition for sunlight) based on Pretzsch et al. (B). In the bottom right corner of (A), the conversion of CCS is indicated in CLE values. Source: (Pace et al. 2018)

Herein, I calculated CLE based on a routine introduced within the framework of the single-tree-based stand simulator SILVA (Pretzsch et al. 2002). This model calculates single-tree growth in relation to its surrounding three-dimensional space to produce the competition index CCS.



CCS aids in identifying the competitors of single trees by considering a virtual reverse cone with an axis equal to the tree axis and its vertex placed within the crown of the tree (Fig. 10). The model determines the angle  $\beta$  between the insertion point of the cone and the top of any competitor tree. This angle is multiplied by the crown cross-sectional areas (CCAs) of the competitors and the tree of interest considering a species-specific light transmission coefficient:

$$CCS_i = \sum_{j=1}^n \left( \beta_i \frac{CCA_j}{CCA_i} TM_j \right) \quad (1)$$

where  $CCS_i$  is the competition index for tree  $i$ ;  $\beta_i$  is the angle between cone vertex and top of competitor  $j$ ;  $CCA_j$  and  $CCA_i$  are the CCAs of trees  $j$  and  $i$ , respectively;  $TM_j$  is the species-specific light transmission coefficient for tree  $j$ ;  $n$  is the number of competitors of tree  $i$  (Pretzsch et al. 2002).

The competition index  $CCS$  was calculated for each tree before converting the results into a CLE classification. Therefore, we assumed that the trees without competition ( $CCS = 0$ ) correspond to the highest CLE value (CLE = 5), while other CLE classes are assigned to  $CCS$  values according to the relative abundance of trees (Figure 12).

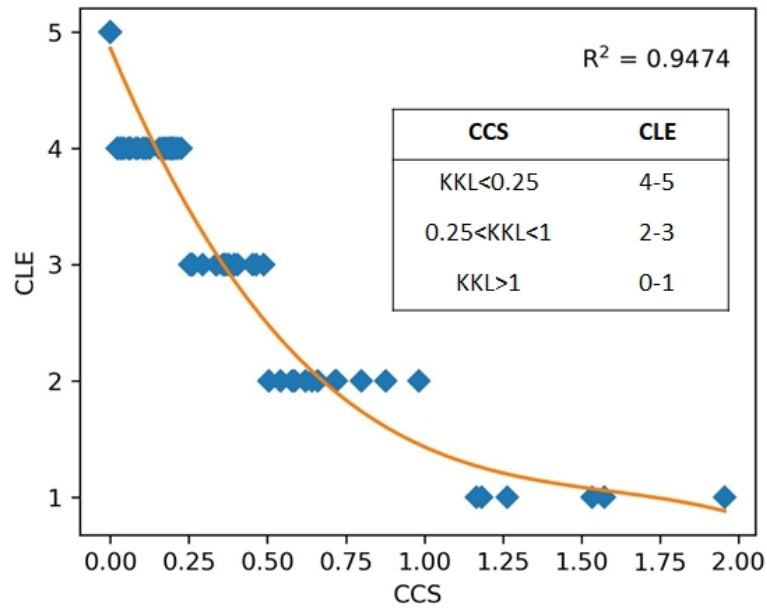


**Figure 10.** Relationship CCS-CLE and relative conversion classes determined from 100 sampled trees.

The shading by buildings and other trees not included in our inventory has been evaluated considering a fixed buffer distance of 15 m around the trees using the open source Quantum GIS (QGIS) software. For all trees falling within this distance, we reduced the CLE by one unit (Fig. 11).

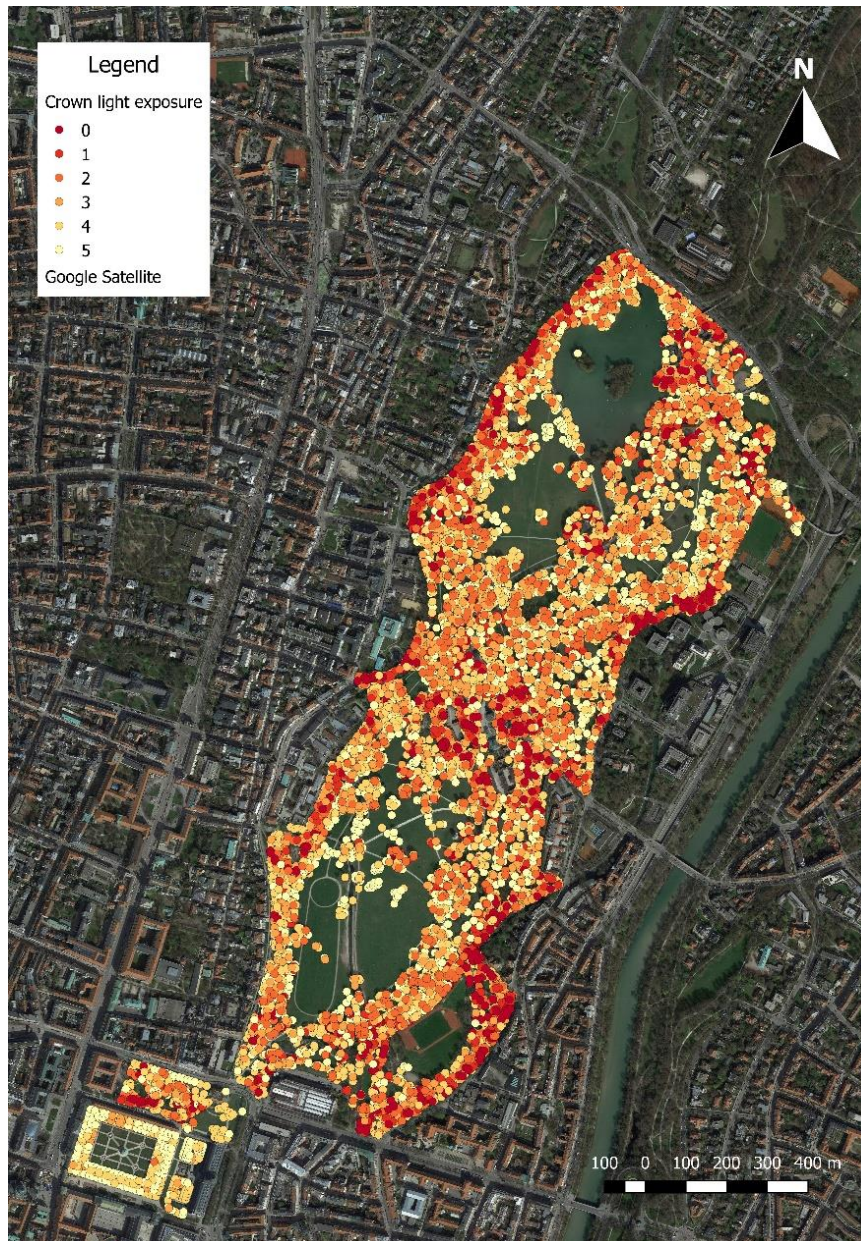


**Figure 11.** All trees in the south of Englischer Garten with relative crown light exposure (CLE) classes calculated by the CCS (crown competition for sunlight) competition index which is based on the algorithms provided in Pretzsch et al. (2002). In addition to competition between trees, shading by buildings has been considered as well. [CLE 0 = no direct light, CLE 1 = Top or one side, CLE 2 = Top and one side, CLE 3 = Top and two sides, CLE 4 = Top and 3 sides, CLE 5 = Top and 4 sides].  
Source: (Pace et al. 2018)

### - CLE effects on leaf area

The i-Tree Eco model calculates LA according to tree-specific CLE classes: the open-grown (CLE = 4–5), park (CLE = 2–3), and closed forest (CLE = 0–1) conditions. Under the open-grown condition, LA is calculated either from DBH only or from crown length (H) and crown width (D) if available (Nowak 1996):



- CLE = 4–5 (open-grown trees)

$$\ln(\text{LA}) = b_0 + b_1\text{DBH} + b_2\text{S} \quad (2)$$

$$\ln(\text{LA}) = b_0 + b_1\text{H} + b_2\text{D} + b_3\text{S} + b_4\text{C} \quad (3)$$

In these calculations, S is a species-specific shading factor, which is defined as the percentage of light intensity intercepted by foliated tree crowns, and C is the outer surface area of the tree crown calculated from H and D as  $C = \pi D(H + D)/2$ . S varies with species for deciduous trees, and if it is not defined for individual species, the averages for the genus or general hardwoods are used. For conifer trees, the model applies a shading factor of 0.91 for all species, except for pines (0.83) (Nowak 1996; Nowak et al. 2008a). For the closed forest condition, LA is calculated using the following equation based on the Beer-Lambert law:

- CLE = 0–1 (forest stand condition)

$$\text{LA} = (\ln(1 - S)/-k) \times \pi \times (D/2)^2 \quad (4)$$

where  $k$  is a light extinction coefficient that is differentiated between conifers (0.52) and hardwoods (0.65) (Nowak et al. 2008a). For CLE = 2–3 (park condition), LA is calculated as the average value determined by the open-grown (CLE = 4–5) and closed canopy equations (CLE = 0–1). Leaf biomass is calculated by converting leaf area estimates using species-specific measurements of grams of leaf dry weight/m<sup>2</sup> of leaf area (Nowak et al. 2008a).

The CLE is influencing the leaf area of a tree and thus the deposition as well as emission surfaces. Deposition is explained later in chapters ii) for gaseous pollutants and iii) for particles, while emissions of isoprene (C<sub>5</sub>H<sub>8</sub>) and monoterpenes (C<sub>10</sub> terpenoids) were estimated using an approach proposed by Guenther et al. 1993 and Geron et al. 1994. In this approach, emission is calculated by multiplying leaf biomass (derived from LA with species-specific conversion factors) with emission rates (Hirabayashi 2012). These in turn depend on temperature and light (isoprene) or temperature only (monoterpenes) as well as on genus-specific parameters that represent emissions at 30 °C and 1000  $\mu\text{mol m}^{-2} \text{s}^{-1}$  photosynthetically active radiation (PAR) (Nowak et al. 2002).

Median emissions values for the family, order, or superorder are used if genus-specific emission is not available (Nowak et al. 2008a). Incoming PAR is calculated as 46% of total solar radiation input (Monteith and Unsworth 2013). Because isoprene emission has a nonlinear dependence on light, PAR was estimated for 30 canopy levels using the sunfleck canopy environment model with the LAI of the analyzed structure (Nowak et al. 2008a). Hourly leaf temperature was calculated from air temperature while considering the again the LAI (Hirabayashi 2012).

### - CLE effects on tree growth

In addition, the CLE is also used to modify tree growth and thus carbon sequestration. Carbon sequestration or wood biomass increase is generally calculated based on tree dimensions using allometric equations (Nowak 1994; Nowak and Crane 2002), also considering a fixed root-to-shoot ratio of 0.26 to account for below ground growth (Cairns et al. 1997).

Because the allometric equations are diameter-based and developed for closed canopies, biomass that has been calculated for open-grown trees (those with a small CLE value), which tend to be shorter and thus have less above-ground biomass at a given diameter, is reduced by an additional factor of 0.8 (Nowak 1994).

Total carbon storage is then calculated by multiplying tree dry weight biomass by an assumed carbon density of 0.5 (Nowak et al. 2008a). Hence, assuming that there is no change in soil carbon, annual carbon sequestration is directly calculated from tree growth (Nowak et al. 2008a). Average diameter growth is added to tree diameter (year  $x$ ) to estimate the tree diameter in year  $x + 1$  (Nowak and Crane 2002). In i-Tree Eco, a standard diameter growth (SG) that can be reduced is defined for open-grown trees (CLE = 4–5) when the number of frost-free days is smaller than a defined value:

$$\text{Standard diameter growth (SG)} = 0.83 \text{ cm/year} \times (\text{number of frost-free days}/153) \quad (5)$$

Park tree growth (CLE = 2–3) is calculated by dividing SG of open-grown trees by 1.78 and that of forest trees (CLE = 0–1) by 2.29.

The new routine for estimating CLE compared to visual observations is objective and easily coupled with remote sensing inventories because based on tree position and crown dimension. Therefore, it does not require trained people for tree measurements saving time and efforts for big city inventories such as the London case demanded (Kenton Rogers et al. 2015). However, it is important to stress that tree crowns are often pruned in the city for safety reasons or to maintain their size assuming in some cases a singular shape and size (Peper et al. 2001a, b) that is hardly evaluable from the model.

### 3.3.2. A soil water balance module to affect stomatal conductance

#### - The Berry-Ball stomatal conductance model

The calculation of transpiration ( $T_f$ ,  $\text{g m}^{-2} \text{hr}^{-1}$ ) is basically calculated using the i-Tree Eco model methodology (Hirabayashi et al. 2015). The amount of water evaporating through stomata is controlled by the leaf and boundary layer resistances (Kramer 1983):

$$T_f = \frac{C_{leaf} - C_{air}}{\frac{1}{gs} + R_a} \cdot \frac{3600}{LAI} \quad (6)$$

where  $C_{leaf}$  is the water vapor concentration of evaporating surfaces within the leaf ( $\text{g m}^{-3}$ ),  $C_{air}$  is the water vapor concentration in the air ( $\text{g m}^{-3}$ ),  $1/g_s$  is the stomatal resistance ( $r_s$ ) ( $\text{s m}^{-1}$ ,  $g_s$  = stomatal conductance),  $R_a$  is the aerodynamic resistance ( $\text{s m}^{-1}$ ), and LAI is the leaf area index.

The parameters  $C_{leaf}$  and  $C_{air}$  can be calculated as follows (Monteith and Unsworth 2013):

$$C_{leaf} = \frac{M_w e_s}{R T} \quad (7a)$$

$$C_{air} = \frac{M_w e}{R T} \quad (7b)$$

where  $M_w$  is the molecular weight of water ( $18 \text{ g mol}^{-1}$ ),  $R$  is the universal gas constant ( $8.314 \text{ J mol}^{-1} \text{ K}^{-1}$ ),  $e_s$  is the saturation vapor pressure (kPa),  $e$  is the vapor pressure (kPa), and  $T$  is the temperature (K).

The stomatal conductance of each layer of the canopy can be then calculated based on the methods presented in Baldocchi, 1994, Farquhar et al., 1980, Harley et al., 1992, summarized as:

$$gs = \frac{m A rh}{C_s} + gm \quad (8)$$

where  $A$  is the photosynthetic carbon flux into the leaf,  $m$  is the Ball–Berry coefficient (or slope of the relationship between stomatal conductance and  $A$ ),  $rh$  is the relative humidity,  $C_s$  is the  $\text{CO}_2$  concentration at the leaf surface, and  $gm$  is the minimum conductance ( $0.02 \text{ mol m}^{-2} \text{ s}^{-1}$ ) when the stomata are closed ( $A = 0$ ). The model calculates stomatal resistance ( $r_s$ ) as the inverse of stomatal conductance.

The aerodynamic resistance ( $R_a$ ) is calculated as follows:

$$R_a = \frac{u(z)}{u_*^2} \quad (9)$$

where  $u(z)$  is the mean wind speed at the height of the weather station  $z$  ( $\text{m s}^{-1}$ ) and  $u_*$  is the friction velocity ( $\text{m s}^{-1}$ ).

This calculation routine does not include any consideration of soil water limitation, which however, is very well known to affect stomatal behavior (e.g. Medrano et al. 2002). Applying the model without soil water constraints, implicitly assumes that there is always sufficient rainfall, the vegetation has groundwater access, or trees are continuously watered during dry periods. Since this is not realistic, a soil water balance model that is suitable for application under urban conditions has been developed and coupled to the stomatal routines.

### - Soil water balance module

The new module is based on the DeNitrification and DeComposition (DNDC) model (Li et al. 1992). The following water fluxes are considered:

$$P = T + I + E + R + S \quad (10)$$

where  $P$  is the precipitation,  $T$  is the transpiration,  $I$  is the interception,  $E$  is the evaporation,  $R$  is the runoff, and  $S$  is the seepage (percolation below the last considered soil layer).

The model determines the daily potential evapotranspiration from the daily temperature based on a modified Thornthwaite equation (Thornthwaite and Mather 1957) considering a dependency on latitude (Camargo et al. 1999; Pereira and Pruitt 2004). The potential demand for hourly evaporation was determined by dividing the daily evaporation by 24. The interception is assumed to be linearly related to LAI and retained water evaporates from leaves according to the evaporation demand. Water drawn from the soil by evaporation and transpiration can be calculated as the minimum of either the remaining potential evapotranspiration or water demand, which in turn depends on photosynthesis and the species-specific water-use efficiency ( $3 \mu\text{mol CO}_2$  per  $\text{mmol H}_2\text{O}$ ; Gillner et al., 2015). The soil evaporation was determined from the residual evaporation demand and soil water available below a predefined depth (0.3 m).

The water movement within the soil depends on the difference between the relative water contents of the three adjacent soil layers and is regulated by the soil hydraulic conductivity. For the evaluation at the sites in Munich, we assumed a runoff of 40% for Pariser Platz because of its impervious surface and lower soil depth (0.1, 0.2, and 0.4 m for the three layers, respectively, compared with 0.2, 0.3, and 0.5 m, respectively, at Bordeaux Platz). A drought index (DI) was defined to limit the stomatal conductance and reduce the Ball–Berry constant ( $m$ ) from 10 to 3 according to the soil water availability:

$$DI = \frac{(\text{water content} - \text{wilting point})}{(\text{field capacity} - \text{wilting point})} \quad (11)$$

where:

- $if\ DI \leq 0.3 \rightarrow m = 3$
- $0.3 < DI < 0.5 \rightarrow m = 3 + 35 \times (DI - 0.3)$
- $DI \geq 0.5 \rightarrow m = 10$

### - Gaseous pollutant uptake affected by stomatal conductance

The dry deposition of O<sub>3</sub>, SO<sub>2</sub>, NO<sub>2</sub>, CO, and PM<sub>2.5</sub> is hourly determined throughout the year (Hirabayashi et al. 2011; Nowak et al. 2014). During precipitation events, deposition is assumed to be zero. Using the following equation, for other periods, the pollutant flux into the biosphere (F; in g m<sup>-2</sup> s<sup>-1</sup>) is calculated as the product of deposition velocity (V<sub>d</sub>; in m s<sup>-1</sup>) and pollutant concentration (C; in g m<sup>-3</sup>) (Nowak et al. 2006):

$$F = V_d C \quad (12)$$

Using the following equation, the deposition velocities of CO, NO<sub>2</sub>, SO<sub>2</sub>, and O<sub>3</sub> are calculated as the inverse of the sum of the aerodynamic resistance  $R_a$ , a quasi-laminar boundary layer ( $R_b$ ), and the canopy resistance  $R_c$  expressed in s m<sup>-1</sup> (Baldocchi et al. 1987):

$$V_d = (R_a + R_b + R_c)^{-1} \quad (13)$$

where  $R_a$  is determined from meteorological data (wind speed and atmospheric stability) and it is assumed to be independent of air pollution type or plant species (see equation 9).

$R_b$  is based on a value defined in a study by Pederson et al., 1995 using a specific Schmidt number (Sc) for each air pollutant (Hirabayashi et al. 2015):

$$R_b = 2(Sc)^{\frac{2}{3}} (Pr)^{-\frac{2}{3}} (ku_*)^{-1} \quad (14)$$

where Sc is the Schmidt number (1), Pr is the Prandtl number (0.72), k is the von Karman constant (0.41), and  $u_*$  is the friction velocity (m s<sup>-1</sup>).

$R_c$  is calculated using the following equation:

$$1/R_c = 1/(r_s + r_m) + 1/r_{soil} + 1/r_t \quad (15)$$

where  $r_s$  is the stomatal resistance (s m<sup>-1</sup>),  $r_m$  is the mesophyll resistance (s m<sup>-1</sup>),  $r_{soil}$  is the soil resistance (2941 s m<sup>-1</sup> in growing season and 2000 otherwise), and  $r_t$  is the cuticular resistance (s m<sup>-1</sup>).

Hourly canopy resistance values for O<sub>3</sub>, SO<sub>2</sub>, and NO<sub>2</sub> were calculated based on a modified hybrid of big leaf and multilayer canopy deposition models (Baldocchi et al. 1987; Baldocchi 1988).

The mesophyll and cuticular resistance values are set based on those reported in the literature: for NO<sub>2</sub>,  $r_m = 100$  s m<sup>-1</sup> (Hosker and Lindberg 1982) and  $r_t = 20,000$  s m<sup>-1</sup> (Wesley 1989); for O<sub>3</sub>,  $r_m = 10$  s m<sup>-1</sup>

(Hosker and Lindberg 1982) and  $r_t = 10,000 \text{ s m}^{-1}$  (Taylor et al. 1988; Lovett 1994); and for  $\text{SO}_2$ ,  $r_m = 0$  (Wesley 1989) and  $r_t = 8000 \text{ s m}^{-1}$ . As CO reduction is assumed to be independent of photosynthesis and transpiration, the resistance value for CO is set to  $50,000 \text{ s m}^{-1}$  in the in-leaf season and  $1,000,000 \text{ s m}^{-1}$  in the out-leaf season for all trees (Bidwell and Fraser 1972).

The new soil water routine enables to consider the drought effects on stomatal conductance and thus on transpiration and gaseous uptake of trees based on a simple parametrization of boundary conditions. This integration compared to the i-Tree model, which instead assumes a sufficient level of water in all conditions, not only allows a more realistic evaluation of the actual contribution of trees to the improvement of air quality and microclimate, but also helps to define the irrigation demand to ensure the health of trees and the provision of ecosystem services. However, cities are often characterized by a mixture of soil types combined with impermeable surfaces (Rossiter 2007) with properties difficult to derive which might increase uncertainties of the assessments.

### 3.3.3. Consideration of specific leaf properties to determine PM deposition

The deposition flux of  $\text{PM}_{2.5}$  is generally calculated according to the method used in the i-Tree Eco model (Hirabayashi et al. 2015):

$$f_t = Vd_t \times C \times \text{LAI} \times 3600 \quad (16)$$

$$R_t = (A_{t-1} + f_t) \times \frac{rr_t}{100} \quad (17)$$

$$A_t = (A_{t-1} + f_t) - R_t \quad (18)$$

$$F_t = f_t - R_t \quad (19)$$

where  $f_t$  is the  $\text{PM}_{2.5}$  flux at time  $t$  ( $\text{g m}^{-2} \text{ hour}^{-1}$ ),  $C$  is pollutant concentration ( $\text{g m}^{-3}$ ), and  $Vd_t$  is the deposition velocity at time  $t$  ( $\text{m s}^{-1}$ ) that is calculated from wind speed ( $\text{windSp}$ ) as  $vds \times \text{windSp}^x$ , with  $vds$  being the ‘specific deposition velocity’.  $R_t$  is the  $\text{PM}_{2.5}$  flux resuspended in the atmosphere at time  $t$  ( $\text{g m}^{-2} \text{ h}^{-1}$ ),  $A_{t-1}$  is the  $\text{PM}_{2.5}$  accumulated on leaves at time  $t$  ( $\text{g m}^{-2} \text{ h}^{-1}$ ) depending on previous deposition as well as precipitation,  $rr_t$  is the relative amount deposited  $\text{PM}_{2.5}$  that is resuspended at a specific wind speed at time  $t$  (%) which has been defined according to the i-tree model standards, and  $F_t$  is the net  $\text{PM}_{2.5}$  removal at time  $t$  after considering resuspension.

Resuspension depends on wind speed considering a specific resuspension rate for each of 13 specific wind speed classes ( $rr_t$ ) (Hirabayashi et al. 2015). Finally, washing from the leaves (and thus final pollution removal) is calculated when precipitation events are higher than the maximum water storage capacity of the canopy, which is defined by potential leaf water storage  $plws$  ( $\text{mm m}^{-2}$ ) (leaf water storage

$= plws \times LAI$ ). If such an event occurs, all  $PM_{2.5}$  accumulated on leaves is assumed to be washed off and  $A_{t-1}$  is set to 0 (Hirabayashi et al. 2015). Additional information on the site-specific parametrization has been described in Pace and Grote, 2020.

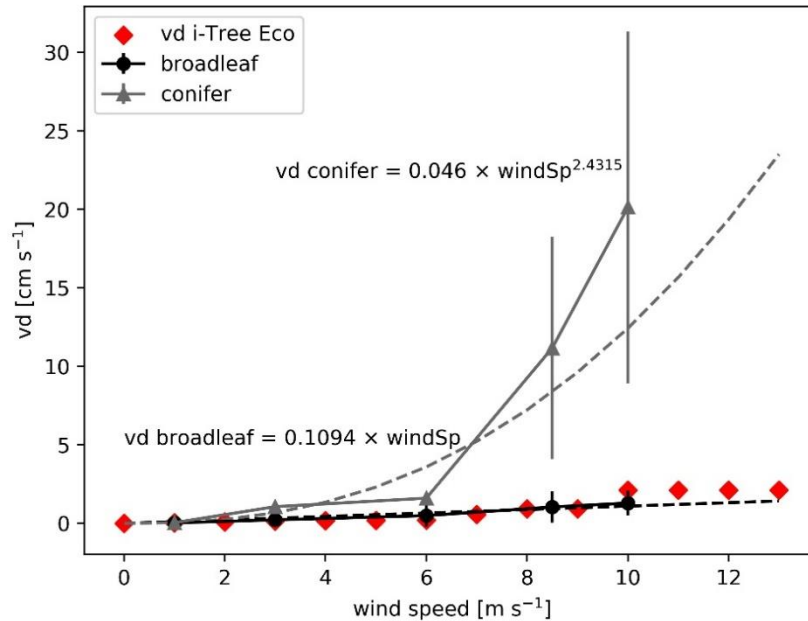


**Figure 12.** Deposition velocities ( $vd$ ) of coniferous and broadleaved tree types in dependence on wind-speed ( $windSp$ ). Red diamonds indicate the relationship as implemented in the original *i-Tree* model. Source: (Pace and Grote 2020)

Deposition velocity determined only from wind speed and one general parameter doesn't account for the multitude of real surface influences such as leaf orientation, morphology and structure (Hicks et al. 2016). Therefore, a literature survey has been carried out about for species-specific deposition velocities as a function of wind speed (Beckett et al. 2000; Freer-Smith et al. 2004; Pullman 2009). According to these data, regression functions separately for the coniferous and broadleaf tree type have been developed (Pace and Grote 2020) (Fig. 12).

For broadleaf evergreen trees (mostly species originating from southern Europe), the same deposition velocity as that of broadleaf deciduous trees was assumed because the deposition process seems to depend more on leaf shape (needle vs. flat leaf) than on other differences that might characterize evergreen vs. deciduous broadleaves and literature information does not provide sufficient information to derive a separate function for evergreen broadleaves. With this differentiation, the suggested model improvement accounts for the most obvious and simple differences in surface properties only. A more comprehensive approach would certainly be desirable but lacks the necessary database.

## 3.3.4. A new energy balance routine to calculate temperature changes

Many concepts of energy balance calculations exist that are implemented in various models of different degree of complexity, however these require a considerable parametrization based on information hardly to get in a city environment (e.g. lateral energy transport). The proposed approach instead allows to evaluate the cooling and shading effect of trees using the physiological calculation of transpiration (see Eq. 6) and an energy balance routine with a simple parametrization, respectively.

The total energy reduction  $E$  ( $\text{W m}^{-2}$ ) was calculated as the sum of two effects, shading from the canopy ( $E_{\text{shading}}$ ,  $\text{W m}^{-2}$ ) and cooling by water evaporation ( $E_{\text{cooling}}$ ,  $\text{W m}^{-2}$ ). Cooling is described based on average hourly transpiration rate  $T$  ( $\text{ml hr}^{-1} \text{m}^{-2}$ ), which is converted into energy loss ( $\text{W m}^{-2}$ ) by multiplication with the latent heat of vaporization  $L_v$ , which is  $2450 \text{ J kg}^{-1}$  and division by 3600 s:

$$E_{\text{cooling}} = \frac{T \times L_v}{3600} \quad (20)$$

The energy reduction due to shading is based on calculations for concrete surfaces that was assessed by determining the equilibrium temperature of the pavement surface based on the heat transfer and energy balance according to Solaimanian and Kennedy (Solaimanian and Kennedy 1993):

$$q_a + q_s - q_c - q_k - q_r = 0 \quad (21)$$

where  $q_a$  is the absorbed energy,  $q_s$  is the Longwave radiation,  $q_c$  is the convection energy,  $q_k$  is the conduction energy, and  $q_r$  is the surface emission.

$$q_a = (1 - a) \times R \quad (22)$$

where  $a$  is the albedo (0.3) and  $R$  is the direct radiation (determined from the global radiation as described in Spitters et al. 1986).

$$q_s = \varepsilon_a \sigma T_{\text{air}}^4 \quad (23)$$

$$\varepsilon_a = 0.77 - 0.28 \times 10^{(-V_p \times 0.074)} \quad (\text{Geiger 1959})$$

$V_p$  = vapor pressure (mmHg)

$\sigma$  = Stefan–Boltzmann constant ( $= 5.68 \times 10^{-8} \text{ W m}^{-2} \text{ K}^{-4}$ )

$T_{\text{air}}$  = air temperature (K)

$$q_c = h_c(T_s - T_{\text{air}}) \quad (24)$$

$h_c$  = surface coefficient of heat transfer =  $698.24[0.00144 T_m^{0.3} U^{0.7} + 0.00097(T_s - T_{\text{air}})^{0.3}]$

$T_s$  = surface temperature (K)

$T_m$  = average of the surface and air temperature (K)

$U$  = average daily wind speed ( $\text{m s}^{-1}$ )



$$q_k = -k \frac{T_d - T_s}{d} \quad (25)$$

$k$  = thermal conductivity ( $1.65 \text{ W m}^{-1} \text{ K}^{-1}$ )

$d$  = depth (0.5 m)

$T_d$  = temperature at depth  $d$  ( $20 \text{ }^\circ\text{C}$ )

$$q_r = \varepsilon_b \sigma T_s^4 \quad (26)$$

$\varepsilon_b = 1.24 \times (10 \times V_p / T_{air})^{\frac{1}{7}}$  (Brutsaert 1982).

The reduction of the direct radiation through the tree crown was calculated using a modified Beer–Lambert law considering a uniform leaf arrangement in the canopy:

$$R_{in} = R \times e^{-k \times LAI} \quad (27)$$

where  $R_{in}$  is the irradiance under the tree canopy ( $\text{W m}^{-2}$ ) and  $k$  is the extinction coefficient (see Eq. 4).

Finally, the energy reduction by shading ( $E_{shading}$ ;  $\text{W m}^{-2}$ ) can be calculated as the absolute difference between the energy balance outside and inside the tree canopy:

$$E_{shading} = |q_{a,out} - q_{a,in}| + |q_{s,out} - q_{s,in}| + |q_{c,out} - q_{c,in}| + |q_{k,out} - q_{k,in}| + |q_{r,out} - q_{r,in}| \quad (29)$$

The new energy balance routine is thus directly coupled to the water balance model including stomatal responses to drought. It is easy to parametrize and many parameters and variables are used in other modules too. Thus, it seems to be able for consistent application to estimate ecosystem services related to temperature mitigation. In the example calculations carried out within this thesis, energy reduction is based on cooling and shading and was evaluated for midday hours only (12:00–15:00, CET).

## 4) Results

### 4.1. Sensitivity of i-Tree Eco simulations to parameterization and competition determination

The tree crowns of Englischer Garten based on calculations with individual determination of CLE and species-specific parameterization, were estimated to cover an area of 73.2 ha and have a total LA of 467.5 ha with a leaf biomass of 301.7 tons. The most dominant species in terms of number and basal area were *A. platanoides* and *F. sylvatica* (Tab. 1). Overall, carbon stored in the trees was estimated to be 6225 tons. In accordance with their fraction of basal area, *F. sylvatica* and *A. platanoides* stored the most carbon (31.4% and 29.1% of the total, respectively). The amount of carbon sequestered in 2012 was calculated to be 214 tons (Fig. 13). The model further indicates that the trees in Englischer Garten removed 2610 kg of O<sub>3</sub>, 845 kg of NO<sub>2</sub>, 186 kg of PM<sub>2.5</sub>, 171 kg of SO<sub>2</sub>, and 62 kg of CO (Fig. 14). In addition, the trees emitted an estimated BVOC amount of 550 kg (158 kg isoprene and 392 kg monoterpenes; Fig. 15).

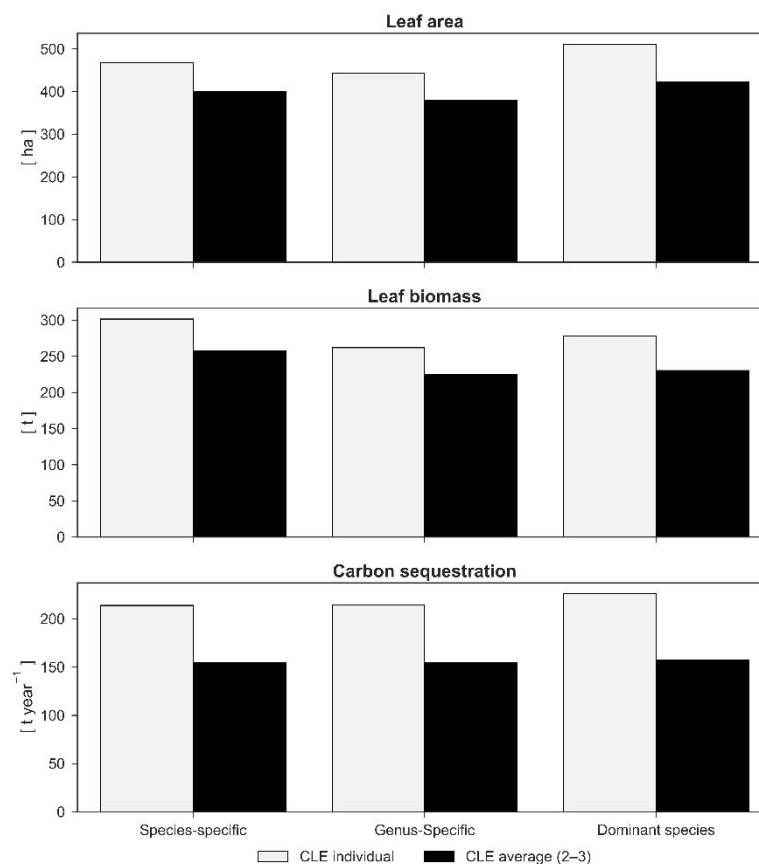


**Figure 13.** Leaf area (LA), leaf biomass, and carbon sequestration comparison between the “species-specific”, “genus-specific”, and “dominant species” simulations considering the crown light exposure (CLE) value for each tree (CLE individual) and the average CLE values (CLE average). Source: (Pace et al. 2018)

Simulation with average CLE values (CLE average) resulted in a 14% reduction in LA and leaf biomass (379.9 vs. 443 ha year<sup>-1</sup>; 224.9 vs. 262 t year<sup>-1</sup>) compared to the run with individually determined CLE (Fig. 13). This directly affected BVOC emissions (494 vs. 550 kg year<sup>-1</sup>; Fig. 15) as well as pollution removal (Fig. 14). Except for CO (in both cases, 62 kg year<sup>-1</sup>), more pollutants were removed in the “CLE individual” simulation compared to the “CLE average” simulation (2610 vs. 2482 kg year<sup>-1</sup> for O<sub>3</sub>, 845 vs. 794 kg year<sup>-1</sup> for NO<sub>2</sub>, 186 vs. 165 kg year<sup>-1</sup> for PM<sub>2.5</sub>, and 171 vs. 164 kg year<sup>-1</sup> for SO<sub>2</sub>). Carbon sequestration was also affected by individual light exposure (Fig. 13): 214 tons of carbon (784 CO<sub>2</sub> equivalent) removed in the “CLE individual” simulation compared to 155 tons of carbon (567 CO<sub>2</sub> equivalent) removed in the “CLE average” simulation, indicating that the trees in Englischer Garten were more open grown than expressed by the average CLE value.

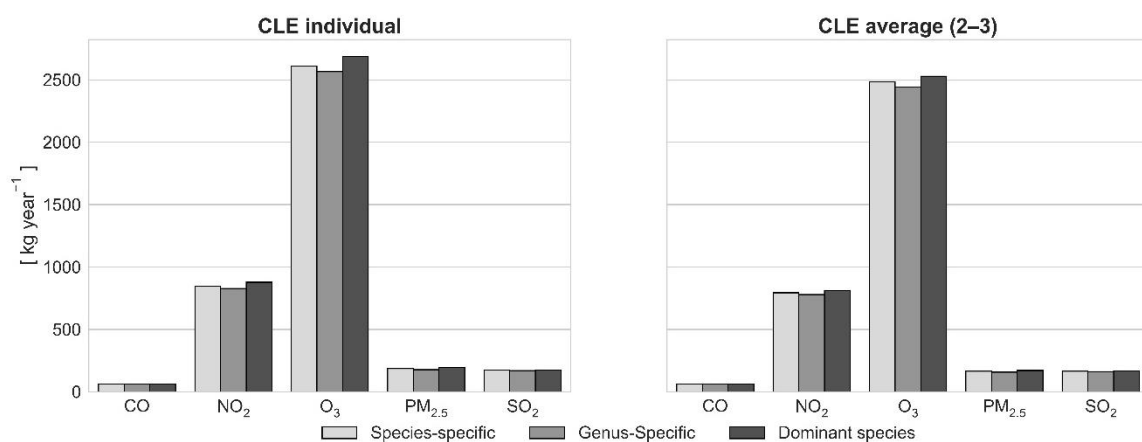


**Figure 14.** Air pollution removal comparison between the “species-specific”, “genus-specific”, and “dominant species” simulations considering the crown light exposure (CLE) for each tree (CLE individual) and the average CLE values (CLE average). Source: (Pace et al. 2018)

Compared to simulations with species-specific parameterization, the results obtained with the genus-specific simulation showed lower LA (−5%; 443.7 ha) and leaf biomass (−13%; 262 t). The dominant species simulation demonstrated higher LA values (511.3 ha; 9% higher than the species-specific parameterization), but leaf biomass results were lower (−8%; 278.4 t) (Fig. 13).

According to the lower LA, pollutants removed with genus-specific parameterization were fewer than those removed with species-specific parameterization (−2% of O<sub>3</sub>, −2% of NO<sub>2</sub>, −5% of PM<sub>2.5</sub>, and −1% of SO<sub>2</sub>), except for CO (62 kg year<sup>-1</sup>), as shown in Fig. 14. The effects of species differentiation were small. LA also had a minor effect on BVOC emissions, which are otherwise driven by marginally different parameters for the species- and genus-specific simulations. However, when the parameters were set according to the dominant species approach, monoterpene emissions were considerably higher (+93%) and isoprene emissions tended to be zero (−89%) compared to the species-specific simulation (Fig. 15).

Carbon sequestration (214 t) was not altered by the species- and genus-specific parameterizations because biomass growth was found to solely depend on the tree size and competition state (Fig. 13).

Instead, the dominant species simulation showed higher carbon sequestration (+5.7%; 226 t) because a larger number of trees fell into class 4–5 due to the smaller transmission coefficients for maples in comparison with the species average (Pace et al. 2018).

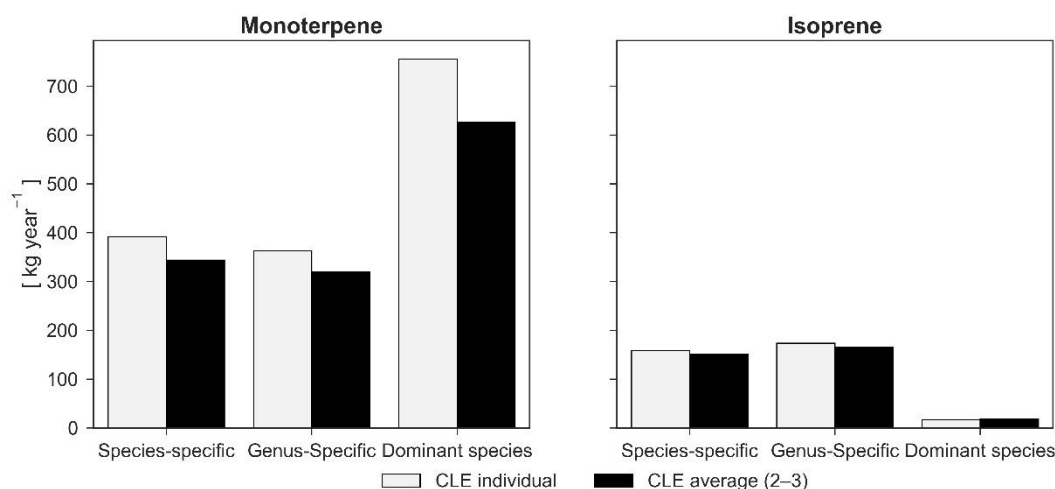


**Figure 15.** Comparison of monoterpene and isoprene emissions between the “species-specific”, “genus-specific”, and “dominant species” simulations considering the crown light exposure (CLE) for each tree (CLE individual) and the average CLE values (CLE average). Source: (Pace et al. 2018)

#### 4.2. Particulate matter removal in dependence on plant-type specific deposition velocities

In general, the highest  $PM_{2.5}$  deposition into urban tree canopies was calculated for Berlin, followed by Munich and Rome. Applying the new deposition velocity differentiation for conifers, deciduous and evergreen broadleaves, the simulations show that the difference is particularly large for conifers, which remove seven times more air pollutants than the broadleaf deciduous trees in Berlin, and about five times more than in Munich and Rome, respectively (Tab. 4). In relative terms, the broadleaf evergreen trees remove twice as much air pollutants as broadleaf deciduous trees. The difference is smallest in Munich (factor 1.8) and largest in Rome (factor 2.5) with Berlin close to Munich (factor 2.1). Also, the data show inter-annual differences of  $\pm 24\%$  over the 3 years for conifers,  $\pm 7\%$  broadleaf evergreens, and  $\pm 2\%$  broadleaf deciduous, indicating that not only plant type properties but also air-pollution distribution and seasonal weather conditions are influencing PM removal (Tab. 4).

**Table 4.** Annual  $PM_{2.5}$  removal by different tree types in three cities. Source: (Pace and Grote 2020).

$PM_{2.5}$ ( $g\ m^{-2}\ yr^{-1}$ )	Berlin			Munich			Rome		
	Conifer	Evergreen	Deciduous	Conifer	Evergreen	Deciduous	Conifer	Evergreen	Deciduous
2013	2.4	0.7	0.3	1.7	0.7	0.3	1.4	0.6	0.2
2014	2.8	0.8	0.4	1.5	0.6	0.4	1.1	0.6	0.2
2015	2.9	0.7	0.4	1.4	0.5	0.3	0.9	0.5	0.2
Average	2.7	0.8	0.4	1.5	0.6	0.3	1.2	0.6	0.2

Since bark and branch deposition is not considered, deciduous trees do not deposit particles outside the vegetation period, i.e., in the winter (the deposition in Rome during this time occurs because the vegetation period here prolongs into the winter period) (Fig. 16). For the other two tree types, the seasonal pattern is similar for Berlin and Rome, with the highest deposition rates in the autumn and winter, but different for Munich, where these months are often those with the lowest deposition rates (with some exceptions, e.g., high removal rate for Berlin in summer 2015, for Rome in spring 2013, and for Munich in autumn 2013) (Figure 16).

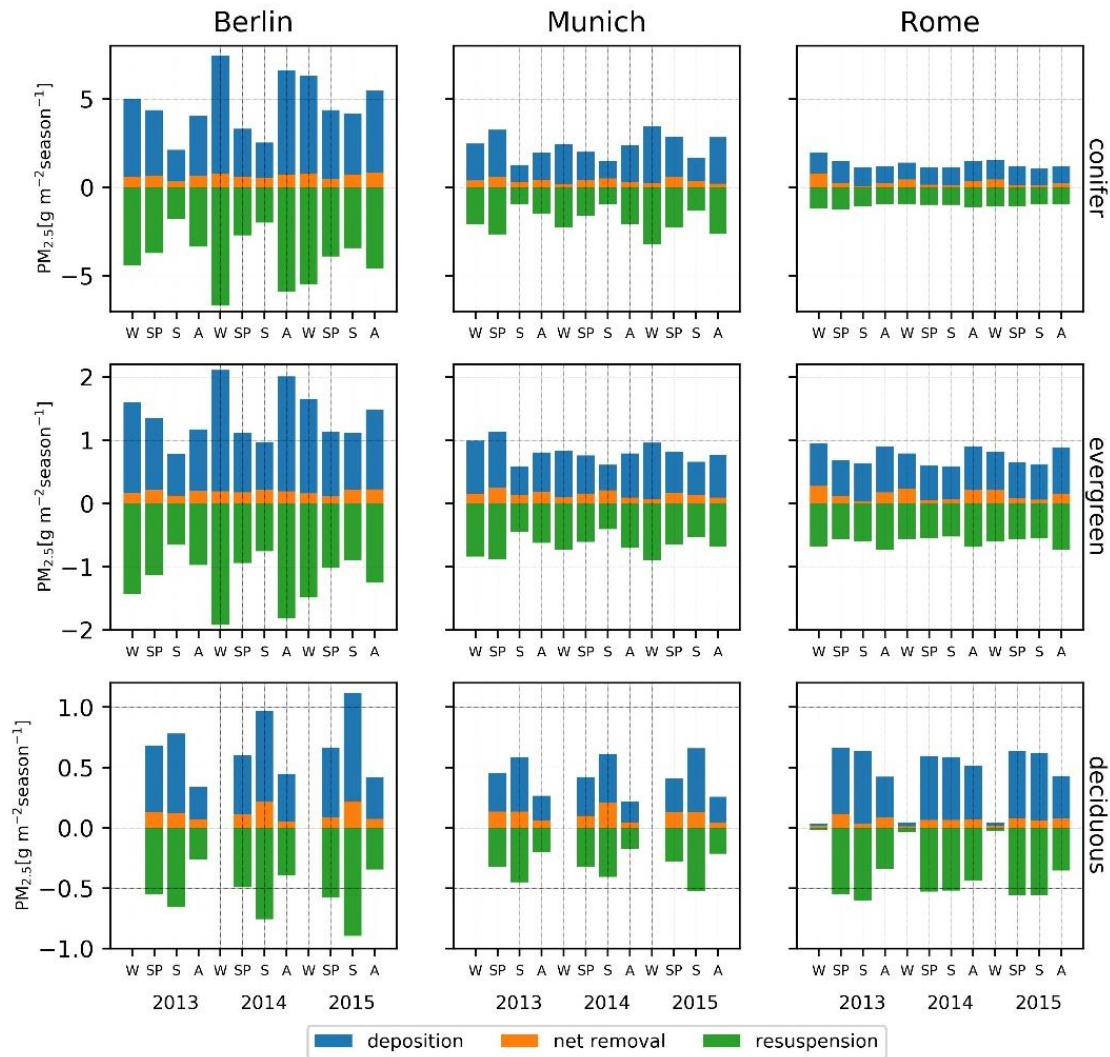


**Figure 16.** Seasonal  $PM_{2.5}$  deposition, removal, and resuspension for three cities, 2013–2015 [seasons: W, winter; SP, spring; S, summer; A, autumn]. Source: (Pace and Grote 2020)

The calculated deposition increases during the day with a peak at mid-day, closely following the development of wind speed. In parallel also resuspension rises because it depends on deposition. In the absence of rainfall, as in the case of Rome in summer, particulate matter is not washed off from leaves which leads to large accumulation, increased resuspension, and thus to negative values of net removal in particular during the middle hours of the day since it is more sensitive to higher wind speeds than deposition (Fig. 17).

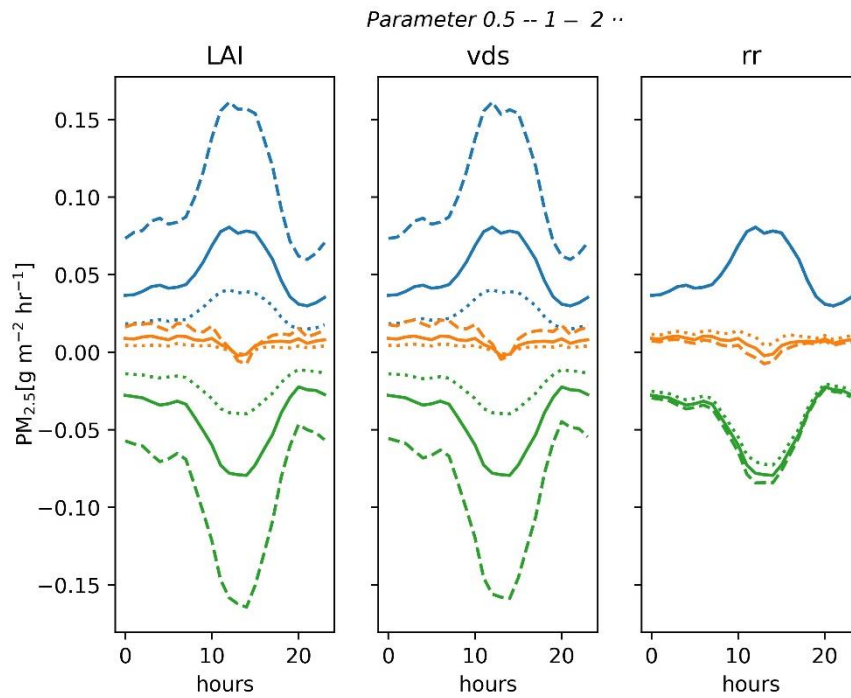


**Figure 17.** Sensitivity of deposition (blue lines), net removal (orange), and resuspension (green) to parameter changes of leaf area index (LAI, left), specific deposition velocity (vds, middle), and resuspension percentages (rr, right). All simulations were run with half, normal and double values relative to standard parameters and carried out for selected periods for Rome in 2014-2015. Source: (Pace and Grote 2020)

The higher  $PM_{2.5}$  concentration and wind speed promote a larger dry deposition in Berlin compared to the other cities. The effect is particularly expressed in winter and autumn, when repeated rainfall events also provide a regular washing of the leaves, increasing the overall effectiveness of conifers. Thus, the highest seasonal net removal rates calculated was for conifers in Berlin during the winter of 2014/2015 (Fig. 16). Although pollution and wind speed are somewhat smaller, the overall net removal for broadleaf deciduous trees in Munich is almost as high in Berlin (Tab. 4). Here, the reason is that summer precipitation in Munich is much higher and thus resuspension in summer is smaller. In Rome, resuspension during summer is particularly high and wind speed is relatively low, both resulting in a smaller  $PM_{2.5}$  removal compared to that in the other cities (Fig. 16). In addition, the vegetation period in Rome is longer, starting early in spring and sometimes reaching into the winter period. Therefore, the spring removal rates in Rome are more similar for broadleaf deciduous and evergreen trees than those in the other two cities where leaves were not fully developed at the time (Fig. 16).

### 4.3. Gaseous pollutants uptake as a function of dynamic stomatal regulation

The two squares in Munich are not significantly different in terms of air temperature, relative humidity, and vapor pressure deficit. However, the wind speed at Bordeaux Platz (mean =  $0.9 \text{ m s}^{-1}$ ) is much higher than that at Pariser Platz (mean =  $0.5 \text{ m s}^{-1}$ ; Fig. 9). Consequently, the resistances of the aerodynamic and quasi-laminar boundary layer were considerably lower at Bordeaux Platz (on average  $105.9$  and  $60 \text{ s m}^{-1}$ , respectively) than at Pariser Platz ( $222.4$  and  $125.9 \text{ s m}^{-1}$ , respectively; Fig. 18), which explains the higher transpiration demand at the former location.

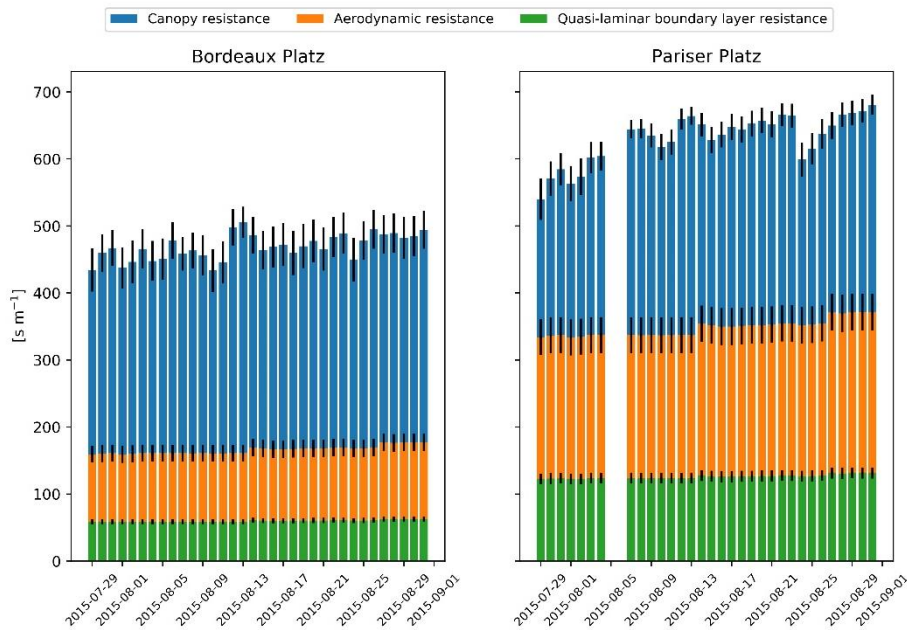


**Figure 18.** Model resistances at the two sites. The quasi-laminar boundary layer is referred to as  $O_3$ .  
Source: (Pace et al. submitted)

During the observation period (August 2015), the negative soil water potential in Munich increased until mid-month when several precipitation events occurred, leading to the replenishment of the soil water and increase in soil moisture potential. This trend could be represented using the newly implemented soil water balance module, considering differences in the soil depth and surface sealing. It should be noted that the recovery of the relative water content at Pariser Platz is considerably slower than that at Bordeaux Platz because the water supply is reduced due to larger runoff (Fig. 19).

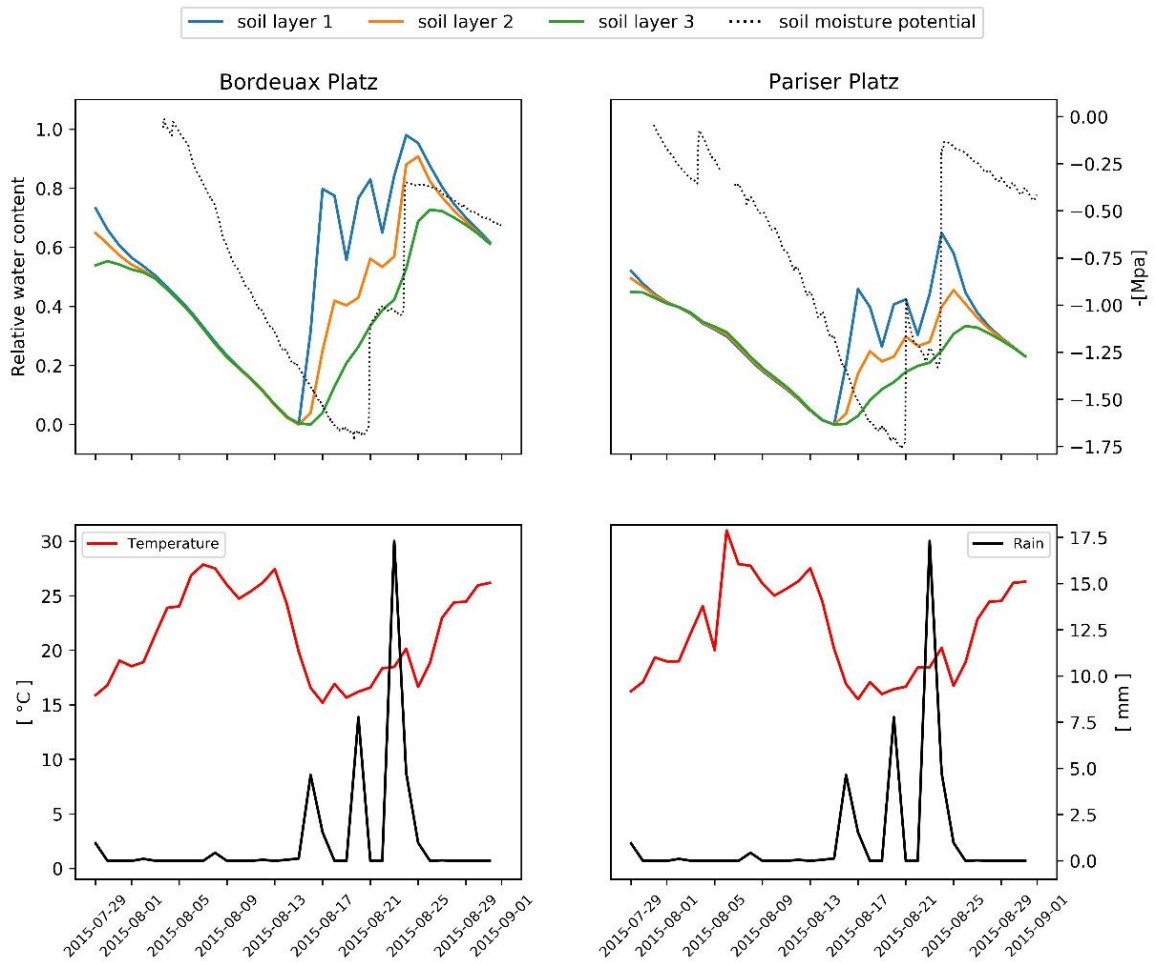


**Figure 19.** Upper panels: Relative water content in each soil layer and measured soil moisture potential. Lower panels: Average daily temperature and rain events in the study period. Source: (Pace et al. submitted)

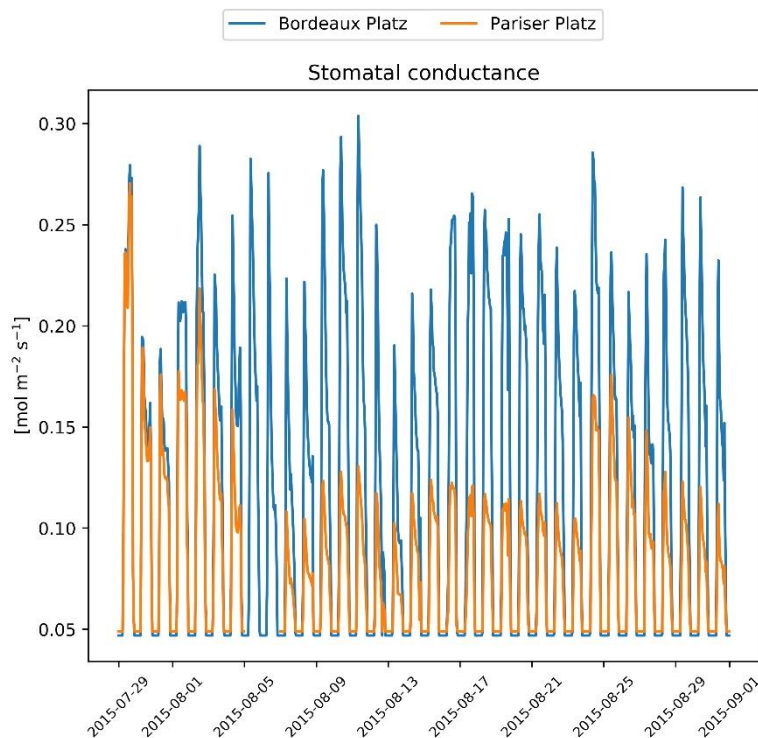


**Figure 20.** Stomatal conductance ( $g_s$ ) at two sites. Source: (Pace et al. submitted)



The calculated differences in stomatal conductance due to both, the different wind conditions and the different soil water availability at the two places (Fig. 20) result in remarkable differences in  $vd$ , as indicated in Fig. 21. Thus, it can be assumed that the conditions at Bordeaux Platz lead to a higher removal of gaseous pollutants than at Pariser Platz. For sites with comparable ozone formation and transport, this may ultimately lead to a relatively better air quality.

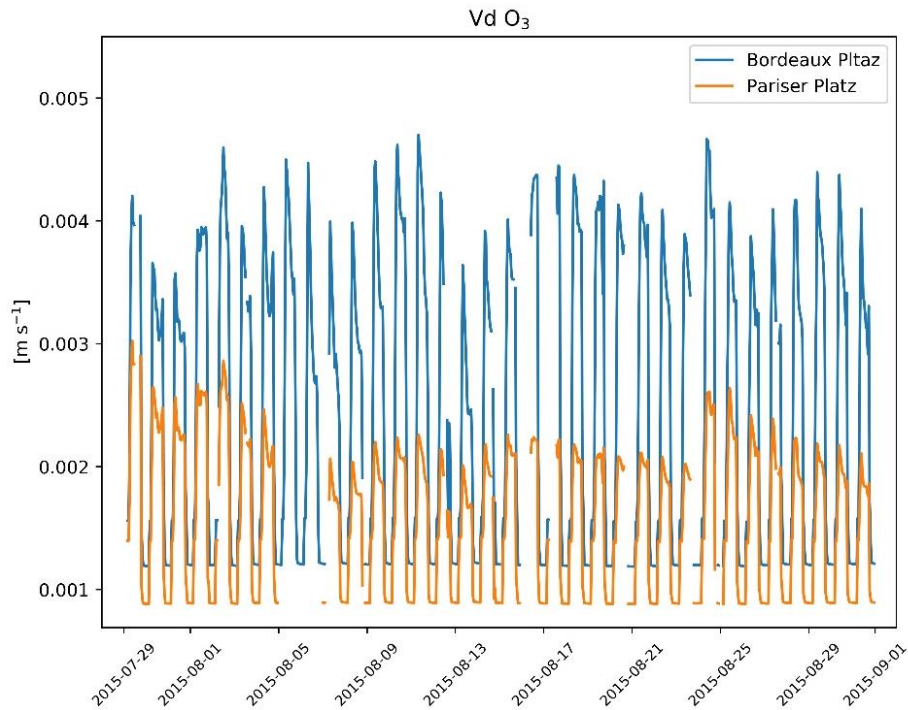


**Figure 21.** Dry deposition velocity ( $vd$ ) of  $O_3$  at the two sites. Missing values correspond to hours with precipitation. Source: (Pace et al. submitted)

#### 4.4. Temperature mitigation by cooling and shading

The impact of drought on stomatal conductance adds to the differences between the two study sites in Munich (Fig. 20) leading to a lower transpiration at Pariser Platz than at Bordeaux Platz. This should affect not only the deposition, but also the transpiration and thus the energy balance around the investigated trees. Indeed, the modeled and measured transpiration values at the two sites overall agree, highlighting the ability of the model to cope with the differences between the two sites (Fig. 22).

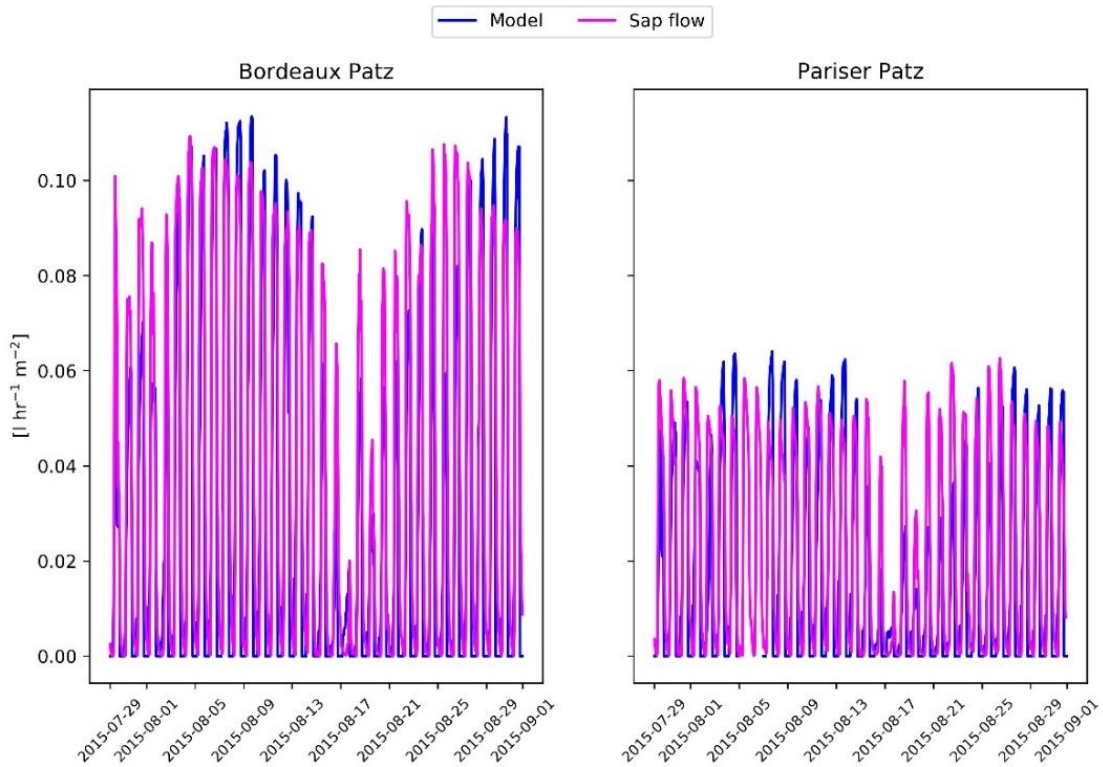


**Figure 22.** Comparison of modeled transpiration and values measured using the sap flow for the two sites. Source: (Pace et al. submitted)

For the whole temperature mitigation effect, however, the shading effect has also to be considered. Based on the new energy balance calculations, the simulated surface temperature was much lower under the tree canopy at the hottest days (up to 20.6 °C in Pariser Platz and 17.2 °C in Bordeaux Platz), while during the cool period without much direct radiation, the shading effect is negligible (Pace et al.). The differences between the places originate again from the lower wind speed at Pariser Platz, which limits the heat flow by convection to the surrounding air and thus leads to higher temperatures in the sun. On the other hand, the surface temperature under shaded conditions at this site is slightly lower because of the slightly higher leaf area index of the trees.

The transpiration performance particularly influences the cooling effect at Pariser Platz (mean = 0.03; max = 0.04 kW/m<sup>2</sup>) compared with Bordeaux Platz (mean = 0.05; max = 0.075 kW/m<sup>2</sup>). Instead, the energy reduction by shading is similar at the two locations (mean = 0.3; max = 0.6 kW/m<sup>2</sup>), indicating that the largest energy reduction occurs at midday (Fig. 23).

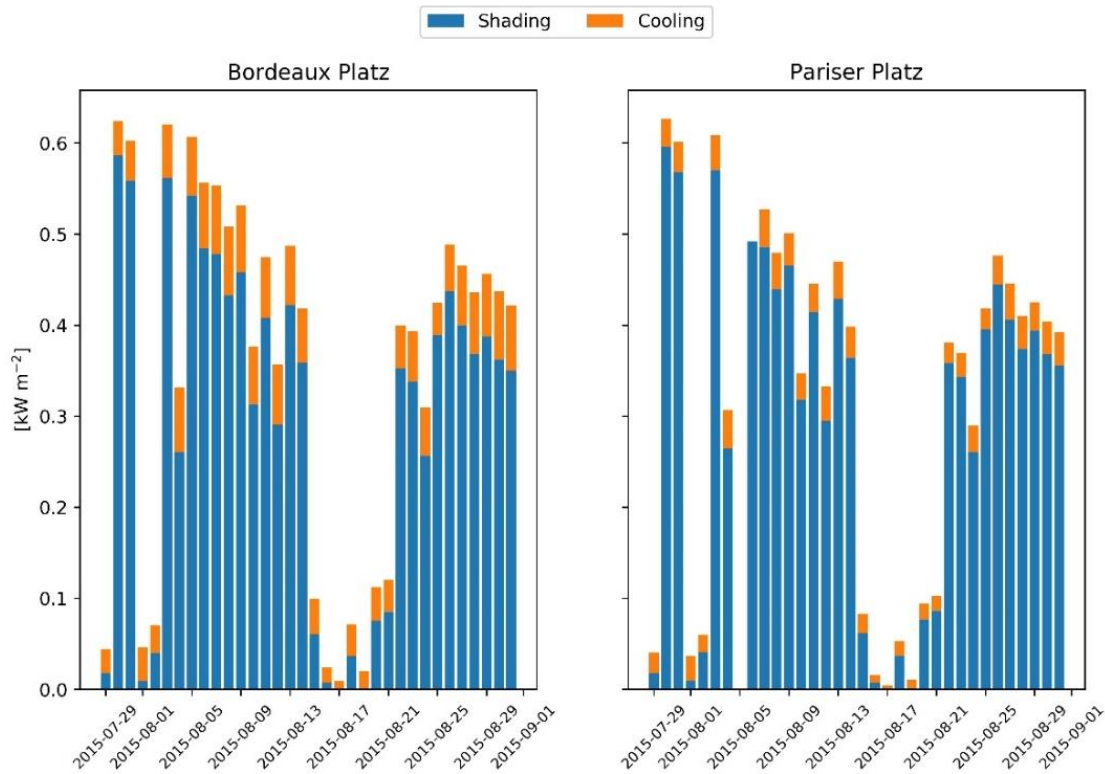


**Figure 23.** Energy reduction by concrete shading and cooling by transpiration at the two sites at midday. Source: (Pace et al. submitted)

## 5) Discussion

### 5.1. i-Tree Eco model sensitivity to species composition and light exposure

The Englischer Garten park provides a considerable amount of environmental services, i.e., air pollution reduction and carbon sequestration. Simulated removals of  $O_3$  and  $NO_2$  were at the highest rates (3.6 and  $1.1 \text{ g m}^{-2}$ , respectively). A comparison with the estimates for other European cities showed that the total pollutant (combining  $CO$ ,  $O_3$ ,  $NO_2$ ,  $SO_2$ , and  $PM_{2.5}$ ) removal rate, which was  $5.3 \text{ g m}^{-2}$  of tree cover per year, was similar to that for the city of Strasbourg ( $5.1 \text{ g m}^{-2}$ ) (Selmi et al. 2016) but lower than that for London ( $8.7 \text{ g m}^{-2}$ ) (Kenton Rogers et al. 2015). The simulated  $PM_{2.5}$  removal rate for the park ( $0.25 \text{ g m}^{-2}$ ) was of the same magnitude as that determined for U.S. cities ( $0.25 \text{ g m}^{-2}$ ) (Nowak et al. 2013), but the total removal rate (considering  $PM_{2.5}$  instead of  $PM_{10}$ ) was lower than the average value calculated for the U.S. cities ( $7.5 \text{ g m}^{-2}$ ) (Nowak et al. 2006).

The total LA in the “genus-specific” simulation was approximately 5% lower than that in the “species-specific” simulation, which slightly reduced pollution removal. This reflects the similarity between species- and genus-based parameters, exhibiting the almost linear scaling of LA and deposition in i-Tree Eco. The differences are more comprehensively expressed with BVOC emissions that are higher for isoprene (+10%) and lower for monoterpene (−7%) using only genus-specific parameterization. This highlights the additional influence of species-specific conversion factors between LA and leaf biomass.

However, there were no differences between the two simulations concerning carbon sequestration because it is based on a fixed diameter growth rate and allometric equations from the literature that are used to calculate biomass change from the dimensional change (Nowak 1994; Nowak et al. 2002). Such allometric equations are usually derived from forest trees and, although they have been adjusted for urban conditions, they might not exactly reflect the actual tree forms and wood density. For example, various investigations show that high ozone concentration can cause a reduction in the root/shoot ratios of trees (Grantz et al. 2006), especially for deciduous species (Landolt et al. 2000).

This approach might be improved by introducing a dependency on climate and soil type, particularly by encompassing drought stress events (Moser et al. 2016) and other stress factors that might depend on the degree of air pollution or salt application. Pretzsch et al. (2017) showed that the urban trees in Europe have accelerated their growth since 1960 because of the effects of climate change, with considerable differences in different climate regions. Currently, the i-Tree Eco model only considers the limited number of frost-free days but representing the growth demands the introduction of direct sensitivity to temperature, competition, and possibly other factors that will vary from those of the city of interest. In addition, wood density and growth form might require parameterization that is regionally adapted to European species (McHale et al. 2009; Russo et al. 2014).

The dominant species parameterization assumes all deciduous trees (99.4% of total population) to be Norway maple (*A. platanoides*) and uses the parameters of spruce (*P. abies*) for all the evergreen trees (0.6%). Although the effects were found to strongly depend on the species composition and the dominant species used for representation, the results showed that tree species misclassification particularly affects BVOC emission estimates. Additionally, important information concerning LA and related air pollution reduction rates was derived. The effect of parameterization on emissions was expressed because emissions factors change strongly between species. For example, high monoterpene emissions resulted from *A. platanoides*—a dominant species having one of the highest monoterpene emission factors (1.6) of all species in the inventory (0.6 for *Fagus*, 0.1 for *Fraxinus*, and 0 for *Tilia*). In contrast, maples had a considerably lower isoprene emission factor (0.1) compared to that of a number of species that were neglected in the dominant species runs, reducing the overall emission estimate for this compound. For example, *Quercus robur*, *Robinia pseudoacacia*, *Platanus × Acerifolia*, and *Salix alba* were all assumed to be high isoprene emitters (with emission factor equal to 70) (Nowak et al. 2002).

However, it is worth noting that emission parameters are uncertain. For subtropical street trees, Dunn-Johnston et al. (2016) showed that a considerable difference exists between species-derived isoprene emission rates and those assumed (genus-specific emission rates) in i-Tree Eco. Additionally, the potential effects of air pollution (Ghirardo et al. 2016) or drought (Grote et al. 2009; Bourtsoukidis et al. 2014), which might increase or decrease emissions, have been neglected. Since emissions are supposed to trigger aerosol production and ozone formation (Derwent et al. 1996), these deficits may

need consideration in order to be appropriately used in combination with regional air chemistry and climate models (Cabaraban et al. 2013).

Another form of influential information is the determination of competition, which represents the light that an individual tree is able to utilize during photosynthesis. Neglecting an individual CLE determination (CLE average) can strongly affect LA and thus pollution reduction (except for CO), carbon sequestration, and BVOC emissions. The intensity of this effect depended on the degree to which tree size and position differed from a homogeneous distribution with medium tree distances. Free-standing trees requiring more sunlight are therefore underrepresented in terms of LA and growth when only using average CLE determination (McPherson and Peper 2012). Since Englischer Garten is characterized by many open spaces and areas where trees are found to clump together, the divergence from the mean conditions is relatively large. However, this is not an exception, since parks are often characterized by a complex tree distribution pattern in order to optimize recreational activities. Therefore, the structure of the Englischer Garten is representative for urban forests highlighting the significance of considering individual crown exposure to properly evaluate ecosystem services. Finally, the new automated method to calculate CLE in the light of new advances in tree classification from remote sensing data (Fassnacht et al. 2016) allows to considerably increase the time and accuracy of the urban forests assessments which are time-consuming and required trained people (Nowak et al. 2008b).

## 5.2. Effect of tree species properties and weather conditions on PM removal

The  $PM_{2.5}$ -deposition difference for leaves from conifers and broadleaf trees that has been obtained from the model is quite similar to that reported by Chen et al. (2017), who found an accumulation of particles on conifers that was up to six times the amount of that on broadleaf trees measured in summer through autumn (with no distinction between evergreen and deciduous broadleaves). This result is related to leaf size, with smaller leaves being more effective per  $m^2$  leaf surface (Weerakkody et al. 2018) and surface properties such as the occurrence of waxes, which are prominent in conifers, increasing the deposition capacity due to their lipophilic properties that are able to bind particles composed of organic pollutants (Dzierzanowski et al. 2011).

Furthermore, their crown shape, as cone-shaped conifers are commonly more exposed to turbulent air movements than spherical broadleaved trees and narrow conifer needles are more efficient capturing particles compared to flat leaves as expressed by the Stoke number, which describes the ability of stopping a particle in dependence on the specific foliage traits of conifers vs. broadleaved (Beckett et al. 2000).

Other leaf characteristics that affect deposition and that are specific to species rather than to coarsely lumped tree types include in particular surface roughness and trichomes (Sæbø et al. 2012; Räsänen et al. 2013; Chen et al. 2017; Muhammad et al. 2019). This is the most important reason for the large

variation that can be found in the literature regarding leaf deposition. Chen et al. (2017) indicate that the accumulated  $\text{PM}_{2.5}$  for conifers is in the range of 10–30  $\mu\text{g cm}^{-2}$  and for broadleaf trees it is 3–17  $\mu\text{g cm}^{-2}$ . Similar values are also found for the broadleaf-evergreen Holm oak (*Quercus ilex* L.) (Sgrigna et al. 2015), which accumulated 4, 13, and 2  $\mu\text{g cm}^{-2}$  in January, August, and October, respectively.

The deposition of particles on tree leaves changes during the year because not only PM concentration but also weather conditions such as precipitation and wind speed affect the deposition and resuspension of particles on and from leaves (Mori et al. 2015). Thus, although the PM concentration is higher in all cities in the winter and autumn, the deposition does not always follow the same pattern. The models assume that sufficient rainfall resets the potential deposition storage to zero, and thus precipitation events are a precondition to enable particle removal over a prolonged period. For example, the effect dominated the simulations for the summer 2014 in Munich, as high precipitation continuously increased cumulative deposition. In contrast, long dry periods such as those that frequently occur in Rome lead to a high resuspension rate, decreasing the actual net PM removal.

Another aspect that needs to be considered is that wind speed and PM concentration are generally negatively correlated diurnally, which may even lead to a net emission during mid-day when wind speed is highest (Fig. 17). This highlights the importance of including more mechanistic processes into the PM removal calculation that account for species-specific and rainfall-intensity dependent variation. For example, it might be favorable to consider that rainfall intensities differ within a canopy, with upper-canopy layers wetted first and lower layers affected only after prolonged precipitation. For example, Xu et al. (2017) found that PM wash-off rates increase with cumulative rainfall up to a maximum amount of 12.5 mm of rain removing 51 to 70% of PM accumulation, with a small amount of particles still retained on the leaf surface. Also, the removal of deposited PM from leaves depends on species-specific properties, as trichomes, or rough surfaces hold PM much more tightly, requiring more water for washing off (Hofman et al. 2014; Blanusa et al. 2015; Xu et al. 2017).

### 5.3. Physiological effects on temperature mitigation and pollution uptake

The implemented and tested model allows to calculate heat mitigation in terms of energy reduction due to cooling and shading but also to consider the impact of drought stress on evaporation and the stomatal uptake. Environmental conditions include direct influences of local climate and indirect influences, particularly the soil water availability (Livesley et al. 2016). Increased drought can be expected to affect the plant properties and thus the ecosystem services that are related to water evaporation (cooling) and pollution uptake (Stratópoulos et al. 2019; Zhang et al. 2020).

The test simulations demonstrate that the energy reduction of urban trees is particularly high at midday on sunny and warm days due to the shading provided by tree crowns. The effectiveness of this process scales with LAI, crown depth, and width (Sanusi et al. 2017). For example, in a recent study in which a

thermal camera was used to determine the surface temperature change of asphalt, porphyry, and grass based on shading of different tree species, median average cooling values of 16.4, 12.9, and 8.5 °C were reported, respectively (Speak et al. 2020), which confirm the results of shading simulation (Pace et al. submitted).

The transpiration effect depends on the meteorological conditions (wind speed, vapor pressure deficit) and soil water availability (pervious or impervious surfaces) and represents on average 12% of the total energy reduction (15% at Bordeaux Platz and 9% at Pariser Platz). The differences between the investigated sites have highlighted the importance of considering impervious surfaces, which characterize the urban fabric, enhances the water runoff and reduces soil water infiltration (Wang et al. 2008). A limited water availability reduces the potential for evaporative cooling, in particular because of transpiration reduction (Gillner et al. 2015a). This effect might significantly affect the immediate environment. For example, the results of experimental studies showed that evaporative cooling alone contributes to an air temperature reduction up to 3° within the canopies (Rahman et al. 2017a, 2020a) and the canopy-to-air temperature difference depends on meteorological conditions, tree species and, urban site-specific characteristics (Meier and Scherer 2012).

The cooling effect by transpiration depends to a large extent on stomatal conductance (Tan et al. 2018) and our results are in agreement with measured values at midday on *Tilia europaea* in Sweden (0.1 – 0.2 mol m<sup>-2</sup> s<sup>-1</sup>) (Konarska et al. 2016). The energy loss due to tree transpiration for commonly planted species in Central Europe including *T. cordata* range between 0.059 and 0.075 kW m<sup>-2</sup> (Rötzer et al. 2019) which are similar to results in Bordeaux Platz.

The new model introduced in this thesis can capture the effect of drought on gaseous pollution uptake, as previously suggested by Wang et al. (2017). This may be of particular importance for future studies in Mediterranean cities characterized by climate with pronounced drought events; neglecting the effects of stomatal conductance may result in a significant overestimation of gaseous pollutant deposition (Morani et al. 2014). However, long periods of heat and drought exacerbated by the high percentage of sealed surfaces have also been recorded in cities at higher latitudes, which affected transpiration and reduced cooling (Gillner et al. 2015b; Rahman et al. 2017b). Furthermore, the gaseous pollution deposition also depends on species and considering a single deposition velocity, as currently used in the i-Tree Eco model, can produce uncertain estimates and does not allow to properly evaluate suitable plants for urban greenery.

## 6) Conclusions and Prospects

Trees and forests play an important role in improving the urban sustainability of cities ensuring essential ecosystem services for citizens. However, cities are also hot-spots of pollution and climate stressors indicated by the common ‘urban heat island’ effect. These stressors are going to increase in the future with ongoing climate change so that adaptation measures in particular to higher temperatures are urgently needed. Designing high-quality green spaces with nature-based solutions and in particular green infrastructure as parks, urban forests, tree-lined streets by selecting the appropriate species should and can improve the urban environment and contribute to the development of green cities.

Models are useful decision-support tools for city planning and to evaluate or optimize the impacts of urban greening but they need to be properly validated to provide accurate estimates. In fact, modeling ecosystem services of urban trees requires a species-specific consideration to accurately estimate the temperature mitigation effect as well as air quality impacts due to either BVOC emissions or pollution removal. The efficiency of these ecosystem services, however, depend on plant physiology, in particular leaf surface properties and stomatal conductance, which in turn is determined by local pollution as well as meteorological conditions such as the soil water content, wind speed and light exposure.

The current functions and parameters implemented in the i-Tree Eco model, the most commonly used model for environmental services in urban areas, do not adequately represent species-specific properties or plant physiology. For example, deposition velocity for gaseous pollutants and particles, which clearly depends on foliage properties is not differentiated. Furthermore, the model neglects the effect of drought stress on stomatal uptake assuming sufficient water availability or irrigation for the street and park trees even in dry summer periods. This is unreasonable for many regions and represents a major limitation for the application of the model in Mediterranean climates or for global warming scenarios.

In this thesis, model improvements have been suggested and tested that 1) improve the determination of environmental conditions of the individual trees so that physiological responses can be better considered, 2) encourage a better differentiation of parameterization between species or plant types, and 3) establish a consistent link between (gaseous) air pollution removal and temperature mitigation effects by introducing a model approach that links stomatal conductance to water supply.

Specifically, the work consists of an automated determination method to derive light competition for individual trees that allows to objectively determine the dimensions and leaf surface of urban trees and forests based on basic tree information such as that available from city or park management administration. Furthermore, the importance to account for basic leaf properties when calculating particle deposition has been demonstrated by model calculations in three European cities, Berlin, Munich and Rome. Based on these simulations, a differentiation of specific deposition velocity for conifers and broadleaved trees has been suggested. Finally, a new single-tree model coupled with a water balance routine has been introduced that is able to consistently calculate temperature mitigation



effects as well as the removal of various pollutants depending on environmental conditions. Species-specific responses can be considered by parameters that determine water use strategies as well as morphological and anatomical properties. The physiological basis of the model facilitates in particular the simultaneous and consistent consideration of cooling effects by transpiration, and uptake of gaseous pollutants taking into account the drought effect on stomatal conductance. The negative relationship between pollutant removal and drought is particularly important for tree species selection and management of urban greens in the light of global warming. Here, the model may be applied for example to determine the irrigation demand of urban trees given some targets for pollution removal and microclimate improvement.

This work, however, can only represent a step forward into the direction of a fully climate sensitive tool to evaluate various ecosystem services. Considerable potential for improving the suggested model exists in defining more parameters as species-specific properties, introducing climate sensitive processes such as phenology (bud burst, leaf shedding) or stomatal regulation in dependence on environment. In addition, also tree growth and thus carbon sequestration may be consistently described in dependence on carbon gain (that is also computed to estimate stomatal conduction) and allocation. Since urban trees are often different from their forest counterparts, an urban-tree-specific data base for parametrization of such processes would be highly useful. Considering that urban environments are also a stressful place for trees, it is also important to consider negative environmental impacts (soil sealing, drought, de-icing salt in winter, high pollution levels) on growth and physiology. In particular, the consideration of air pollution and drought-stress effects on gas exchange and foliage phenology (and eventually tree mortality) would principally enable the representation of important long-term feedbacks between environment and ecosystem service delivery. In the following paragraphs, some specific suggestions are presented that are derived from the investigation within the thesis.

Based on the investigated uncertainties related to the calculation of PM removal from the air, it can be deduced that it would be beneficial to consider species-specific deposition velocities, resuspension, and washing threshold that are defined from leaf characteristics. For example, the dependence of resuspension rates on wind speed might be possibly defined by various foliage traits such as trichome or wax abundance. Also, washing of deposited PM from leaves should principally depend on such leaf properties but may also be likely to depend on leaf distribution within a canopy since upper-canopy layers are wetted first while lower layers are only affected after prolonged precipitation. Considering a vertically distributed leaf area and thus a differentiation into fractions of leaves subjected to specific wind speeds would also increase the accuracy of deposition calculation.

A considerable part of this thesis aims to improve the mechanistic representation of stomatal conductance in order to better describe gaseous air pollution uptake. This enables also to consider a still neglected effect, namely the damages that these pollutants do to the physiological mechanisms of trees. In particular, the effects of ozone on stomata might be introduced, which are usually reflected by a short-

term stomatal closure (less conductance) and a long-term loss of the stomatal control (higher conductance) under high ozone concentrations. The introduction of such a feature would also provide the means for considering the potential positive effects of reduced ozone concentrations on the water balances. In addition, seasonal responses of trees, such as leaf shedding, xylem embolism, and higher root turnover or the death of trees might be introduced in response to pollution or drought stress. However, the stomatal conductance also interacts with particle deposition and the heavy particle absorption can affect the stomatal functionality. Finally, not only direct temperature effects but also changes in the air humidity might be simulated based on evaporation, which also improves the human thermal comfort and thus may add to the benefit of urban tree abundance.

Overall, the introduction of models that quantify ecosystem services based on physiologically-oriented models may in particular serve to select tree species best suited for specific environmental conditions. A model can find an appropriated species selection to maximize specific ecosystem services but cannot overall evaluate which ecosystems are most urgently needed or which mixture of ecosystem services is desired. Also, other services that cannot objectively be quantified such as beauty or suitability for insects, mammals or birds might play additional roles. For example, it may be desired to plant native trees together with exotic species in order to make the city environment unique or more biodiverse.

Consideration for species selection that can be guided by models are, however, manifold. In the past, the choice of species was mostly based on aesthetic, cultural or practical reasons such as the availability of plants in local nurseries or the survival rate of newly planted trees. As a result, tree species were often planted outside their climatic optimum range, possibly increasing their vulnerability under further climate changes. For this reason, the consideration of projected climate changes may be the first important aspect for the planning of future green areas. In particular, heat waves accompanied with severe drought conditions might increase and require the selection of drought-tolerant tree species.

Secondly, ecosystem services that can be quantified can be supplied by models in order to improve the basis for decisions. For example, if CO<sub>2</sub> sequestration should be maximized, species that combine rapid growth and longevity must be preferred. Fast-growing species initially fix larger amounts of carbon dioxide but can be more susceptible to environmental stresses that are usually more pronounced in urban than natural areas.

Another important issue is the amount of air pollution that the trees are able to remove, which requires to account for uptake capacity but also for phenological criteria. For example, high levels of particulate matter mainly occur in winter where only evergreen species provide foliage as deposition surface. Nevertheless, particle deposition is also strongly related to leaf characteristics (e.g. trichomes, waxes, roughness) and weather conditions (e.g. regular rainfall throughout the year better than long dry periods). For the uptake of gaseous pollutant such as ozone, it is additionally important to ensure an adequate light exposure of the canopy as well as a sufficient water supply to support photosynthesis and stomatal opening. Models that quantify this uptake need to consider that tree species can have different

water-use strategies (anisohydric vs. isohydric), which are suited to maximize stomatal uptake under either short- or long periods of drought.

Apart from pollution removal, temperature mitigation is arguably the most important quantifiable service of urban trees. In general, a higher leaf area that also promotes pollution deposition enhances the shading effect, indicating a double impact of the same property. For example, it is desirable to ensure a year-round canopy in Mediterranean cities by planting evergreen trees to mitigate high temperatures during autumn and to remove particulate matter from the air. However, the decrease of light during cooler periods in the year reverse the benefit of shading during winter in northern latitudes leading to a preference for deciduous species. In addition, cooling also appears by means of transpiration although this effect is usually more pronounced on a larger scale instead in the immediate environment. In order to have an optimized mitigation of the urban heat island effect, tree selection is therefore bound to the same criteria as indicated for the gaseous pollutant uptake.

Apart from climate changes, socio-economic developments might also impact the importance of specific ecosystem and thus the criteria for the selection of particular species. For example, an increase in electric mobility will significantly reduce  $\text{NO}_x$  emission and thus pollution concentration in urban areas. This not only reduces the need for species with high pollution removal but also demands for low BVOC emitters, since in a limited  $\text{NO}_x$  condition, BVOCs do increasingly promote  $\text{O}_3$  formation.

Overall, it is an established fact that urban green spaces provide many environmental benefits and will play a key role in ensuring and possibly enhancing the life quality in cities in the future. In this regard, urban forestry, which deals with the management of urban trees, is bound to consider biosphere-atmosphere interactions in particular to improve air quality and microclimate of urban areas. This can only be guided with adequate models that account for changing environmental conditions as well as for species-specific properties that can be used as decision criteria by urban planners. In this sense, the thesis will hopefully help to develop such models in order to provide this kind of support.

## Literature

- Baldocchi D (1994) An analytical solution for coupled leaf photosynthesis and stomatal conductance models. *Tree Physiol* 14:1069–1079 . doi: 10.1093/treephys/14.7-8-9.1069
- Baldocchi D (1988) A Multi-layer model for estimating sulfur dioxide deposition to a deciduous oak forest canopy. *Atmos Environ* 22:869–884 . doi: 10.1016/0004-6981(88)90264-8
- Baldocchi DD, Hicks BB, Camara P (1987) A canopy stomatal resistance model for gaseous deposition to vegetated surfaces. *Atmos Environ* 21:91–101 . doi: 10.1016/0004-6981(87)90274-5
- Baldwin JW, Dessy JB, Vecchi GA, Oppenheimer M (2019) Temporally Compound Heat Wave Events and Global Warming: An Emerging Hazard. *Earth's Futur* 7:411–427 . doi: 10.1029/2018EF000989
- Bechtold WA (2003) Crown position and light exposure classification - An alternative to field-assigned crown class. *North J Appl For* 20:154–160 . doi: 10.1093/njaf/20.4.154
- Beck I, Jochner S, Gilles S, et al (2013) High environmental ozone levels lead to enhanced allergenicity of birch pollen. *PLoS One* 8: . doi: 10.1371/journal.pone.0080147
- Beckett KP, Freer-Smith PH, Taylor G (1998) Urban woodlands: Their role in reducing the effects of particulate pollution. *Environ Pollut* 99:347–360 . doi: 10.1016/S0269-7491(98)00016-5
- Beckett KP, Freer-Smith PH, Taylor G (2000) Particulate pollution capture by urban trees: Effect of species and windspeed. *Glob Chang Biol* 6:995–1003 . doi: 10.1046/j.1365-2486.2000.00376.x
- Bidwell RGS, Fraser DE (1972) Carbon monoxide uptake and metabolism by leaves. *Can J Bot* 50:1435–1439 . doi: 10.1139/b72-174
- Blanusa T, Fantozzi F, Monaci F, Bargagli R (2015) Leaf trapping and retention of particles by holm oak and other common tree species in Mediterranean urban environments. *Urban For Urban Green* 14:1095–1101 . doi: 10.1016/j.ufug.2015.10.004
- Bourtsoukidis E, Kawaletz H, Radacki D, et al (2014) Impact of flooding and drought conditions on the emission of volatile organic compounds of *Quercus robur* and *Prunus serotina*. *Trees - Struct Funct* 28:193–204 . doi: 10.1007/s00468-013-0942-5
- Brilhante O, Klaas J (2018) Green city concept and a method to measure green city performance over time applied to fifty cities globally: Influence of GDP, population size and energy efficiency. *Sustain* 10: . doi: 10.3390/su10062031
- Brink E, Aalders T, Ádám D, et al (2016) Cascades of green: A review of ecosystem-based adaptation

- in urban areas. *Glob Environ Chang* 36:111–123 . doi: 10.1016/j.gloenvcha.2015.11.003
- Brune M (2016) Urban trees under climate change. Potential impacts of dry spells and heat waves in three German regions in the 2050s. Hamburg, Germany
- Brutsaert W (1982) *Evaporation into the atmosphere: theory, history, and applications*. D.Reidel, Hingham MA.
- Cabaraban MTI, Kroll CN, Hirabayashi S, Nowak DJ (2013) Modeling of air pollutant removal by dry deposition to urban trees using a WRF/CMAQ/i-Tree Eco coupled system. *Environ Pollut* 176:123–133 . doi: 10.1016/j.envpol.2013.01.006
- Cai M, Xin Z, Yu X (2017) Spatio-temporal variations in PM leaf deposition: A meta-analysis. *Environ Pollut* 231:207–218 . doi: 10.1016/j.envpol.2017.07.105
- Cairns MA, Brown S, Helmer EH, Baumgardner GA (1997) Root biomass allocation in the world's upland forests. *Oecologia* 111:1–11 . doi: 10.1007/s004420050201
- Calfapietra C, Cherubini L (2019) Green Infrastructure: Nature-Based Solutions for sustainable and resilient cities. *Urban For Urban Green* 37:1–2 . doi: 10.1016/j.ufug.2018.09.012
- Calfapietra C, Fares S, Manes F, et al (2013) Role of Biogenic Volatile Organic Compounds (BVOC) emitted by urban trees on ozone concentration in cities: A review. *Environ Pollut* 183:71–80 . doi: 10.1016/j.envpol.2013.03.012
- Camargo AP, Marin FR, Sentelhas PC, Picini AG (1999) Adjust of the Thornthwaite's method to estimate the potential evapotranspiration for arid and superhumid climates, based on daily temperature amplitude. *Bras Agrometeorol* 251–257
- Caneva G, Bartoli F, Zappitelli I, Savo V (2020) Street trees in italian cities: story, biodiversity and integration within the urban environment. *Rend Lincei Sci Fis e Nat*. doi: 10.1007/s12210-020-00907-9
- Cariñanos P, Adinolfi C, Díaz de la Guardia C, et al (2016) Characterization of Allergen Emission Sources in Urban Areas. *J Environ Qual* 45:244–252 . doi: 10.2134/jeq2015.02.0075
- Chen L, Liu C, Zhang L, et al (2017) Variation in Tree Species Ability to Capture and Retain Airborne Fine Particulate Matter (PM<sub>2.5</sub>). *Sci Rep* 7:1–11 . doi: 10.1038/s41598-017-03360-1
- Churkina G, Grote R, Butler TM, Lawrence M (2015) Natural selection? Picking the right trees for urban greening. *Environ Sci Policy* 47:12–17 . doi: 10.1016/j.envsci.2014.10.014
- Derwent RG, Jenkin ME, Saunders SM (1996) Photochemical ozone creation potentials for a large number of reactive hydrocarbons under European conditions. *Atmos Environ* 30:181–199 . doi: 10.1016/1352-2310(95)00303-G

- Dunn-Johnston KA, Kreuzwieser J, Hirabayashi S, et al (2016) Isoprene Emission Factors for Subtropical Street Trees for Regional Air Quality Modeling. *J Environ Qual* 45:234–243 . doi: 10.2134/jeq2015.01.0051
- Dzierzanowski K, Popek R, Gawrońska H, et al (2011) Deposition of particulate matter of different size fractions on leaf surfaces and in waxes of urban forest species. *Int J Phytoremediation* 13:1037–1046 . doi: 10.1080/15226514.2011.552929
- Endreny T, Santagata R, Perna A, et al (2017) Implementing and managing urban forests: A much needed conservation strategy to increase ecosystem services and urban wellbeing. *Ecol Modell* 360:328–335 . doi: 10.1016/j.ecolmodel.2017.07.016
- European Commission (2008) Directive 2008/50/Ec on Ambient Air Quality and Cleaner Air for Europe
- European Commission (2015) Towards an EU Research and Innovation policy agenda for Nature-Based Solutions & Re-Naturing Cities. Final Report of the Horizon 2020 Expert Group on “Nature-Based Solutions and Re-Naturing Cities” (full version)
- European Environment Agency (2018) Air quality in Europe — 2018 report
- European Environment Agency (2019) Air quality in Europe — 2019 report
- Farquhar GD, Caemmerer S Von, Berry J a. (1980) A biochemical model of photosynthesis CO<sub>2</sub> fixation in leaves of C<sub>3</sub> species. *Planta* 149:78–90
- Fassnacht FE, Latifi H, Stereńczak K, et al (2016) Review of studies on tree species classification from remotely sensed data. *Remote Sens Environ* 186:64–87 . doi: 10.1016/j.rse.2016.08.013
- Freer-Smith PH, El-Khatib AA, Taylor G (2004) Capture of Particulate Pollution by Trees: A Comparison of Species Typical of Semi-Arid Areas (*Ficus Nitida* and *Eucalyptus Globulus*) with European and North American Species. *Water Air Soil Pollut* 155:173–187 . doi: 10.1023/B:WATE.0000026521.99552.fd
- Geiger R (1959) *The Climate Near the Ground*. Harvard University Press, Cambridge
- Geron CD, Guenther AB, Pierce TE (1994) An improved model for estimating emissions of volatile organic compounds from forests in the eastern United States. *J Geophys Res*
- Ghirardo A, Xie J, Zheng X, et al (2016) Urban stress-induced biogenic VOC emissions and SOA-forming potentials in Beijing. *Atmos Chem Phys* 16:2901–2920 . doi: 10.5194/acp-16-2901-2016
- Gillner S, Korn S, Roloff A (2015a) Leaf-gas exchange of five tree species at urban street sites. *Arboric Urban For* 41:113–124

- Gillner S, Vogt J, Tharang A, et al (2015b) Role of street trees in mitigating effects of heat and drought at highly sealed urban sites. *Landsc Urban Plan* 143:33–42 . doi: 10.1016/j.landurbplan.2015.06.005
- Grantz DA, Gunn S, Vu HB (2006) O<sub>3</sub> impacts on plant development: A meta-analysis of root/shoot allocation and growth. *Plant, Cell Environ* 29:1193–1209 . doi: 10.1111/j.1365-3040.2006.01521.x
- Grote R (2019) Environmental impacts on biogenic emissions of volatile organic compounds (VOCs)
- Grote R, Lavoit AV, Rambal S, et al (2009) Modelling the drought impact on monoterpene fluxes from an evergreen Mediterranean forest canopy. *Oecologia* 160:213–223 . doi: 10.1007/s00442-009-1298-9
- Grote R, Samson R, Alonso R, et al (2016) Functional traits of urban trees: air pollution mitigation potential. *Front Ecol Environ* 14:543–550 . doi: 10.1002/fee.1426
- Guenther AB, Zimmerman PR, Harley PC, et al (1993) Isoprene and monoterpene emission rate variability: model evaluations and sensitivity analyses. *J Geophys Res* 98: . doi: 10.1029/93jd00527
- Guo Y, Gasparri A, Li S, et al (2018) Quantifying excess deaths related to heatwaves under climate change scenarios: A multicountry time series modelling study. *PLoS Med* 15:1–17 . doi: 10.1371/journal.pmed.1002629
- Hansen R, Olafsson AS, van der Jagt APN, et al (2019) Planning multifunctional green infrastructure for compact cities: What is the state of practice? *Ecol Indic* 96:99–110 . doi: 10.1016/j.ecolind.2017.09.042
- Harley PC, Thomas RB, Reynolds JF, Strain BR (1992) Modelling photosynthesis of cotton grown in elevated CO<sub>2</sub>. *Plant Cell Environ* 15:271–282 . doi: 10.1111/j.1365-3040.1992.tb00974.x
- Hicks BB, Saylor RD, Baker BD (2016) Dry deposition of particles to canopies-A look back and the road forward. *J Geophys Res* 121:14691–14707 . doi: 10.1002/2015JD024742
- Hirabayashi S (2012) i-Tree Eco Biogenic Emissions Model Descriptions. i-Tree, USDA For. Serv. 8
- Hirabayashi S, Kroll CN, Nowak DJ (2015) i-Tree Eco Dry Deposition Model Descriptions
- Hirabayashi S, Kroll CN, Nowak DJ (2011) Component-based development and sensitivity analyses of an air pollutant dry deposition model. *Environ Model Softw* 26:804–816 . doi: 10.1016/j.envsoft.2010.11.007
- Hofman J, Wuyts K, Van Wittenberghe S, Samson R (2014) On the temporal variation of leaf magnetic parameters: Seasonal accumulation of leaf-deposited and leaf-encapsulated particles of

- a roadside tree crown. *Sci Total Environ* 493:766–772 . doi: 10.1016/j.scitotenv.2014.06.074
- Hosker RP, Lindberg SE (1982) Review: Atmospheric deposition and plant assimilation of gases and particles. *Atmos Environ* 16:889–910 . doi: 10.1016/0004-6981(82)90175-5
- i-Tree (2020) i-Tree Eco: Application Overview. <https://www.itreetools.org/tools/i-tree-eco/i-tree-eco-overview>. Accessed 25 Apr 2020
- Janhäll S (2015) Review on urban vegetation and particle air pollution - Deposition and dispersion. *Atmos Environ* 105:130–137 . doi: 10.1016/j.atmosenv.2015.01.052
- Kenton Rogers, Sacre K, Goodenough J, Doick K (2015) Valuing London’s Urban Forest
- Konarska J, Uddling J, Holmer B, et al (2016) Transpiration of urban trees and its cooling effect in a high latitude city. *Int J Biometeorol* 60:159–172 . doi: 10.1007/s00484-015-1014-x
- Kramer JP (1983) Water relations of plants. Academic Press
- Landolt W, Bühlmann U, Bleuler P, Bucher JB (2000) Ozone exposure-response relationships for biomass and root/shoot ratio of beech (*Fagus sylvatica*), ash (*Fraxinus excelsior*), Norway spruce (*Picea abies*) and Scots pine (*Pinus sylvestris*). *Environ Pollut* 109:473–478 . doi: 10.1016/S0269-7491(00)00050-6
- Li C, Frolking S, Frolking TA (1992) A model of nitrous oxide evolution from soil driven by rainfall events: 2. Model applications. *J Geophys Res* 97:9777–9783 . doi: 10.1029/92jd00510
- Lin J, Kroll CN, Nowak DJ, Greenfield EJ (2019) A review of urban forest modeling: Implications for management and future research. *Urban For Urban Green* 43: . doi: 10.1016/j.ufug.2019.126366
- Livesley SJ, McPherson EG, Calfapietra C (2016) The Urban Forest and Ecosystem Services: Impacts on Urban Water, Heat, and Pollution Cycles at the Tree, Street, and City Scale. *J Environ Qual* 45:119–124 . doi: 10.2134/jeq2015.11.0567
- Loreto F (2002) Distribution of isoprenoid emitters in the *Quercus* genus around the world: Chemo-taxonomical implications and evolutionary considerations based on the ecological function of the trait. *Perspect Plant Ecol Evol Syst* 5:185–192 . doi: 10.1078/1433-8319-00033
- Lovett G (1994) Atmospheric Deposition of Nutrients and Pollutants in North America : An Ecological Perspective. *Ecol Appl* 4:629–650
- Lu S, Yang X, Li S, et al (2018) Effects of plant leaf surface and different pollution levels on PM2.5 adsorption capacity. *Urban For Urban Green* 34:64–70 . doi: 10.1016/j.ufug.2018.05.006
- Maes J, Egoh B, Willemsen L, et al (2012) Mapping ecosystem services for policy support and decision making in the European Union. *Ecosyst Serv* 1:31–39 . doi: 10.1016/j.ecoser.2012.06.004



- McHale MR, Burke IC, Lefsky MA, et al (2009) Urban forest biomass estimates: Is it important to use allometric relationships developed specifically for urban trees? *Urban Ecosyst* 12:95–113 . doi: 10.1007/s11252-009-0081-3
- McPherson EG, Peper PJ (2012) Urban tree growth modeling. *Arboric Urban For*
- Medrano H, Escalona JM, Bota J, et al (2002) Regulation of photosynthesis of C3 plants in response to progressive drought: Stomatal conductance as a reference parameter. *Ann Bot* 89:895–905 . doi: 10.1093/aob/mcf079
- Meier F, Scherer D (2012) Spatial and temporal variability of urban tree canopy temperature during summer 2010 in Berlin, Germany. *Theor Appl Climatol* 110:373–384 . doi: 10.1007/s00704-012-0631-0
- Monteith JL, Unsworth MH (2013) *Principles of Environmental Physics*, Fourth Edi. Academic Press
- Morani A, Nowak D, Hirabayashi S, et al (2014) Comparing i-Tree modeled ozone deposition with field measurements in a periurban Mediterranean forest. *Environ Pollut* 195:202–209 . doi: 10.1016/j.envpol.2014.08.031
- Mori J, Sæbø A, Hanslin HM, et al (2015) Deposition of traffic-related air pollutants on leaves of six evergreen shrub species during a Mediterranean summer season. *Urban For Urban Green* 14:264–273 . doi: 10.1016/j.ufug.2015.02.008
- Moser A, Rötzer T, Pauleit S, Pretzsch H (2016) The urban environment can modify drought stress of small-leaved lime (*Tilia cordata* Mill.) and black locust (*Robinia pseudoacacia* L.). *Forests* 7: . doi: 10.3390/f7030071
- Muhammad S, Wuyts K, Samson R (2019) Atmospheric net particle accumulation on 96 plant species with contrasting morphological and anatomical leaf characteristics in a common garden experiment. *Atmos Environ* 202:328–344 . doi: 10.1016/j.atmosenv.2019.01.015
- Nowak DJ (1996) Estimating leaf area and leaf biomass of open-grown deciduous urban trees. *For Sci* 42:504–507 . doi: 10.1093/forestscience/42.4.504
- Nowak DJ (1994) Atmospheric Carbon Dioxide Reduction by Chicago's urban forest. In: McPherson EG, Nowak DJ, Rowntree RA (eds) *Chicago's Urban Forest Ecosystem: Results of the Chicago Urban Forest Climate Project*. US Department of Agriculture, Forest Service, Northeastern Forest Experiment Station, Radnor, PA, USA, pp 83–94
- Nowak DJ, Crane DE (2002) Carbon storage and sequestration by urban trees in the USA. *Environ Pollut* 116:381–389 . doi: 10.1016/S0269-7491(01)00214-7
- Nowak DJ, Crane DE, Stevens JC (2006) Air pollution removal by urban trees and shrubs in the

- United States. *Urban For Urban Green* 4:115–123 . doi: 10.1016/j.ufug.2006.01.007
- Nowak DJ, Crane DE, Stevens JC, et al (2008a) A Ground-Based Method of Assessing Urban Forest Structure and Ecosystem Services. *Arboric Urban For* 34:347–358
- Nowak DJ, Crane DE, Stevens JC, Ibarra M (2002) Brooklyn' s Urban Forest
- Nowak DJ, Hirabayashi S, Bodine A, Greenfield E (2014) Tree and forest effects on air quality and human health in the United States. *Environ Pollut* 193:119–129 . doi: 10.1016/j.envpol.2014.05.028
- Nowak DJ, Hirabayashi S, Bodine A, Hoehn R (2013) Modeled PM<sub>2.5</sub> removal by trees in ten U.S. cities and associated health effects. *Environ Pollut* 178:395–402 . doi: 10.1016/j.envpol.2013.03.050
- Nowak DJ, Walton JT, Stevens JC, et al (2008b) Effect of plot and sample size on timing and precision of urban forest assessments. *Arboric Urban For* 34:386–390
- Oke TR (2002) *Boundary Layer Climates*
- Pace R (2019) La modellistica applicata agli alberi in ambiente urbano per ottimizzare la scelta della specie. *Arbor - Soc. Ital. di Arboric.*
- Pace R, Biber P, Pretzsch H, Grote R (2018) Modeling ecosystem services for park trees: Sensitivity of i-tree eco simulations to light exposure and tree species classification. *Forests* 9:1–18 . doi: 10.3390/f9020089
- Pace R, Churkina G (submitted) How green are European “Green Cities”? Insights on their environmental performance from a global perspective. *npj Urban Sustain*
- Pace R, Churkina G, Rivera M (2016) How green is a “ Green City ”? A review of existing indicators and approaches
- Pace R, De Fino F, Rahman MA, et al (submitted) A single tree model to consistently simulate cooling, shading, and pollution uptake of urban trees. *Int J Biometeorol*
- Pace R, Grote R (2020) Deposition and Resuspension Mechanisms Into and From Tree Canopies: A Study Modeling Particle Removal of Conifers and Broadleaves in Different Cities. *Front For Glob Chang* 3:26 . doi: 10.3389/ffgc.2020.00026
- Pederson JR, Massman WJ, Mahrt L, et al (1995) California ozone deposition experiment: Methods, results, and opportunities. *Atmos Environ* 29:3115–3132 . doi: 10.1016/1352-2310(95)00136-M
- Peper PJ, McPherson GE, Mori SM (2001a) Equations for predicting diameter, height, crown width, and leaf area of San Joaquin Valley street trees. *J Arboric* 27:306–317

- Peper PJ, McPherson GE, Mori SM (2001b) Predictive equations for dimensions and leaf area of coastal Southern California street trees. *J Arboric* 27:169–180
- Pereira AR, Pruitt WO (2004) Adaptation of the Thornthwaite scheme for estimating daily reference evapotranspiration. *Agric Water Manag* 66:251–257 . doi: 10.1016/j.agwat.2003.11.003
- Perkins SE, Alexander L V., Nairn JR (2012) Increasing frequency, intensity and duration of observed global heatwaves and warm spells. *Geophys Res Lett* 39:1–5 . doi: 10.1029/2012GL053361
- Poelman H (2018) A walk to the park? Assessing access to green areas in Europe’s cities. Update using completed Copernicus Urban Atlas data
- Pretzsch H, Biber P, Ďurský J (2002) The single tree-based stand simulator SILVA: construction, application and evaluation. *For Ecol Manage* 162:3–21 . doi: [https://doi.org/10.1016/S0378-1127\(02\)00047-6](https://doi.org/10.1016/S0378-1127(02)00047-6)
- Pretzsch H, Biber P, Uhl E, et al (2017) Climate change accelerates growth of urban trees in metropolises worldwide. *Sci Rep* 7:15403 . doi: 10.1038/s41598-017-14831-w
- Pullman MR (2009) Conifer PM2.5 deposition and re-suspension in wind and rain events. Cornell University, Ithaca, NY, United States.
- Rahman MA, Hartmann C, Moser-Reischl A, et al (2020a) Tree cooling effects and human thermal comfort under contrasting species and sites. *Agric For Meteorol* 287:107947 . doi: 10.1016/j.agrformet.2020.107947
- Rahman MA, Moser A, Gold A, et al (2018) Vertical air temperature gradients under the shade of two contrasting urban tree species during different types of summer days. *Sci Total Environ* 633:100–111 . doi: 10.1016/j.scitotenv.2018.03.168
- Rahman MA, Moser A, Rötzer T, Pauleit S (2017a) Within canopy temperature differences and cooling ability of *Tilia cordata* trees grown in urban conditions. *Build Environ* 114:118–128 . doi: 10.1016/j.buildenv.2016.12.013
- Rahman MA, Moser A, Rötzer T, Pauleit S (2017b) Microclimatic differences and their influence on transpirational cooling of *Tilia cordata* in two contrasting street canyons in Munich, Germany. *Agric For Meteorol* 232:443–456 . doi: 10.1016/j.agrformet.2016.10.006
- Rahman MA, Stratopoulos LMF, Moser-Reischl A, et al (2020b) Traits of trees for cooling urban heat islands: A meta-analysis. *Build Environ* 170: . doi: 10.1016/j.buildenv.2019.106606
- Räsänen J V., Holopainen T, Joutsensaari J, et al (2013) Effects of species-specific leaf characteristics and reduced water availability on fine particle capture efficiency of trees. *Environ Pollut* 183:64–70 . doi: 10.1016/j.envpol.2013.05.015

- Robine JM, Cheung SLK, Le Roy S, et al (2008) Death toll exceeded 70,000 in Europe during the summer of 2003. *Comptes Rendus - Biol* 331:171–178 . doi: 10.1016/j.crv.2007.12.001
- Rossiter DG (2007) Classification of urban and industrial soils in the World Reference Base for Soil Resources. *J Soils Sediments* 7:96–100 . doi: 10.1065/jss2007.02.208
- Rötzer T, Rahman MA, Moser-Reischl A, et al (2019) Process based simulation of tree growth and ecosystem services of urban trees under present and future climate conditions. *Sci Total Environ* 676:651–664 . doi: 10.1016/j.scitotenv.2019.04.235
- Russo A, Escobedo FJ, Timilsina N, et al (2014) Assessing urban tree carbon storage and sequestration in Bolzano, Italy. *Int J Biodivers Sci Ecosyst Serv Manag* 10:54–70 . doi: 10.1080/21513732.2013.873822
- Sæbø A, Popek R, Nawrot B, et al (2012) Plant species differences in particulate matter accumulation on leaf surfaces. *Sci Total Environ* 427–428:347–354 . doi: 10.1016/j.scitotenv.2012.03.084
- Sanusi R, Johnstone D, May P, Livesley SJ (2017) Microclimate benefits that different street tree species provide to sidewalk pedestrians relate to differences in Plant Area Index. *Landsc Urban Plan* 157:502–511 . doi: 10.1016/j.landurbplan.2016.08.010
- Schaubroeck T, Deckmyn G, Neiryneck J, et al (2014) Multilayered modeling of particulate matter removal by a growing forest over time, from plant surface deposition to washoff via rainfall. *Environ Sci Technol* 48:10785–10794 . doi: 10.1021/es5019724
- Selmi W, Weber C, Rivière E, et al (2016) Air pollution removal by trees in public green spaces in Strasbourg city, France. *Urban For Urban Green* 17:192–201 . doi: 10.1016/j.ufug.2016.04.010
- Sgrigna G, Sæbø A, Gawronski S, et al (2015) Particulate Matter deposition on *Quercus ilex* leaves in an industrial city of central Italy. *Environ Pollut* 197:187–194 . doi: 10.1016/j.envpol.2014.11.030
- Shao F, Wang L, Sun F, et al (2019) Study on different particulate matter retention capacities of the leaf surfaces of eight common garden plants in Hangzhou, China. *Sci Total Environ* 652:939–951 . doi: 10.1016/j.scitotenv.2018.10.182
- Solaimanian M, Kennedy TW (1993) Predicting Maximum Pavement Surface Temperature Using Maximum Air Temperature and Hourly Solar Radiation. *Transp Res Rec* 1–11
- Speak A, Montagnani L, Wellstein C, Zerbe S (2020) The influence of tree traits on urban ground surface shade cooling. *Landsc Urban Plan* 197: . doi: 10.1016/j.landurbplan.2020.103748
- Spitters CJT, Toussaint HAJM, Goudriaan J (1986) Separating the diffuse and direct component of global radiation and its implications for modeling canopy photosynthesis Part I. Components of

- incoming radiation. *Agric For Meteorol* 38:217–229 . doi: 10.1016/0168-1923(86)90060-2
- Stratópoulos LMF, Zhang C, Häberle KH, et al (2019) Effects of drought on the phenology, growth, and morphological development of three urban tree species and cultivars. *Sustain* 11:1–15 . doi: 10.3390/su11185117
- Tan PY, Wong NH, Tan CL, et al (2018) A method to partition the relative effects of evaporative cooling and shading on air temperature within vegetation canopy. *J Urban Ecol* 4:1–11 . doi: 10.1093/jue/juy012
- Taylor GE, Hanson PJ, Baldocchi DD (1988) Pollutant deposition to individual leaves and plant canopies: sites of regulation and relationship to injury. *Assess Crop loss from air Pollut* 227–257 . doi: 10.1007/978-94-009-1367-7\_11
- Thornthwaite CW, Mather JR (1957) Instructions and tables for computing potential evapotranspiration and the water balance. *Publ Climatol* 183–311
- Tigges J, Churkina G, Lakes T (2017) Modeling above-ground carbon storage: a remote sensing approach to derive individual tree species information in urban settings. *Urban Ecosyst* 20:97–111 . doi: 10.1007/s11252-016-0585-6
- Tiwari S, Grote R, Churkina G, Butler T (2016) Ozone damage, detoxification and the role of isoprenoids-new impetus for integrated models. *Funct Plant Biol* 43:324–336 . doi: 10.1071/FP15302
- TUM (2016) Trees Transpire for a Cool City. <https://www.tum.de/nc/en/about-tum/news/press-releases/details/33394/>
- UN-Habitat (2016) Urbanization and development: emerging futures. World cities report 2016. United Nations Human Settlements Programme, Nairobi
- United Nations (2014) World Urbanization Prospects: The 2014 Revision, Highlights (ST/ESA/SER.A/352)
- Wang J, Endreny TA, Nowak DJ (2008) Mechanistic simulation of tree effects in an urban water balance model. *J Am Water Resour Assoc* 44:75–85 . doi: 10.1111/j.1752-1688.2007.00139.x
- Wang L, Gong H, Liao W, Wang Z (2015) Accumulation of particles on the surface of leaves during leaf expansion. *Sci Total Environ* 532:420–434 . doi: 10.1016/j.scitotenv.2015.06.014
- Wang Y, Xie Y, Dong W, et al (2017) Adverse effects of increasing drought on air quality via natural processes. *Atmos Chem Phys* 17:12827–12843 . doi: 10.5194/acp-17-12827-2017
- Watts N, Amann M, Arnell N, et al (2019) The 2019 report of The Lancet Countdown on health and climate change: ensuring that the health of a child born today is not defined by a changing

- climate. *Lancet* 394:1836–1878 . doi: 10.1016/S0140-6736(19)32596-6
- Weerakkody U, Dover JW, Mitchell P, Reiling K (2018) Quantification of the traffic-generated particulate matter capture by plant species in a living wall and evaluation of the important leaf characteristics. *Sci Total Environ* 635:1012–1024 . doi: 10.1016/j.scitotenv.2018.04.106
- Wesley ML (1989) Parameterization of Surface Resistances to Gaseous Dry Deposition in Regional-Scale Numerical Models. *Atmos Environ* 23:1293–1304 . doi: 10.1016/S0950-351X(05)80241-1
- Wilby RL (2003) Past and projected trends in London's Urban heat island. *Weather* 58:251–260 . doi: 10.1256/wea.183.02
- World Health Organization (2013) Health Effects of Particulate Matter. Policy Implications for Countries in Eastern Europe, Caucasus and Central Asia. World Health Organization, Regional Office for Europe, Copenhagen
- World Health Organization (2016) Ambient air pollution: A global assessment of exposure and burden of disease
- Xu X, Zhang Z, Bao L, et al (2017) Influence of rainfall duration and intensity on particulate matter removal from plant leaves. *Sci Total Environ* 609:11–16 . doi: 10.1016/j.scitotenv.2017.07.141
- Zhang C, Stratópoulos LMF, Xu C, et al (2020) Article Development of fine root biomass of two contrasting urban tree cultivars in response to drought stress. *Forests* 11:1–14 . doi: 10.3390/f11010108
- Zhang W, Wang B, Niu X (2017) Relationship between leaf surface characteristics and particle capturing capacities of different tree species in Beijing. *Forests* 8:1–12 . doi: 10.3390/f8030092
- Zölch T, Maderspacher J, Wamsler C, Pauleit S (2016) Using green infrastructure for urban climate-proofing: An evaluation of heat mitigation measures at the micro-scale. *Urban For Urban Green* 20:305–316 . doi: 10.1016/j.ufug.2016.09.011

## Contributions and other publications

### - Journal papers:

Pace, R., Churkina, G., Rivera, M., (2016) How green is a “Green City”? A review of existing indicators and approaches, IASS Working Paper. <https://doi.org/10.2312/iass.2016.035>

Pace, R., (2019) La modellistica applicata agli alberi in ambiente urbano per ottimizzare la scelta della specie. *Arbor - Soc. Ital. di Arboric.*

Pace, R., Liberati, D., Sconocchia, P., De Angelis, P., (2019) Lead transfer into the vegetation layer growing naturally in a Pb-contaminated site. *Environ. Geochem. Health* 1–9. <https://doi.org/10.1007/s10653-019-00429-w>

Zhang, J., Ghirardo, A., Gori, A., Albert, A., Buegger, F., Pace, R., Georgii, E., Grote, R., Schnitzler, J.-P., Durner, J., Lindermayr, C. (2020) Improving air quality by nitric oxide consumption of climate-resilient trees suitable for urban greening. *Front. Plant Sci.* <https://doi.org/10.3389/fpls.2020.549913>

### - Conferences:

Pace, R., Guidolotti, G., Baldacchini, C., Calfapietra, C. (2019) Comparing the modeled deposition of PM<sub>2.5</sub> with the eddy covariance flux and SEM analysis of an urban forest in Naples. *La scienza utile per le foreste: ricerca e trasferimento. XII Congresso Nazionale SISEF, Palermo (Italy), 12-15 Nov 2019. [oral presentation]*

Amini, S., Gaglio, M., Pace, R., Muresan, A.N., Grote, R., Fano, E.A. (2019) Modelling the performances of different tree species to remove PM<sub>2.5</sub> from the air. *XXIX Congresso Società Italiana di Ecologia (SItE), Ferrara (Italy), 10-12 Sept 2019. [poster]*

Pace, R., De Fino, F., Rahman, M.A., Pauleit, S., Nowak, D., Grote, R. (2019) Temperature mitigation by urban trees: Modelling the cooling effect of transpiration and shading on a single tree basis. *European Forum on Urban Forestry 2019. Cologne (Germany), 22-24 May 2019. [poster]*

Pace, R., De Fino, F., Grote, R. (2018) How ecosystem services provided by urban green spaces change according to new city planning strategies? The case study of Berlin. *World Forum on Urban Forests. Mantova (Italy), 27 Nov - 1 Dec 2018. [oral presentation]*

Pace, R., Grote, R. (2018) Evaluierung des i-Tree Eco Modells zur Bestimmung von Ökosystemdienstleistungen von Stadtbäumen. *FOWITA 2018 - Forstwissenschaftlichen Tagung, Göttingen (Germany), 24-27 Sept 2018. [oral presentation]*

Pace, R., Pretzsch, H., Grote, R. (2018) Influence of park stand structure on ecosystem services modeling. European Forum on Urban Forestry 2018, Helsinki and Vantaa (Finland), 15-19 May 2018. [oral presentation]

Pace, R., Grote, R., Calfapietra, C. (2017) Are current models reliable in assessing ecosystem services provided by urban forests in the Mediterranean climate? La foresta che cambia: ricerca, qualità della vita e opportunità. XI SISEF National Congress, Rome (Italy) 10-13 Sept 2017. [short oral presentation]

Pace, R., Liberati, D., Sconocchia, P., De Angelis, P. (2017) Pb distribution within vertical and horizontal mixed vegetation layers growing in a lead contaminated site. Green infrastructure: nature based solutions for sustainable and resilient cities, Orvieto (Italy), 4-7 April 2017. [oral presentation]

Grote, R., Pace, R. (2017) Are air quality related ecosystem services of European tree species adequately represented in current models? Green infrastructure: nature based solutions for sustainable and resilient cities, Orvieto (Italy), 4-7 April 2017. [oral presentation]

Pace, R., Churkina, G., Rivera, M., Grote, R. (2017) How green is a “Green City”? A review of existing indicators and approaches. Green infrastructure: nature based solutions for sustainable and resilient cities, Orvieto, 4-7 April 2017. [poster]



# Curriculum vitae



## Eidesstattliche Erklärung

Ich erkläre an Eides statt, dass ich die bei der promotionsführenden Einrichtung  
Wissenschaftszentrum Weihenstephan für Ernährung, Landnutzung und Umwelt

der TUM zur Promotionsprüfung vorgelegte Arbeit mit dem Titel:

Modeling ecosystem services of urban trees to improve air quality and microclimate

in Lehrstuhl für Waldwachstumskunde

Fakultät, Institut, Lehrstuhl, Klinik, Krankenhaus, Abteilung

unter der Anleitung und Betreuung durch: Prof. Dr. Dr. Hans Pretzsch ohne sonstige Hilfe erstellt und bei der Abfassung nur die gemäß § 6 Ab. 6 und 7 Satz 2 angebotenen Hilfsmittel benutzt habe.

Ich habe keine Organisation eingeschaltet, die gegen Entgelt Betreuerinnen und Betreuer für die Anfertigung von Dissertationen sucht, oder die mir obliegenden Pflichten hinsichtlich der Prüfungsleistungen für mich ganz oder teilweise erledigt.

Ich habe die Dissertation in dieser oder ähnlicher Form in keinem anderen Prüfungsverfahren als Prüfungsleistung vorgelegt.

Die vollständige Dissertation wurde in \_\_\_\_\_ veröffentlicht. Die promotionsführende Einrichtung

\_\_\_\_\_ hat der Veröffentlichung zugestimmt.

Ich habe den angestrebten Doktorgrad noch nicht erworben und bin nicht in einem früheren Promotionsverfahren für den angestrebten Doktorgrad endgültig gescheitert.

Ich habe bereits am \_\_\_\_\_ bei der Fakultät für \_\_\_\_\_ der Hochschule \_\_\_\_\_ unter Vorlage einer Dissertation mit dem Thema \_\_\_\_\_ die Zulassung zur Promotion beantragt mit dem Ergebnis: \_\_\_\_\_

Die öffentlich zugängliche Promotionsordnung der TUM ist mir bekannt, insbesondere habe ich die Bedeutung von § 28 (Nichtigkeit der Promotion) und § 29 (Entzug des Doktorgrades) zur Kenntnis genommen. Ich bin mir der Konsequenzen einer falschen Eidesstattlichen Erklärung bewusst.

Mit der Aufnahme meiner personenbezogenen Daten in die Alumni-Datei bei der TUM bin ich

einverstanden,  nicht einverstanden.

Bozen, 08-06-2020,

*Rocco Pak*

Ort, Datum, Unterschrift

## Appendix

### Published Articles and Manuscripts

#### 1. Paper I

Pace, R.; Biber, P.; Pretzsch, H.; Grote, R. (2018): Modeling Ecosystem Services for Park Trees: Sensitivity of i-Tree Eco Simulations to Light Exposure and Tree Species Classification. *Forests* 9 (2): 89-106, 10.3390/f9020089.

© [2018] *Forests* MDPI. Reprinted with permission of open access license.



Article

# Modeling Ecosystem Services for Park Trees: Sensitivity of i-Tree Eco Simulations to Light Exposure and Tree Species Classification

Rocco Pace <sup>1</sup> , Peter Biber <sup>2</sup> , Hans Pretzsch <sup>2</sup> and Rüdiger Grote <sup>1,\*</sup>

<sup>1</sup> Karlsruhe Institute of Technology (KIT), Institute of Meteorology and Climate Research, Atmospheric Environmental Research (IMK-IFU), Kreuzteckbahnstraße 19, 82467 Garmisch-Partenkirchen, Germany; rocco.pace@kit.edu

<sup>2</sup> Chair for Forest Growth and Yield Science, Faculty of Forest Science and Resource Management, Technical University of Munich, Hans-Carl-von-Carlowitz-Platz 2, 85354 Freising, Germany; peter.biber@lrz.tu-muenchen.de (P.B.); hans.pretzsch@lrz.tu-muenchen.de (H.P.)

\* Correspondence: ruediger.grote@kit.edu

Received: 18 January 2018; Accepted: 10 February 2018; Published: 13 February 2018

**Abstract:** Ecosystem modeling can help decision making regarding planting of urban trees for climate change mitigation and air pollution reduction. Algorithms and models that link the properties of plant functional types, species groups, or single species to their impact on specific ecosystem services have been developed. However, these models require a considerable effort for initialization that is inherently related to uncertainties originating from the high diversity of plant species in urban areas. We therefore suggest a new automated method to be used with the i-Tree Eco model to derive light competition for individual trees and investigate the importance of this property. Since competition depends also on the species, which is difficult to determine from increasingly used remote sensing methodologies, we also investigate the impact of uncertain tree species classification on the ecosystem services by comparing a species-specific inventory determined by field observation with a genus-specific categorization and a model initialization for the dominant deciduous and evergreen species only. Our results show how the simulation of competition affects the determination of carbon sequestration, leaf area, and related ecosystem services and that the proposed method provides a tool for improving estimations. Misclassifications of tree species can lead to large deviations in estimates of ecosystem impacts, particularly concerning biogenic volatile compound emissions. In our test case, monoterpene emissions almost doubled and isoprene emissions decreased to less than 10% when species were estimated to belong only to either two groups instead of being determined by species or genus. It is discussed that this uncertainty of emission estimates propagates further uncertainty in the estimation of potential ozone formation. Overall, we show the importance of using an individual light competition approach and explicitly parameterizing all ecosystem functions at the species-specific level.

**Keywords:** air pollution removal; BVOC emission; carbon sequestration; tree competition; urban forest

## 1. Introduction

Population growth, climate change, and high and increasing air pollution levels are known to pose risks to health and safety in cities [1]. Therefore, sustainable urban planning is necessary to improve the quality of life and preserve the integrity of natural ecosystems [2]. Urban forests and trees can significantly contribute to mitigating climate change effects and improving air quality in residential areas [3]. Pollution caused by tree removal in cities considerably depends on the species

and their properties [4]. For this reason, species selection is important to achieve optimal results of city greening [5]. To find the most suitable trees or tree mixture, ecosystem services models can be particularly useful as decision-support tools for city planning [6,7].

The i-Tree Eco model is an ecosystem service model for urban trees developed by the US Department of Agriculture (USDA) Forest Service for application in the U.S., and it has been adopted by the U.K., Australia, and Canada [8,9]. The model is widely used to evaluate urban vegetation-induced environmental services [10–12], e.g., carbon storage and sequestration, air pollution reduction, and water runoff reduction, the effects of trees on energy consumed by buildings, and some disservices, such as the emission of biogenic volatile organic compounds (BVOCs).

The i-Tree Eco requires information concerning the species and the stem diameter at breast height (DBH) as the input data. Additional data, including land use criteria, total tree height, crown size (height to live top, height to the crown base, crown width, and percentage of crown missing), crown health (dieback or condition), and competition status, can improve the model accuracy. Most of these input data are usually determined in the field by explicit visual inventories. This determination method is relatively easy to learn but remains subjective and prone to errors. For large areas, sample plots are required to be investigated and scaled to the whole region, leading to considerable uncertainties when the species distribution is non-homogeneous [13]. In addition, the efforts involved in defining the sample plots, educating the field researchers, and applying the inventory requires more time and money [14] compared to the case wherein the i-Tree Eco protocol, which refers to the data available from remote sensing or GIS, is used. The latter facilitates the assessment of pollution reduction in cities using the input of leaf area index (LAI) as a structural characteristic [15–18]. However, it is worth noting that in many cases, urban forest inventories are unsuitable for deriving all the required parameters, e.g., crown light exposure (CLE), making the use of default model parameterization for many tree properties more appealing.

Species characterization data is important for i-Tree Eco initialization because these data define the basic parameters used for calculating all ecosystem services and disservices (e.g., leaf area (LA), leaf biomass, allometric equations, BVOCs emission rates). If the species information is not available, the i-Tree Eco model uses values that are defined by the genus, family, or type (evergreen/deciduous). This may be particularly problematic if the model is applied to regions other than the U.S., for which the parameters were designed. Another important characterization is the degree of competition that a tree experiences. This is expressed as “CLE” in the i-Tree Eco model based on a visual estimate according to Bechtold (2003) [19]. Because this parameter is evaluated by educated investigators, it is expensive and remains subjective. The default value for the competition is differentiated into street trees and trees within urban parks and forests but is independent of size or closeness to neighbors. Hence, it is desirable to define i-Tree Eco initialization for species, size, and composition of each tree using cost-effective and objective methods, particularly when large areas are concerned.

A promising approach to achieve an automated initialization is the application of remote sensing methods, which has been attempted in recent investigations [15,20–22]. However, because of the complexity associated with urban areas (e.g., high spectral similarity of vegetation types or overlooked small trees in high-density stands), initializations using remote sensing data have an inevitable degree of uncertainty concerning species differentiation [23]. Additionally, it should be considered that most urban trees are deciduous [4,24]. This creates difficulties in species distinction because the photogrammetric interpretation of aerial photographs generally allows only the separation of evergreen from deciduous trees, particularly when the plant species diversity is as high as that in the urban context [25]. Furthermore, although tree position and size can be reasonably well determined, automatic information on light competition between trees is not provided by these approaches [26,27].

The actual competition between trees has been estimated using multiple approaches. These estimations include the influence zone of each tree and the degree and nature of interaction [28]; a competition algorithm based on light intensity [29]; the “moving average autoregression” method to assess the spatial dependence attributable to the competition and micro-site influences [30]; and the

calculation of the inter-tree competition between each tree based on the position, height, and crown size of a tree and its competitors [31]. The aforementioned methods provide objective measures because they are based on tree position and size, i.e., the remote sensing data.

Herein, we propose a methodology to derive competition data from dimensional tree information and investigate uncertainties inherent in i-Tree Eco model applications related to species determination. Therefore, we apply the model to Englischer Garten—a large urban park in Munich, Germany—where detailed inventory data are available, to assess how the estimates of ecosystem services and disservices change when we gradually decrease the degree of initialization detail. In particular, we hypothesized that accurate species information is crucial for determining several ecosystem processes and functions.

## 2. Materials and Methods

### 2.1. Site Description and Model Inputs

In this study, we analyzed the south of “Englischer Garten”, a 330-ha park located in Munich, Germany (Figure 1). The site is mainly comprised of a mix of deciduous trees dominated ( $\approx 77\%$ ) by the species Norway maple (*Acer platanoides* L.), European beech (*Fagus sylvatica* L.), small-leaved lime (*Tilia cordata* MILL.), sycamore maple (*Acer pseudoplatanus* L.), and European ash (*Fraxinus excelsior* L.). Evergreen species contribute less than 1% to the total tree number (Table 1). The inventory comprises 9391 trees growing within the “Englischer Garten” park, which have been collected by the Bavarian Administration of State-Owned Palaces, Gardens and Lakes. These tree data (species, tree height, DBH, crown diameter, and height to the crown base) were used as input parameters in i-Tree Eco to calculate the ecosystem services provided by the park. Since information about the crown condition has not been collected, we assumed a crown condition involving the best tress, i.e., 0% crown missing and 100% healthy (or 0% dieback). Further, these input parameters can be used for increasing the accuracy of LA and carbon sequestration estimations [32].

**Table 1.** Species composition of the south part of Englischer Garten (a total of 9391 trees).

Species	Relative Number (%)	Basal Area (m <sup>2</sup> )
Norway maple ( <i>Acer platanoides</i> L.)	32.9	453.6
European beech ( <i>Fagus sylvatica</i> L.)	12.6	447.4
Small-leaved lime ( <i>Tilia cordata</i> MILL.)	11.2	160.1
Sycamore maple ( <i>Acer pseudoplatanus</i> L.)	10.4	122.8
European ash ( <i>Fraxinus excelsior</i> L.)	10.1	223.2
Field maple ( <i>Acer campestre</i> L.)	3.7	35.8
European hornbeam ( <i>Carpinus betulus</i> L.)	3.6	43.6
Horse-chestnut ( <i>Aesculus hippocastanum</i> L.)	2.6	70.1
English oak ( <i>Quercus robur</i> L.)	2	32.4
Scotch elm ( <i>Ulmus glabra</i> Huds.)	1.8	28.8
Black locust ( <i>Robinia pseudoacacia</i> L.)	1.6	21.7
London plane ( <i>Platanus × acerifolia</i> Aiton)	1.3	19.4
White willow ( <i>Salix alba</i> L.)	1.0	43.3
Willows ( <i>Salix</i> spp.), poplars ( <i>Populus</i> spp.), cherries ( <i>Prunus</i> spp.), Caucasian wingnut ( <i>Pterocarya fraxinifolia</i> ), birches ( <i>Betula</i> spp.), hazels ( <i>Corylus</i> spp.), walnuts ( <i>Juglans</i> spp.), common pear ( <i>Pyrus communis</i> ), honey locust <i>Gleditsia triacanthos</i> , tulip tree ( <i>Liriodendron tulipifera</i> ), hawthorns ( <i>Crataegus</i> spp.), ginkgo ( <i>Ginkgo biloba</i> ), whitebeams ( <i>Sorbus</i> spp.), grey alder ( <i>Alnus incana</i> ), tree of heaven ( <i>Ailanthus altissima</i> ), cornelian cherry ( <i>Cornus mas</i> ), Japanese pagoda tree ( <i>Sophora japonica</i> ), yew ( <i>Taxus baccata</i> ), pines ( <i>Pinus</i> spp.), and spruce ( <i>Picea abies</i> ), magnolia ( <i>Magnolia</i> spp.)	5.2 (evergreen species <1%)	82.6

The model simulations were conducted in 2012 using hourly meteorological data registered at the Munich Airport (temperature, wind speed, and radiation from the National Oceanic and Atmospheric Administration (NOAA, Silver Spring, MD, USA) database that is directly accessed by i-Tree Eco, Farnham, UK) and the München Theresienstrasse (precipitation) weather stations, which are about 40 and 1 km away from the study site, respectively. The average hourly concentration data for ozone (O<sub>3</sub>), sulfur dioxide (SO<sub>2</sub>), nitrogen dioxide (NO<sub>2</sub>), carbon monoxide (CO), and particulate matter with



a diameter of 2.5 ( $PM_{2.5}$ ) were provided from the Bavarian Environment Agency (LFU), Augsburg, Germany.  $PM_{10}$  data are no longer analyzed in the latest i-Tree Eco version (version 6) because  $PM_{2.5}$  is generally more relevant for human health [33]. This information was checked for quality and fed into the USDA Forest Service database for its use in our investigation.

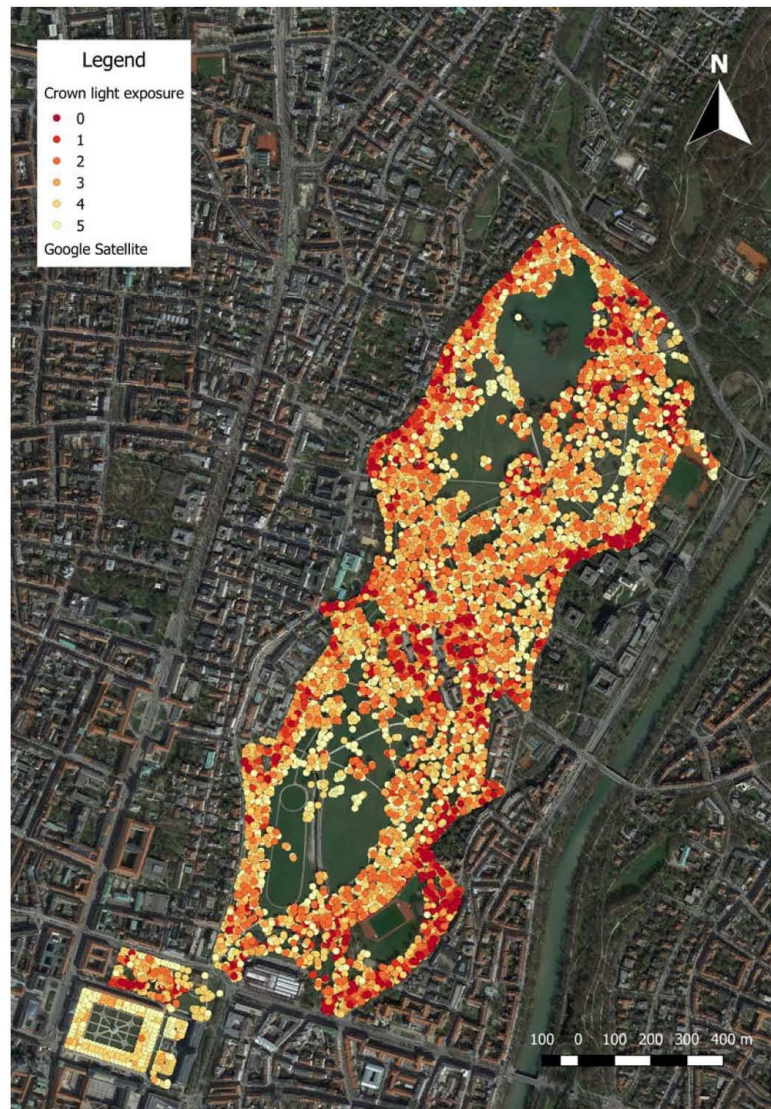


**Figure 1.** All trees in the south of Englischer Garten with relative crown light exposure (CLE) classes calculated by the CCS (crown competition for sunlight) competition index which is based on the algorithms provided in Pretzsch et al. [31]. In addition to competition between trees, shading by buildings has been considered as well.



## 2.2. CLE Effects

The i-Tree Eco model considers the average competition of a tree as the degree of crown exposure to sunlight, which is not supposed to change during the simulation. This competition is expressed as CLE (crown light exposure), which is an empirical index that reflects the number of sides of a tree receiving direct sunlight [32]. Therefore, the tree crown is virtually divided into the four cardinal directions and an additional surface on top of the crown (Figure 2) [19]. A classification can thus result in a CLE value between 0 (which would characterize a fully suppressed tree in the understorey of a closed canopy, only receiving diffuse light) and 5 (solitary tree not shaded by surrounding trees or other obstacles). CLE reflects broadly the capability for photosynthesis and is used to calculate LA and tree growth estimates. While growth directly determines carbon sequestration, LA influences various ecosystem services. Herein, we investigate air pollution reduction and biogenic emissions to determine the CLE sensitivity (see Section 2.4).

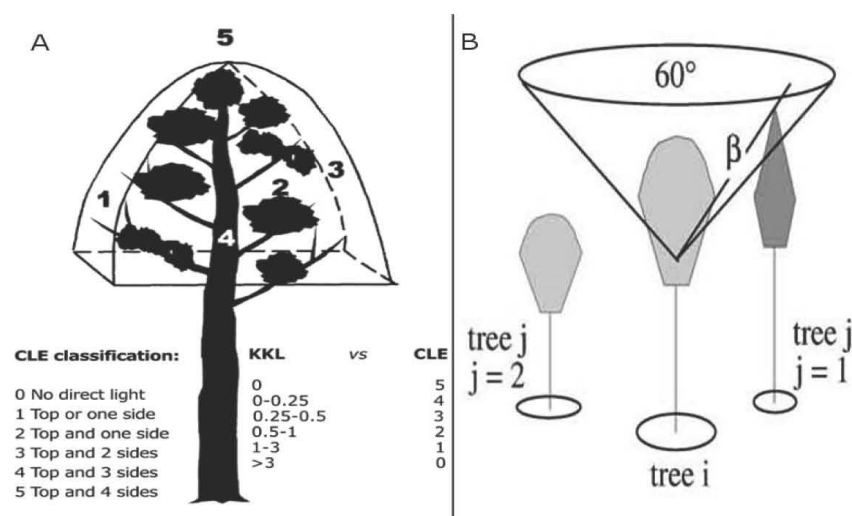


**Figure 2.** Crown light exposure (CLE) classification (A) and calculation of the competition index CCS (crown competition for sunlight) based on Pretzsch et al. (B). In the bottom right corner of (A), the conversion of CCS is indicated in CLE values. Sources: [19,31].

### 2.2.1. Calculation of Leaf Area (LA)

The i-Tree Eco model uses tree-specific CLE values that are grouped into three states in order to calculate LA: the open-grown (CLE = 4–5), park (CLE = 2–3), and closed forest (CLE = 0–1) conditions. Under the open-grown condition, LA is calculated either from DBH only (measured at 1.37 m above ground) or from crown length (H) and crown width (D) if available [34]:

- CLE = 4–5 (open-grown trees)

$$\ln(LA) = b_0 + b_1 DBH + b_2 S \quad (1)$$

$$\ln(LA) = b_0 + b_1 H + b_2 D + b_3 S + b_4 C \quad (2)$$

In these calculations, S is a species-specific shading factor, which is defined as the percentage of light intensity intercepted by foliated tree crowns, and C is the outer surface area of the tree crown calculated from H and D as  $C = \pi D(H + D)/2$ . S varies with species for deciduous trees, and if it is not

defined for individual species, the averages for the genus or general hardwoods are used. For conifer trees, the model applies a shading factor of 0.91 for all species, except for pines (0.83) [32,34]. For the closed forest condition, LA is calculated using the following equation based on the Beer-Lambert law:

- CLE = 0–1 (forest stand condition)

$$LA = (\ln(1 - S)/-k) \times \pi \times (D/2)^2 \quad (3)$$

where  $k$  is a light extinction coefficient that is differentiated between conifers (0.52) and hardwoods (0.65) [32]. For CLE = 2–3 (park condition), LA is calculated as the average value determined by the open-grown (CLE = 4–5) and closed canopy equations (CLE = 0–1).

### 2.2.2. Effects on Tree Growth

Average diameter growth is added to tree diameter (year  $x$ ) to estimate the tree diameter in year  $x + 1$  [35]. In i-Tree Eco, a standard diameter growth (SG) that can be reduced is defined for open-grown trees (CLE = 4–5) when the number of frost-free days is smaller than a defined value:

$$\text{Standard diameter growth (SG)} = 0.83 \text{ cm/year} \times (\text{number of frost-free days}/153) \quad (4)$$

Park tree growth (CLE = 2–3) is calculated by dividing SG of open-grown trees by 1.78 and that of forest trees (CLE = 0–1) by 2.29.

### 2.2.3. Automated Competition Calculations

Herein, we calculated CLE based on a routine introduced within the framework of the single-tree-based stand simulator SILVA [31]. This model calculates single-tree growth in relation to its surrounding three-dimensional space to produce the competition index  $CCS$  value.  $CCS$  aids in identifying the competitors of single trees by considering a virtual reverse cone with an axis equal to the tree axis and its vertex placed within the crown of the tree (Figure 2b). The model determines the angle  $\beta$  between the insertion point of the cone and the top of any competitor tree. This angle is multiplied by the crown cross-sectional areas (CCAs) of the competitors and the tree of interest considering a species-specific light transmission coefficient:

$$CCS_i = \sum_{j=1}^n \left( \beta_i \frac{CCA_j}{CCA_i} TM_j \right) \quad (5)$$

where  $CCS_i$  is the competition index for tree  $i$ ;  $\beta_i$  is the angle between cone vertex and top of competitor  $j$ ;  $CCA_j$  and  $CCA_i$  are the CCAs of trees  $j$  and  $i$ , respectively;  $TM_j$  is the species-specific light transmission coefficient for tree  $j$ ;  $n$  is the number of competitors of tree  $i$  [31].

We calculated the competition index  $CCS$  for each tree before converting the results into a CLE classification. Therefore, we assumed that the trees without competition ( $CCS = 0$ ) correspond to the highest CLE value (CLE = 5), while other CLE classes are assigned to  $CCS$  values according to the relative abundance of trees (see Figure 2a). Thus, there is approximately the same number of trees in each CLE class. We also considered shading by buildings and other trees not included in our inventory using the open source Quantum GIS (QGIS) software and a fixed buffer distance of 15 m around the trees. For all trees falling within this distance, we reduced the CLE by one unit.

### 2.3. Model Sensitivity Studies

The importance of individually determined CLEs was tested by comparing simulated carbon sequestration, pollution reduction, and emissions calculated using the SILVA routine (indicated as individual CLE runs) with the results originating from default CLE values (indicated as average CLE runs). The sensitivity connected to uncertain tree species determination was also investigated by deriving parameters from different information sources: (1) individually determined tree species

through field measurements (species-specific runs); (2) assuming a genus-specific inventory that reflects the detail derived by, for example, sophisticated remote sensing techniques, such as LiDAR (light detection and ranging) and high-resolution images (genus-specific runs) [23]; and (3) assuming a distinction between evergreen and deciduous trees representing the detail that can be derived by photogrammetric interpretation of aerial photographs (dominant species runs) [25]. In this context, we hypothesized that all deciduous species were *A. platanoides*, the dominant species of the park (Table 1), and all evergreen trees had the properties of *Picea abies*, the most common conifer species in South Germany [36].

#### 2.4. Model Calculations

For all calculations, the initial dimensional data, hourly temperature and precipitation records, and air pollution concentrations are used as input data [32,37]. Only ecosystem services with a direct link to air chemistry, i.e., air pollution reduction, carbon sequestration, and biogenic emissions, were evaluated. In subsequent paragraphs, we describe how the model calculates these services.

##### 2.4.1. Carbon Storage and Sequestration

The model calculates the above-ground biomass of trees in dry weight using allometric equations [35,38] and the total tree biomass using a root-to-shoot ratio of 0.26 [32,39]. Because the allometric equations are diameter-based and developed for closed canopies, biomass should be corrected for open-grown trees, which tend to be shorter and thus have less above-ground biomass at a given diameter. Therefore, biomass estimates are reduced for urban trees by a factor of 0.8 [38]. Total carbon storage is calculated by multiplying tree dry weight biomass by 0.5 [32]. Hence, assuming that there is no change in soil carbon, annual carbon sequestration is directly calculated from tree growth (see Section 2.2.2) [32].

##### 2.4.2. Air Pollution Reduction

The dry deposition of O<sub>3</sub>, SO<sub>2</sub>, NO<sub>2</sub>, CO, and PM<sub>2.5</sub> is hourly determined throughout the year [40–43]. During precipitation events, deposition is assumed to be zero. Using the following equation, for other periods, the pollutant flux into the biosphere ( $F$ ; in g m<sup>-2</sup> s<sup>-1</sup>) is calculated as the product of deposition velocity ( $V_d$ ; in m s<sup>-1</sup>) and pollutant concentration ( $C$ ; in g m<sup>-3</sup>) [41]:

$$F = V_d C \quad (6)$$

Using the following equation, the deposition velocities of CO, NO<sub>2</sub>, SO<sub>2</sub>, and O<sub>3</sub> are calculated as the inverse of the sum of the aerodynamic resistance  $R_a$ , a quasi-laminar boundary layer ( $R_b$ ), and the canopy resistance  $R_c$  expressed in s m<sup>-1</sup> [44]:

$$V_d = (R_a + R_b + R_c)^{-1} \quad (7)$$

where  $R_a$  is determined from meteorological data (wind speed and atmospheric stability) since it is assumed to be independent of air pollution type or plant species,  $R_b$  is based on a value defined in a study by Pederson et al. (1995) [45] using a specific Schmidt number for each air pollutant [46], and  $R_c$  is calculated using the following equation:

$$1/R_c = 1/(r_s + r_m) + 1/r_{soil} + 1/r_t \quad (8)$$

where  $r_s$  is the stomatal resistance (s m<sup>-1</sup>),  $r_m$  is the mesophyll resistance (s m<sup>-1</sup>),  $r_{soil}$  is the soil resistance (2941 s m<sup>-1</sup> in growing season and 2000 otherwise), and  $r_t$  is the cuticular resistance (s m<sup>-1</sup>).

Hourly canopy resistance values for O<sub>3</sub>, SO<sub>2</sub>, and NO<sub>2</sub> were calculated based on a modified hybrid of big leaf and multilayer canopy deposition models [44,47]. The model calculates stomatal resistance ( $r_s$ ) as the inverse of stomatal conductance, which is estimated based on the leaf photosynthetic rate,



relative humidity, and surface CO<sub>2</sub> concentration using the Ball-Berry formula (for more details, see [46]). The mesophyll and cuticular resistance values are set based on those reported in the literature: for NO<sub>2</sub>,  $r_m = 100 \text{ s m}^{-1}$  [48] and  $r_t = 20,000 \text{ s m}^{-1}$  [49]; for O<sub>3</sub>,  $r_m = 10 \text{ s m}^{-1}$  [48] and  $r_t = 10,000 \text{ s m}^{-1}$  [50,51]; and for SO<sub>2</sub>,  $r_m = 0$  [49] and  $r_t = 8000 \text{ s m}^{-1}$ . As CO reduction is assumed to be independent of photosynthesis and transpiration, the resistance value for CO is set to  $50,000 \text{ s m}^{-1}$  in the in-leaf season and  $1,000,000 \text{ s m}^{-1}$  in the out-leaf season for all trees [52]. The hourly deposition and resuspension rates for PM<sub>2.5</sub> are calculated based on wind speed and LA (for more details, see [42]).

The base deposition velocity  $V_d$  was multiplied by the individual tree LAI based on local field data and local seasonal variation (local leaf-on and leaf-off dates). For deciduous trees, the calculation of pollution deposition is limited to the in-leaf period. Herein, the leaf-on date is 5 April, whereas the leaf-off date is October 28.

#### 2.4.3. Biogenic Emissions

Hourly emissions of isoprene (C<sub>5</sub>H<sub>8</sub>) and monoterpenes (C<sub>10</sub> terpenoids) were estimated using an approach proposed by Guenther et al. 1993 [53] and Geron et al. 1994 [54] with genus-specific parameters [55]. In this approach, emission was calculated by multiplying leaf biomass (derived from LA with species-specific conversion factors) by emission rates. These in turn depend on temperature and light (isoprene) or temperature only (monoterpenes) as well as on genus-specific factors that represent emissions at 30 °C and  $1000 \mu\text{mol m}^{-2} \text{ s}^{-1}$  photosynthetically active radiation (PAR) [56]. Median emissions values for the family, order, or superorder were used if genus-specific emission was not available [32]. Incoming PAR was calculated as 46% of total solar radiation input [57]. Because isoprene emission has a nonlinear dependence on light, PAR was estimated from incoming PAR for 30 canopy levels using the sunfleck canopy environment model with the LAI of the analyzed structure [32]. Hourly leaf temperature was calculated from air temperature while considering the transpiration rate (for unlimited water supply), LAI, and percentage tree cover [55].

### 3. Results

#### 3.1. Ecosystem Services

The tree crowns of Englischer Garten were calculated to cover an area of 73.2 ha and have a total LA of 467.5 ha with a leaf biomass of 301.7 tons. The most dominant species in terms of number and basal area were *A. platanoides* and *F. sylvatica* (Table 1). Overall, carbon stored in the trees was estimated to be 6225 tons. In accordance with their fraction of basal area, *F. sylvatica* and *A. platanoides* stored the most carbon (31.4% and 29.1% of the total, respectively). The amount of carbon sequestered in 2012 was calculated to be 214 tons (Figure 3). The model further indicates that the trees in Englischer Garten removed 2610 kg of O<sub>3</sub>, 845 kg of NO<sub>2</sub>, 186 kg of PM<sub>2.5</sub>, 171 kg of SO<sub>2</sub>, and 62 kg of CO (Figure 4). In addition, the trees emitted an estimated BVOC amount of 550 kg (158 kg isoprene and 392 kg monoterpenes; Figure 5).

#### 3.2. Sensitivity to Average CLE Values

Simulation with average CLE values (CLE average) resulted in a 14% reduction in LA and leaf biomass (379.9 vs. 443 ha year<sup>-1</sup>; 224.9 vs. 262 t year<sup>-1</sup>) compared to the run with individual determination of CLE (Figure 3). This directly affected bioemissions (494 vs. 550 kg year<sup>-1</sup>; Figure 5) and pollution reduction (Figure 4). Except for CO (in both cases, 62 kg year<sup>-1</sup>), more pollutants were removed in the “CLE individual” simulation compared to the “CLE average” simulation (2610 vs. 2482 kg year<sup>-1</sup> for O<sub>3</sub>, 845 vs. 794 kg year<sup>-1</sup> for NO<sub>2</sub>, 186 vs. 165 kg year<sup>-1</sup> for PM<sub>2.5</sub>, and 171 vs. 164 kg year<sup>-1</sup> for SO<sub>2</sub>). Carbon sequestration was also affected by individual light exposure (Figure 3): 214 tons of carbon (784 CO<sub>2</sub> equivalent) removed in the “CLE individual” simulation compared to 155 tons of carbon (567 CO<sub>2</sub> equivalent) removed in the “CLE average” simulation, indicating that the trees in Englischer Garten were more open grown than expressed by the average CLE value.

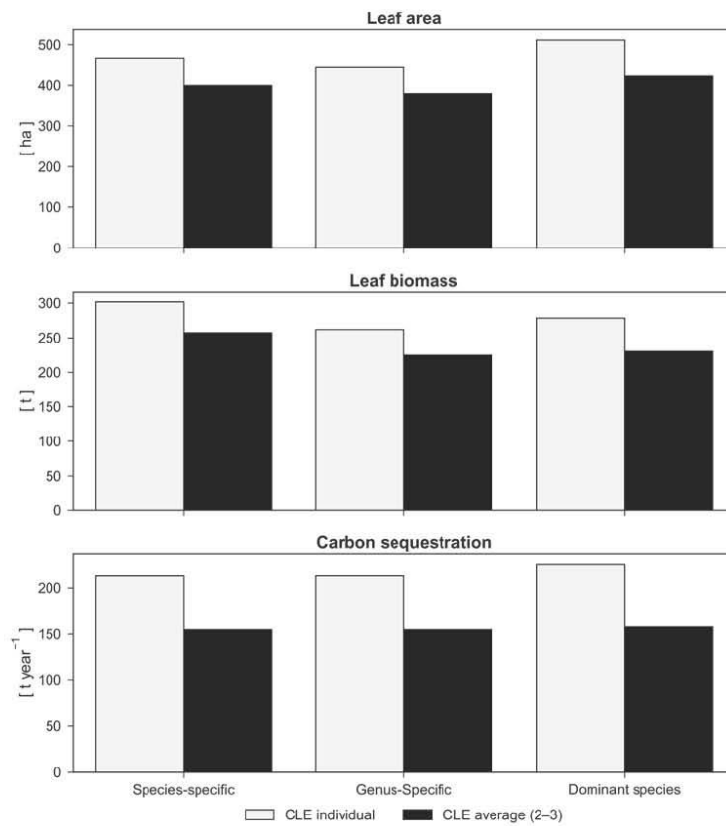


Figure 3. Leaf area (LA), leaf biomass, and carbon sequestration comparison between the “species-specific”, “genus-specific”, and “dominant species” simulations considering the crown light exposure (CLE) value for each tree (CLE individual) and the average CLE values (CLE average).

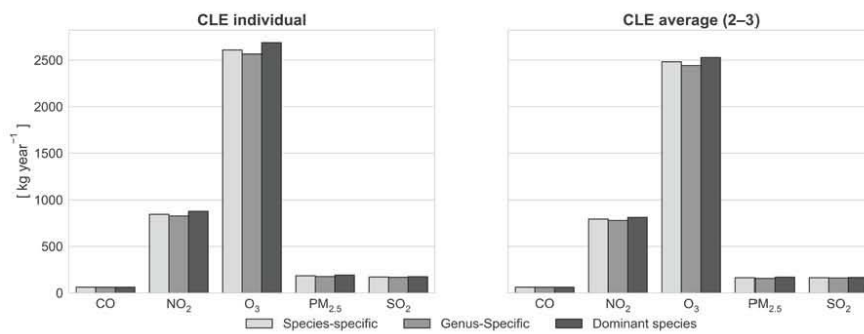


Figure 4. Air pollution reduction comparison between the “species-specific”, “genus-specific”, and “dominant species” simulations considering the crown light exposure (CLE) for each tree (CLE individual) and the average CLE values (CLE average).

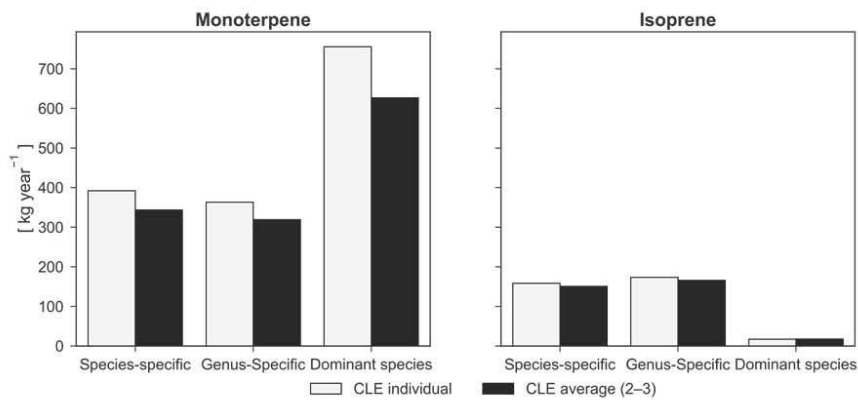


Figure 5. Comparison of monoterpene and isoprene emissions between the “species-specific”, “genus-specific”, and “dominant species” simulations considering the crown light exposure (CLE) for each tree (CLE individual) and the average CLE values (CLE average).

### 3.3. Sensitivity to Different Species Classification

Compared to simulations with species-specific parameterization, the results obtained with the genus-specific simulation showed lower LA (−5%; 443.7 ha) and leaf biomass (−13%; 262 t). The dominant species simulation demonstrated higher LA values (511.3 ha; 9% higher than the species-specific parameterization), but leaf biomass results (−8%; 278.4 t) were almost equivalent (Figure 3).

According to lower LA, pollutants removed with genus-specific parameterization were fewer than those removed with species-specific parameterization (−2% of  $\text{O}_3$ , −2% of  $\text{NO}_2$ , −5% of  $\text{PM}_{2.5}$ , and −1% of  $\text{SO}_2$ ), except for CO ( $62 \text{ kg year}^{-1}$ ), as shown in Figure 4. The effects of species differentiation were small. LA also had a minor effect on BVOC emissions, which are otherwise driven by marginally different parameters for the species- and genus-specific simulations. However, when the parameters were set according to the dominant species approach, monoterpene emissions were considerably higher (+93%) and isoprene emissions tended to be zero (−89%) compared to the species-specific simulation.

Carbon sequestration (214 t) was not altered by the species- and genus-specific parameterizations because biomass growth was found to solely depend on the tree size and competition state (Figure 3). Instead, the dominant species simulation showed higher carbon sequestration (+5.7%; 226 t). In this case, a larger number of trees fell into class 4–5 due to the smaller transmission coefficients for maples in comparison with the species average (Figure 6).

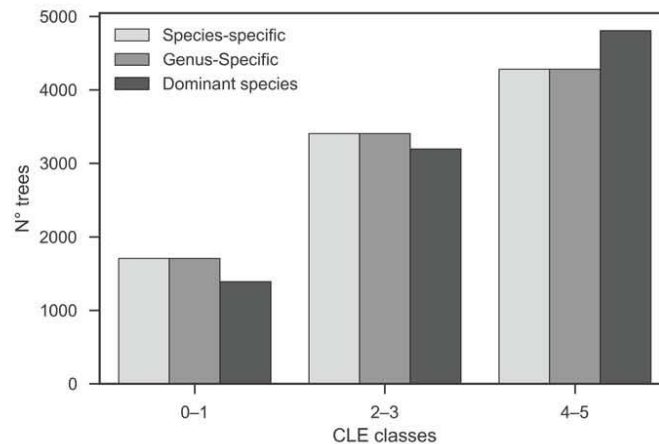


Figure 6. Comparison of crown light exposure (CLE) classes between the “species-specific”, “genus-specific”, and “dominant species” simulations. Class 4–5 (open-grown trees) is dominant in all simulations, particularly in the “dominant-species” simulation (99.4% of *Acer platanoides*).

#### 4. Discussion

Our investigation demonstrates that Englischer Garten—a major park in Munich—provides a considerable amount of environmental services, i.e., air pollution reduction and carbon sequestration. Simulated removals of  $O_3$  and  $NO_2$  were at the highest rates ( $3.6$  and  $1.1$   $g\ m^{-2}$ , respectively). A comparison with the estimates for other European cities showed that the total pollutant (combining  $CO$ ,  $O_3$ ,  $NO_2$ ,  $SO_2$ , and  $PM_{2.5}$ ) removal rate, which was  $5.3$   $g\ m^{-2}$  of tree cover per year, was similar to that for the city of Strasbourg ( $5.1$   $g\ m^{-2}$ ) [12] but lower than that for London ( $8.7$   $g\ m^{-2}$ ) [58]. The simulated  $PM_{2.5}$  removal rate for the park ( $0.25$   $g\ m^{-2}$ ) was of the same magnitude as that determined for U.S. cities ( $0.25$   $g\ m^{-2}$ ) [42], but the total removal rate (considering  $PM_{2.5}$  instead of  $PM_{10}$ ) was lower than the average value calculated for the U.S. cities ( $7.5$   $g\ m^{-2}$ ) [41].

Although we focused on uncertainties associated with parameterization and the determination of light competition (discussed further below), we also addressed the process uncertainty that is tightly linked to parameterization because processes and parameters often share the same knowledge base. Other uncertainties associated with the model inputs were climate conditions, which resulted in different degrees of ecosystem services during different years, and air pollution data measured outside the park, which may not reflect the ambient conditions of the park trees. However, since these aspects do not alter the relative contribution to the ecosystem services of different tree species, their investigation was outside the scope of this study.

##### 4.1. Uncertainties Associated with Parameterization

Species definition is fundamental information on which many properties depend. Therefore, we introduced a degree of uncertainty in species definition based on either imperfect knowledge—as is often the case with species in areas outside the original model development region (genus-specific parameterization)—or what can reasonably be derived from remote sensing measures (dominant species parameterization).

The total LA in the “genus-specific” simulation was approximately 5% lower than that in the “species-specific” simulation, which slightly reduced pollution removal. This reflects the similarity between species- and genus-based parameters, exhibiting the almost linear scaling of LA and deposition in i-Tree Eco. The differences are more comprehensively expressed with BVOC emissions



that are higher for isoprene (+10%) and lower for monoterpene (−7%) using only genus-specific parameterization. This highlights the additional influence of species-specific conversion factors between LA and leaf biomass. However, there were no differences between the two simulations concerning carbon sequestration because it is based on a fixed diameter growth rate and allometric equations from the literature that are used to calculate biomass change from the dimensional change [38,56]. Such allometric equations are usually derived from forest trees and, although they have been adjusted for urban conditions, they might not exactly reflect the actual tree forms and wood density. For example, various investigations show that high ozone concentration can cause a reduction in the root/shoot ratios of trees [59], especially for deciduous species [60]. Under high air pollution a larger root biomass fraction can thus be expected.

This approach might be improved by introducing a dependency on climate and soil type, particularly by encompassing drought stress events [61] and other stress factors that might depend on the degree of air pollution or salt application. Pretzsch et al. (2017) [62] showed that the urban trees in Europe have accelerated their growth since 1960 because of the effects of climate change, with considerable differences in different climate regions. Dahlhausen et al. (2017) [63] demonstrated the effect of urban climate on lime tree growth in Berlin and found that the trees in the city center were more responsive than those in urban boundaries. It is a challenge to represent these findings with the i-Tree Eco model by only considering the limited number of frost-free days, as is currently the case. Instead, representing the growth demands the introduction of direct sensitivity to temperature, competition, and possibly other factors that will vary from those of the city of interest. In addition, wood density and growth form might require parameterization that is regionally adapted to European species [64,65].

The dominant species parameterization assumes all deciduous trees (99.4% of total population) to be Norway maple (*A. platanoides*) and uses the parameters of spruce (*P. abies*) for all the evergreen trees (0.6%). Although the effects were found to strongly depend on the species composition and the dominant species used for representation, the results showed that tree species misclassification particularly affects BVOC emission estimates. Additionally, important information concerning LA and related air pollution reduction rates was derived. The effect of parameterization on emissions was expressed because emissions factors change strongly between species. For example, high monoterpene emissions resulted from *A. platanoides*—a dominant species having one of the highest monoterpene emission factors (1.6) of all species in the inventory (0.6 for *Fagus*, 0.1 for *Fraxinus*, and 0 for *Tilia*). In contrast, maples had a considerably low isoprene emission factor (0.1) compared to that of a number of species that were neglected in the dominant species runs, reducing the overall emission estimate for this compound. For example, *Quercus robur*, *Robinia pseudoacacia*, *Platanus × Acerifolia*, and *Salix alba* were all assumed to be considerably high isoprene emitters (with emission factor equal to 70) [56].

However, it is worth noting that emission parameters are uncertain. For example, monoterpene emission factors reported in the literature vary between 0.1 [66] and 43.5 [67] for *Fagus*, between 0 [68] and 9.6 [69] for *Fraxinus*, and between 0 [70] and 1.2 [71] for *Tilia*. For subtropical street trees, Dunn-Johnston et al. (2016) [72] showed that a considerable difference exists between species-derived isoprene emission rates and those assumed (genus-specific emission rates) in i-Tree Eco. Other uncertainties in the emission pattern of plants were found to originate from seasonal changes that depended on the weather conditions of the previous days and weeks [73], which were not considered herein. Additionally, the potential effects of air pollution [74] or drought [75,76], which might increase or decrease emissions, have been neglected. Since emissions are supposed to trigger aerosol production and ozone formation [77], these deficits may need consideration in order to be appropriately used in combination with regional air chemistry and climate models [78].

#### 4.2. Uncertainties Associated with Competition Calculations

Another form of influential information is the determination of competition, which represents the light that an individual tree is able to utilize during photosynthesis. We demonstrated that neglecting



an individual CLE determination (CLE average) strongly affected LA and thus pollution reduction (except for CO), carbon sequestration, and bioemissions. The intensity of this effect depended on the degree to which tree size and position differed from a homogeneous distribution with medium tree distances. Free-standing trees requiring more sunlight are therefore underrepresented in terms of LA and growth when only using average CLE determination [79]. Since Englischer Garten is characterized by many open spaces and areas where trees are found to clump together, the divergence from the mean conditions is relatively large (Figure 6). However, this is not an exception, since parks are often characterized by a complex tree distribution pattern in order to optimize recreational activities [3]. Therefore, we assumed that the structure of the Englischer Garten park was representative and that the significance of considering individual crown exposure was possibly high.

It is worth noting that the uncertainties associated with competition estimates can multiply with those associated with parameter estimation. In our case, the difference between the individual and mean competition calculations was particularly high when only “dominant species” parameters were used: the class with average competition (CLE = 2–3) was 56% larger than that with high competition (CLE = 0–1) and 51% smaller than that with low competition (CLE = 4–5) (50% and 26% for the species- and genus-specific simulations, respectively; Figure 6). Part of this effect was due to the method we designated CLE classes from competition calculations. Because competition depends on transmission properties of the canopy that differ with species, dominant-species parameterization results in different tree numbers per CLE class than species- or genus-specific parameterization (no difference exists between those two since light transmission factors are homogeneous within a genus) [31].

#### 4.3. Uncertainties Associated with Processes

Pollution deposition was calculated from LA and species-specific deposition velocities. However, uptake processes may need to be differentiated in terms of stomatal uptake and deposition onto the surface of the leaves, both of which are related to further environmental conditions. Stomatal uptake was found to depend on the photosynthetic activity, turgor pressure, and removal time in the intercellular spaces, particularly for O<sub>3</sub> and NO<sub>2</sub>, which were almost immediately metabolized [4]. Therefore, stomatal uptake through stomata could possibly be influenced by drought stress, which the standard i-Tree Eco model neglects, assuming sufficient water availability or irrigation for the street and park trees. In fact, the stomatal closure has been shown to considerably reduce pollution removal in dry periods and alternative model formulations have been suggested [80,81]. Consequently, surface deposition was found to strongly depend on leaf structure [82,83], which determines both velocity and deposition capacity. Deposition capacity in turn is also dynamical, since washing the deposited content from the leaf reduces the pollutant storage at the leaves [84]. In the case of NO<sub>2</sub> and SO<sub>2</sub>, it is also possible that pollution removal occurs by means of dissolving directly into the water film on the plant surface [4]. Although it might have a minor impact compared with the influence of the stomata on the gaseous uptake, the uncertainty associated with leaf-surface properties and the dependency on rainfall are currently underexplored in i-Tree Eco.

In addition, pollutant deposition varies with the canopy structure and tree position because these factors determine the air flow within and around trees [85]. However, the relation between tree traits (e.g., crown geometry and foliage distribution), “urban street canyon”, and weather conditions are complex and cannot be evaluated using i-Tree Eco. For example, low turbulence may promote deposition and increase the N<sub>2</sub>O and CO concentrations or O<sub>3</sub> formation due to longer residence time [86].

Based on the above discussion, it can be easily observed that i-Tree Eco estimates constitute a relatively first-order approximation that is solely related to surface area and uses lumped velocity parameters for pollutants that are nevertheless species specific. Only CO removal is independent of LA, possibly because it is independent of photosynthesis and transpiration [52,87]. This assumption is likely to be defensible because CO deposition in soil has been demonstrated to be considerably larger than that in plant leaves [48,88].

## 5. Conclusions

Englischer Garten trees provide important ecosystem services to Munich. The results of our model simulation revealed that in 2012, they potentially removed 4 t of pollutants, particularly ozone and nitrogen dioxide, and more than 200 t of carbon dioxide. The robustness of the model estimates was found to strongly depend on accurate species-specific parametrization as well as an individual determination of the competition state of the trees. The suggested automated determination process represents an objective procedure that is in many ways preferable to manual investigations, although its applicability and precision remains to be tested against field observations. Species-specific parameterization is particularly necessary for the determination of BVOC emissions. Since the taxonomic approach of i-Tree Eco only assigns genus or family values, simulations have uncertainties associated with species that differ from the genus- or dominating species-based settings, even if their abundance is relatively small. Therefore, it is strongly recommended to complement remote sensing applications with terrestrial observations and improve the database of species-specific parameters. Overall, we highlighted a considerable potential for improvements in the i-Tree Eco model process representations, particularly concerning the climate sensitivity of emission and growth processes.

**Acknowledgments:** This research was supported by Graduate School for Climate and Environment (GRACE). We also acknowledge support by Deutsche Forschungsgemeinschaft and Open Access Publishing Fund of Karlsruhe Institute of Technology. Furthermore, we thank the Bavarian Administration of State-Owned Palaces, Gardens and Lakes for providing the individual tree data, the Bavarian Environment Agency (LFU) for providing air pollution data, the i-Tree support team for assisting us in model implementation and data processing, and the Graduiertenzentrum Weihenstephan of Technical University of Munich and the ENAGO company for the English editing.

**Author Contributions:** R.P. performed the simulation experiments and analyzed the data; R.P. and R.G. conceived and designed the experiments and jointly wrote the text; P.B. and H.P. provided the competition algorithm, supported the implementation, and revised the text.

**Conflicts of Interest:** The authors declare no conflict of interest.

## References

1. United Nations. *World Urbanization Prospects: The 2014 Revision, Highlights (ST/ESA/SER.A/352)*; Department of Economic and Social Affairs, Population Division: New York, NY, USA, 2014; ISBN 9789211515176.
2. UN-Habitat. *Urbanization and Development: Emerging Futures. World Cities Report 2016*; United Nations Human Settlements Programme: Nairobi, Kenya, 2016; ISBN 978-92-1-132708-3.
3. Salbitano, F.; Borelli, S.; Conigliaro, M.; Chen, Y. *Guidelines on Urban and Peri-Urban Forestry*; FAO Forest; Food and Agriculture Organization of the United Nations: Rome, Italy, 2016; ISBN 9789251094426.
4. Grote, R.; Samson, R.; Alonso, R.; Amorim, J.H.; Cariñanos, P.; Churkina, G.; Fares, S.; Thiec, D.L.; Niinemets, Ü.; Mikkelsen, T.N.; et al. Functional traits of urban trees: Air pollution mitigation potential. *Front. Ecol. Environ.* **2016**, *14*, 543–550. [[CrossRef](#)]
5. Churkina, G.; Grote, R.; Butler, T.M.; Lawrence, M. Natural selection? Picking the right trees for urban greening. *Environ. Sci. Policy* **2015**, *47*, 12–17. [[CrossRef](#)]
6. Maes, J.; Egoh, B.; Willemsen, L.; Liquete, C.; Vihervaara, P.; Schägner, J.P.; Grizzetti, B.; Drakou, E.G.; Notte, A.L.; Zulian, G.; et al. Mapping ecosystem services for policy support and decision making in the European Union. *Ecosyst. Serv.* **2012**, *1*, 31–39. [[CrossRef](#)]
7. Endreny, T.; Santagata, R.; Perna, A.; De Stefano, C.; Rallo, R.F.; Ulgiati, S. Implementing and managing urban forests: A much needed conservation strategy to increase ecosystem services and urban wellbeing. *Ecol. Modell.* **2017**, *360*, 328–335. [[CrossRef](#)]
8. Nowak, D.; Crane, D. The urban forest effects (UFORE) model: Quantifying urban forest structure and function. In *Integrated Tools for Natural Resources Inventories in the 21st Century*; Hansen, M., Burk, T., Eds.; U.S. Department of Agriculture, Forest Service, North Central Forest Experiment Station: Saint Paul, MN, USA, 1998; pp. 714–720.

9. Hirabayashi, S.; Kroll, C.N.; Nowak, D.J. Development of a distributed air pollutant dry deposition modeling framework. *Environ. Pollut.* **2012**, *171*, 9–17. [[CrossRef](#)] [[PubMed](#)]
10. Nowak, D.J.; Hoehn, R.E.; Bodine, A.R.; Greenfield, E.J.; O'Neil-Dunne, J. Urban forest structure, ecosystem services and change in Syracuse, NY. *Urban Ecosyst.* **2013**, *19*, 1–23. [[CrossRef](#)]
11. Russo, A.; Escobedo, F.J.; Zerbe, S. Quantifying the local-scale ecosystem services provided by urban treed streetscapes in Bolzano, Italy. *AIMS Environ. Sci.* **2016**, *3*, 58–76. [[CrossRef](#)]
12. Selmi, W.; Weber, C.; Rivière, E.; Blond, N.; Mehdi, L.; Nowak, D. Air pollution removal by trees in public green spaces in Strasbourg city, France. *Urban For. Urban Green.* **2016**, *17*, 192–201. [[CrossRef](#)]
13. Westfall, J. Spatial-scale considerations for a large-area forest inventory regression model. *Forestry* **2015**, *88*, 267–274. [[CrossRef](#)]
14. Nowak, D.J.; Walton, J.; Stevens, J.C.; Crane, D.E.; Hoehn, R.E. Effect of Plot and Sample Size on Timing and Precision of Urban Forest Assessments METHODS Effect of Plot Size on Data Collection Time and Total Population Estimate Precision. *Arboric. Urban For.* **2008**, *34*, 386–390.
15. Bottalico, F.; Chirici, G.; Giannetti, F.; De Marco, A.; Nocentini, S.; Paoletti, E.; Salbitano, F.; Sanesi, G.; Serenelli, C.; Travaglini, D. Air Pollution Removal by Green Infrastructures and Urban Forests in the City of Florence. *Agric. Agric. Sci. Procedia* **2016**, *8*, 243–251. [[CrossRef](#)]
16. Manes, F.; Marando, F.; Capotorti, G.; Blasi, C.; Salvatori, E.; Fusaro, L.; Ciancarella, L.; Mircea, M.; Marchetti, M.; Chirici, G.; et al. Regulating Ecosystem Services of forests in ten Italian metropolitan Cities: Air quality improvement by PM<sub>10</sub> and O<sub>3</sub> removal. *Ecol. Indic.* **2016**, *67*, 425–440. [[CrossRef](#)]
17. Marando, F.; Salvatori, E.; Fusaro, L.; Manes, F. Removal of PM<sub>10</sub> by forests as a nature-based solution for air quality improvement in the Metropolitan city of Rome. *Forests* **2016**, *7*, 150. [[CrossRef](#)]
18. Fusaro, L.; Marando, F.; Sebastiani, A.; Capotorti, G.; Blasi, C.; Copiz, R.; Congedo, L.; Munafò, M.; Ciancarella, L.; Manes, F. Mapping and Assessment of PM<sub>10</sub> and O<sub>3</sub> Removal by Woody Vegetation at Urban and Regional Level. *Remote Sens.* **2017**, *9*, 791. [[CrossRef](#)]
19. Bechtold, W.A. Crown position and light exposure classification—an alternative to field-assigned crown class. *North. J. Appl. For.* **2003**, *20*, 154–160.
20. Alonzo, M.; Bookhagen, B.; Roberts, D.A. Urban tree species mapping using hyperspectral and LiDAR data fusion. *Remote Sens. Environ.* **2014**, *148*, 70–83. [[CrossRef](#)]
21. Alonzo, M.; McFadden, J.P.; Nowak, D.J.; Roberts, D.A. Mapping urban forest structure and function using hyperspectral imagery and LiDAR data. *Urban For. Urban Green.* **2016**, *17*, 135–147. [[CrossRef](#)]
22. Parmehr, E.G.; Amati, M.; Taylor, E.J.; Livesley, S.J. Estimation of urban tree canopy cover using random point sampling and remote sensing methods. *Urban For. Urban Green.* **2016**, *20*, 160–171. [[CrossRef](#)]
23. Shojanoori, R.; Shafri, H.Z.M. Review on the Use of Remote Sensing for Urban Forest Monitoring. *Arboric. Urban For.* **2016**, *42*, 400–417.
24. Yang, J.; Chang, Y.M.; Yan, P.B. Ranking the suitability of common urban tree species for controlling PM<sub>2.5</sub> pollution. *Atmos. Pollut. Res.* **2015**, *6*, 267–277. [[CrossRef](#)]
25. Fassnacht, F.E.; Latifi, H.; Stereńczak, K.; Modzelewska, A.; Lefsky, M.; Waser, L.T.; Straub, C.; Ghosh, A. Review of studies on tree species classification from remotely sensed data. *Remote Sens. Environ.* **2016**, *186*, 64–87. [[CrossRef](#)]
26. Berland, A.; Lange, D.A. Google Street View shows promise for virtual street tree surveys. *Urban For. Urban Green.* **2017**, *21*, 11–15. [[CrossRef](#)]
27. Tanhuanpää, T.; Vastaranta, M.; Kankare, V.; Holopainen, M.; Hyyppä, J.; Hyyppä, H.; Alho, P.; Raisio, J. Mapping of urban roadside trees—A case study in the tree register update process in Helsinki City. *Urban For. Urban Green.* **2014**, *13*, 562–570. [[CrossRef](#)]
28. Bella, I.E. A new competition model for individual trees. *For. Sci.* **1971**, *17*, 364–372.
29. Korol, R.L.; Running, S.W.; Milner, K.S. Incorporating intertree competition into an ecosystem model. *Can. J. For. Res.* **1995**, *25*, 413–424. [[CrossRef](#)]
30. Fox, J.C.; Bi, H.; Ades, P.K. Spatial dependence and individual-tree growth models. II. Modelling spatial dependence. *For. Ecol. Manag.* **2007**, *245*, 20–30. [[CrossRef](#)]
31. Pretzsch, H.; Biber, P.; Dursky, J. The single tree-based stand simulator SILVA: Construction, application and evaluation. *For. Ecol. Manag.* **2002**, *162*, 3–21. [[CrossRef](#)]
32. Nowak, D.J.; Crane, D.E.; Stevens, J.C.; Hoehn, R.E.; Walton, J.T.; Bond, J. A Ground-Based Method of Assessing Urban Forest Structure and Ecosystem Services. *Arboric. Urban For.* **2008**, *34*, 347–358. [[CrossRef](#)]



33. USDA Forest Service. *i-Tree Eco User's Manual v 6.0*; U.S. Forest Service Northern Research Station (NRS): Washington, DC, USA, 2016.
34. Nowak, D.I. Estimating Leaf Area and Leaf Biomass of Open-Grown Deciduous Urban Trees. *For. Sci.* **1996**, *42*, 504–507.
35. Nowak, D.J.; Crane, D.E. Carbon storage and sequestration by urban trees in the USA. *Environ. Pollut.* **2002**, *116*, 381–389. [[CrossRef](#)]
36. BMEL Federal Ministry of Food and Agriculture. *The Forests in Germany: Selected Results of the Third National Forest Inventory*; Federal Ministry of Food and Agriculture: Berlin, Germany, 2015.
37. Hirabayashi, S. *Air Pollutant Removals, Biogenic Emissions and Hydrologic Estimates for i-Tree Applications*; United States Forest Service: Syracuse, NY, USA, 2016.
38. Nowak, D.J. Atmospheric Carbon Dioxide Reduction by Chicago's urban forest. In *Chicago's Urban Forest Ecosystem: Results of the Chicago Urban Forest Climate Project*; McPherson, E.G., Nowak, D.J., Eds.; US Department of Agriculture, Forest Service, Northeastern Forest Experiment Station: Radnor, PA, USA, 1994; pp. 83–94.
39. Cairns, M.A.; Brown, S.; Helmer, E.H.; Baumgardner, G.A. Root biomass allocation in the world's upland forests. *Oecologia* **1997**, *111*, 1–11. [[CrossRef](#)] [[PubMed](#)]
40. Hirabayashi, S.; Kroll, C.N.; Nowak, D.J. Component-based development and sensitivity analyses of an air pollutant dry deposition model. *Environ. Model. Softw.* **2011**, *26*, 804–816. [[CrossRef](#)]
41. Nowak, D.J.; Crane, D.E.; Stevens, J.C. Air pollution removal by urban trees and shrubs in the United States. *Urban For. Urban Green.* **2006**, *4*, 115–123. [[CrossRef](#)]
42. Nowak, D.J.; Hirabayashi, S.; Bodine, A.; Hoehn, R. Modeled PM<sub>2.5</sub> removal by trees in ten US cities and associated health effects. *Environ. Pollut.* **2013**, *178*, 395–402. [[CrossRef](#)] [[PubMed](#)]
43. Nowak, D.J.; Hirabayashi, S.; Bodine, A.; Greenfield, E. Tree and forest effects on air quality and human health in the United States. *Environ. Pollut.* **2014**, *193*, 119–129. [[CrossRef](#)] [[PubMed](#)]
44. Baldocchi, D.D.; Hicks, B.B.; Camara, P. A canopy stomatal resistance model for gaseous deposition to vegetated surfaces. *Atmos. Environ.* **1987**, *21*, 91–101. [[CrossRef](#)]
45. Pederson, J.R.; Massman, W.J.; Mahrt, L.; Delany, A.; Oncley, S.; Hartog, G.D.; Neumann, H.H.; Mickle, R.E.; Shaw, R.H.; Paw U, K.T.; et al. California ozone deposition experiment: Methods, results, and opportunities. *Atmos. Environ.* **1995**, *29*, 3115–3132. [[CrossRef](#)]
46. Hirabayashi, S.; Kroll, C.N.; Nowak, D.J. *i-Tree Eco Dry Deposition Model Descriptions*; United States Forest Service: Syracuse, NY, USA, 2015.
47. Baldocchi, D. A Multi-layer model for estimating sulfur dioxide deposition to a deciduous oak forest canopy. *Atmos. Environ.* **1988**, *22*, 869–884. [[CrossRef](#)]
48. Hosker, R.P.; Lindberg, S.E. Review: Atmospheric deposition and plant assimilation of gases and particles. *Atmos. Environ.* **1982**, *16*, 889–910. [[CrossRef](#)]
49. Wesley, M.L. Parametrization of surface resistance to gaseous dry deposition in regional-scale numerical model. *Atmos. Environ.* **1989**, *23*, 1293–1304. [[CrossRef](#)]
50. Taylor, G.E.; Hanson, P.J.; Baldocchi, D.D. Pollutant deposition to individual leaves and plant canopies: Sites of regulation and relationship to injury. In *Assessment of Crop Loss from Air Pollution*; Heck, W.W., Taylor, O.C., Tingey, D.T., Eds.; Springer: Dordrecht, The Netherlands, 1988; pp. 227–257.
51. Lovett, G.M. Atmospheric deposition of nutrients and pollutants in North America: An ecological perspective. *Ecol. Appl.* **1994**, *4*, 629–650. [[CrossRef](#)]
52. Bidwell, R.G.S.; Fraser, D.E. Carbon monoxide uptake and metabolism by leaves. *Can. J. Bot.* **1972**, *50*, 1435–1439. [[CrossRef](#)]
53. Guenther, A.B.; Zimmerman, P.R.; Harley, P.C.; Monson, R.K. Isoprene and Monoterpene Emission Rate Variability: Model Evaluations and Sensitivity Analyses. *J. Geophys. Res.* **1993**, *98617*, 609–612. [[CrossRef](#)]
54. Geron, C.D.; Guenther, A.B.; Pierce, T.E. An improved model for estimating emissions of volatile organic compounds from forests in the eastern United States. *J. Geophys. Res.* **1994**, *99*, 12773. [[CrossRef](#)]
55. Hirabayashi, S. *i-Tree Eco Biogenic Emissions Model Descriptions*; United States Forest Service: Syracuse, NY, USA, 2012.
56. Nowak, D.J.; Crane, D.E.; Stevens, J.C.; Ibarra, M. *Brooklyn's Urban Forest*; U.S. Department of Agriculture, Forest Service, Northeastern Research Station: Newtown Square, PA, USA, 2002.
57. Monteith, J.L.; Unsworth, M.H. *Principles of Environmental Physics*, 2nd ed.; Edward Arnold: London, UK, 1990.

58. Rogers, K.; Sacre, K.; Goodenough, J.; Doick, K. *Valuing London's Urban Forest*; Treeconomics: London, UK, 2015; ISBN 9780957137110.
59. Grantz, D.A.; Gunn, S.; Vu, H.B. O<sub>3</sub> impacts on plant development: A meta-analysis of root/shoot allocation and growth. *Plant Cell Environ.* **2006**, *29*, 1193–1209. [[CrossRef](#)] [[PubMed](#)]
60. Landolt, W.; Bühlmann, U.; Bleuler, P.; Bucher, J.B. Ozone exposure–response relationships for biomass and root/shoot ratio of beech (*Fagus sylvatica*), ash (*Fraxinus excelsior*), Norway spruce (*Picea abies*) and Scots pine (*Pinus sylvestris*). *Environ. Pollut.* **2000**, *109*, 473–478. [[CrossRef](#)]
61. Moser, A.; Rötzer, T.; Pauleit, S.; Pretzsch, H. The Urban Environment Can Modify Drought Stress of Small-Leaved Lime (*Tilia cordata* Mill.) and Black Locust (*Robinia pseudoacacia* L.). *Forests* **2016**, *7*, 71. [[CrossRef](#)]
62. Pretzsch, H.; Biber, P.; Uhl, E.; Dahlhausen, J.; Schütze, G.; Perkins, D.; Rötzer, T.; Caldentey, J.; Koike, T.; van Con, T.; et al. Climate change accelerates growth of urban trees in metropolises worldwide. *Sci. Rep.* **2017**, *7*, 15403. [[CrossRef](#)] [[PubMed](#)]
63. Dahlhausen, J.; Rötzer, T.; Biber, P.; Uhl, E.; Pretzsch, H. Urban climate modifies tree growth in Berlin. *Int. J. Biometeorol.* **2017**, 1–14. [[CrossRef](#)] [[PubMed](#)]
64. McHale, M.R.; Burke, I.C.; Lefsky, M.A.; Peper, P.J.; McPherson, E.G. Urban forest biomass estimates: Is it important to use allometric relationships developed specifically for urban trees? *Urban Ecosyst.* **2009**, *12*, 95–113. [[CrossRef](#)]
65. Russo, A.; Escobedo, F.J.; Timilsina, N.; Schmitt, A.O.; Varela, S.; Zerbe, S. Assessing urban tree carbon storage and sequestration in Bolzano, Italy. *Int. J. Biodivers. Sci. Ecosyst. Serv. Manag.* **2014**, *10*, 54–70. [[CrossRef](#)]
66. König, G.; Brunda, M.; Puxbaum, H.; Hewitt, C.N.; Duckham, S.C.; Rudolph, J. Relative contribution of oxygenated hydrocarbons to the total biogenic VOC emissions of selected mid-European agricultural and natural plant species. *Atmos. Environ.* **1995**, *29*, 861–874. [[CrossRef](#)]
67. Moukhtar, S.; Bessagnet, B.; Rouil, L.; Simon, V. Monoterpene emissions from Beech (*Fagus sylvatica*) in a French forest and impact on secondary pollutants formation at regional scale. *Atmos. Environ.* **2005**, *39*, 3535–3547. [[CrossRef](#)]
68. Aydin, Y.M.; Yaman, B.; Koca, H.; Dasdemir, O.; Kara, M.; Altiok, H.; Dumanoglu, Y.; Bayram, A.; Tolunay, D.; Odabasi, M.; et al. Biogenic volatile organic compound (BVOC) emissions from forested areas in Turkey: Determination of specific emission rates for thirty-one tree species. *Sci. Total Environ.* **2014**, *490*, 239–253. [[CrossRef](#)] [[PubMed](#)]
69. Papież, M.R.; Potosnak, M.J.; Goliff, W.S.; Guenther, A.B. The impacts of reactive terpene emissions from plants on air quality in Las Vegas, Nevada. *Atmos. Environ.* **2009**, *43*, 4109–4123. [[CrossRef](#)]
70. Tiwary, A.; Namdeo, A.; Fuentes, J.; Dore, A.; Hu, X.; Bell, M. Systems scale assessment of the sustainability implications of emerging green initiatives. *Environ. Pollut.* **2013**, *183*, 213–223. [[CrossRef](#)] [[PubMed](#)]
71. Curtis, A.J.; Helmig, D.; Baroch, C.; Daly, R.; Davis, S. Biogenic volatile organic compound emissions from nine tree species used in an urban tree-planting program. *Atmos. Environ.* **2014**, *95*, 634–643. [[CrossRef](#)]
72. Dunn-Johnston, K.A.; Kreuzwieser, J.; Hirabayashi, S.; Plant, L.; Rennenberg, H.; Schmidt, S. Isoprene Emission Factors for Subtropical Street Trees for Regional Air Quality Modeling. *J. Environ. Qual.* **2016**, *45*, 234–243. [[CrossRef](#)] [[PubMed](#)]
73. Monson, R.K.; Grote, R.; Niinemets, Ü.; Schnitzler, J.P. Modeling the isoprene emission rate from leaves. *New Phytol.* **2012**, *195*, 541–559. [[CrossRef](#)] [[PubMed](#)]
74. Ghirardo, A.; Xie, J.; Zheng, X.; Wang, Y.; Grote, R.; Block, K.; Wildt, J.; Mentel, T.; Kiendler-Scharr, A.; Hallquist, M.; et al. Urban stress-induced biogenic VOC emissions and SOA-forming potentials in Beijing. *Atmos. Chem. Phys.* **2016**, *16*, 2901–2920. [[CrossRef](#)]
75. Grote, R.; Lavoit, A.V.; Rambal, S.; Staudt, M.; Zimmer, I.; Schnitzler, J.P. Modelling the drought impact on monoterpene fluxes from an evergreen Mediterranean forest canopy. *Oecologia* **2009**, *160*, 213–223. [[CrossRef](#)] [[PubMed](#)]
76. Boutsoukidis, E.; Kawaletz, H.; Radacki, D.; Schütz, S.; Hakola, H.; Hellén, H.; Noe, S.; Mölder, I.; Ammer, C.; Bonn, B. Impact of flooding and drought conditions on the emission of volatile organic compounds of *Quercus robur* and *Prunus serotina*. *Trees* **2014**, *28*, 193–204. [[CrossRef](#)]
77. Derwent, R.G.; Jenkin, M.E.; Saunders, S.M. Photochemical ozone creation potentials for a large number of reactive hydrocarbons under European conditions. *Atmos. Environ.* **1996**, *30*, 181–199. [[CrossRef](#)]

78. Cabaraban, M.T.I.; Kroll, C.N.; Hirabayashi, S.; Nowak, D.J. Modeling of air pollutant removal by dry deposition to urban trees using a WRF/CMAQ/i-Tree Eco coupled system. *Environ. Pollut.* **2013**, *176*, 123–133. [[CrossRef](#)] [[PubMed](#)]
79. McPherson, E.; Peper, P. Urban tree growth modeling. *Arboric. Urban For.* **2012**, *38*, 172–180.
80. Fares, S.; Savi, F.; Muller, J.; Matteucci, G.; Paoletti, E. Simultaneous measurements of above and below canopy ozone fluxes help partitioning ozone deposition between its various sinks in a Mediterranean Oak Forest. *Agric. For. Meteorol.* **2014**, *198*, 181–191. [[CrossRef](#)]
81. Morani, A.; Nowak, D.; Hirabayashi, S.; Guidolotti, G.; Medori, M.; Muzzini, V.; Fares, S.; Mugnozza, G.S.; Calfapietra, C. Comparing i-Tree modeled ozone deposition with field measurements in a periurban Mediterranean forest. *Environ. Pollut.* **2014**, *195*, 202–209. [[CrossRef](#)] [[PubMed](#)]
82. Beckett, K.P.; Freer-Smith, P.H.; Taylor, G. Particulate pollution capture by urban trees: Effect of species and windspeed. *Glob. Chang. Biol.* **2000**, *6*, 995–1003. [[CrossRef](#)]
83. Kardel, F.; Wuyts, K.; Babanezhad, M.; Wuytack, T.; Adriaenssens, S.; Samson, R. Tree leaf wettability as passive bio-indicator of urban habitat quality. *Environ. Exp. Bot.* **2012**, *75*, 277–285. [[CrossRef](#)]
84. Hofman, J.; Wuyts, K.; Van Wittenberghe, S.; Samson, R. On the temporal variation of leaf magnetic parameters: Seasonal accumulation of leaf-deposited and leaf-encapsulated particles of a roadside tree crown. *Sci. Total Environ.* **2014**, *493*, 766–772. [[CrossRef](#)] [[PubMed](#)]
85. Amorim, J.H.; Rodrigues, V.; Tavares, R.; Valente, J.; Borrego, C. CFD modelling of the aerodynamic effect of trees on urban air pollution dispersion. *Sci. Total Environ.* **2013**, *461–462*, 541–551. [[CrossRef](#)] [[PubMed](#)]
86. Harris, T.B.; Manning, W.J. Nitrogen dioxide and ozone levels in urban tree canopies. *Environ. Pollut.* **2010**, *158*, 2384–2386. [[CrossRef](#)] [[PubMed](#)]
87. Pihlatie, M.; Rannik, Ü.; Haapanala, S.; Peltola, O.; Shurpali, N.; Martikainen, P.J.; Lind, S.; Hyvönen, N.; Virkajarvi, P.; Zahniser, M.; et al. Seasonal and diurnal variation in CO fluxes from an agricultural bioenergy crop. *Biogeosciences* **2016**, *13*, 5471–5485. [[CrossRef](#)]
88. Sanhueza, E.; Dong, Y.; Scharffe, D.; Lobert, J.M.; Crutzen, P.J.; Dong, Y.; Scharffe, D.; Lobert, J.M.; Carbon, P.J.C. Carbon monoxide uptake by temperate forest soils: The effects of leaves and humus layers. *Tellus B Chem. Phys. Meteorol.* **1998**, *50*, 51–58. [[CrossRef](#)]



© 2018 by the authors. Licensee MDPI, Basel, Switzerland. This article is an open access article distributed under the terms and conditions of the Creative Commons Attribution (CC BY) license (<http://creativecommons.org/licenses/by/4.0/>).

## 2. Paper II

Pace, R.; Grote, R. (2020): Deposition and resuspension mechanisms into and from tree canopies: A study modeling particle removal of conifers and broadleaves in different cities. *Frontiers in Forest and Global Change* 3 (26): 10.3389/ffgc.2020.00026.

© [2020] **Frontiers in Forests and Global Change. Reprinted with permission of open access license.**





# Deposition and Resuspension Mechanisms Into and From Tree Canopies: A Study Modeling Particle Removal of Conifers and Broadleaves in Different Cities

Rocco Pace and Rüdiger Grote\*

*Institute of Meteorology and Climate Research - Atmospheric Environmental Research (IMK-IFU), Karlsruhe Institute of Technology (KIT), Karlsruhe, Germany*

## OPEN ACCESS

### Edited by:

Mark Potosnak,  
DePaul University, United States

### Reviewed by:

Ana María Yáñez-Serrano,  
Ecological and Forestry Applications  
Research Center (CREAF), Spain  
Robert Popek,  
Warsaw University of Life  
Sciences, Poland

### \*Correspondence:

Rüdiger Grote  
rue diger.grote@kit.edu

### Specialty section:

This article was submitted to  
Forests and the Atmosphere,  
a section of the journal  
Frontiers in Forests and Global  
Change

**Received:** 17 July 2019

**Accepted:** 24 February 2020

**Published:** 12 March 2020

### Citation:

Pace R and Grote R (2020) Deposition  
and Resuspension Mechanisms Into  
and From Tree Canopies: A Study  
Modeling Particle Removal of Conifers  
and Broadleaves in Different Cities.  
*Front. For. Glob. Change* 3:26.  
doi: 10.3389/ffgc.2020.00026

With increasing realization that particles in the air are a major health risk in urban areas, strengthening particle deposition is discussed as a means to air-pollution mitigation. Particles are deposited physically on leaves and thus the process depends on leaf area and surface properties, which change throughout the year. Current state-of-the-art modeling accounts for these changes only by altering leaf longevity, which may be selected by vegetation type and geographic location. Particle removal also depends on weather conditions, which determine deposition and resuspension but generally do not consider properties that are specific to species or plant type. In this study, we modeled < 2.5  $\mu\text{m}$ -diameter particulate-matter ( $\text{PM}_{2.5}$ ) deposition, resuspension, and removal from urban trees along a latitudinal gradient (Berlin, Munich, Rome) while comparing coniferous with broadleaf (deciduous and evergreen) tree types. Accordingly, we re-implemented the removal functionality from the i-Tree Eco model, investigated the uncertainty connected with parameterizations, and evaluated the efficiency of pollution mitigation depending on city conditions. We found that distinguishing deposition velocities between conifers and broadleaves is important for model results, i.e., because the removal efficiency of conifers is larger. Because of the higher wind speed, modeled  $\text{PM}_{2.5}$  deposition from conifers is especially large in Berlin compared to Munich and Rome. Extended periods without significant precipitation decrease the amount of  $\text{PM}_{2.5}$  removal because particles that are not occasionally washed from the leaves or needles are increasingly resuspended into the air. The model predicted this effect particularly during the long summer periods in Rome with only very little precipitation and may be responsible for less-efficient net removal from urban trees under climate change. Our analysis shows that the range of uncertainty in particle removal is large and that parameters have to be adjusted at least for major tree types if not only the species level. Furthermore, evergreen trees (broadleaved as well as coniferous) are predicted to be more effective at particle removal in northern regions than in Mediterranean cities, which is unexpected given the higher number of evergreens in southern cities. We discuss to what degree the effect of current  $\text{PM}_{2.5}$  abundance can be mitigated by species selection and which model improvements are needed.

**Keywords:** air quality, model evaluation, urban trees, deposition velocities, resuspension, metropolitan areas



## INTRODUCTION

The high concentration of particulate matter in the air is a problem relevant to human health, particularly in urban areas (World Health Organization, 2013). All combustion processes (such as by vehicle engines or furnaces for heating of buildings) contribute to the emission of fine particles (<10  $\mu\text{m}$  diameter), which represent a considerable hazard for people because they can penetrate deep into the lung tissue and enter the bloodstream (World Health Organization, 2006). The European Union set concentration limits for different sizes of particulate matter (PM) to be 40  $\mu\text{g m}^{-3} \text{ yr}^{-1}$  for  $\text{PM}_{10}$  and 25  $\mu\text{g m}^{-3} \text{ yr}^{-1}$  for  $\text{PM}_{2.5}$  (European Commission, 2008), but these are often exceeded in many European cities, demanding considerable measures to improve air quality (European Environment Agency, 2018). Recently, the European Commission has suggested application of the nature-based solutions concept, which includes preserving, managing, and restoring natural or modified ecosystems in order to respond to societal challenges and contribute to the human well-being and biodiversity (European Commission, 2015). A recommendation for the practical implementation of nature-based solutions is to design green infrastructures (Hansen et al., 2019), which are very efficient in providing ecosystem services for animals and people (Calfapietra and Cherubini, 2019).

Trees remove airborne PM by deposition on leaf, bark, and branch surfaces that is later on washed off by rainfall or deposited on the ground with senescent tissue (Beckett et al., 1998; Janhäll, 2015; Cai et al., 2017). Although bark and branches can substantially contribute to total deposition, smaller particles are preferentially captured by foliage (Xu et al., 2019). Thus, deciduous trees remove pollutants from the air primarily during the vegetative (leaf-on) period, which is a relatively short period compared to the whole year of activity by evergreen plants. The length of the vegetative period varies by geographic location because it is mainly controlled by light and temperature (Badeck et al., 2004; Forrest and Miller-Rushing, 2010). The capacity to remove fine PM depends on the leaf area, also considering phenological transition phases (Wang et al., 2015) as well as on leaf surface properties that are species-specific (Sæbo et al., 2012; Zhang W. et al., 2017; Shao et al., 2019). The actual deposition rate is then modified by weather conditions, such as wind speed or precipitation regime (Schaubroeck et al., 2014) as well as pollution concentration (Lu et al., 2018). Needles of conifers are considered more efficient than broadleaves in removing fine PM because of their shape, abundance of waxes on their surfaces, and their surface structure (Chen et al., 2017; Zhang W. et al., 2017; Muhammad et al., 2019). Species-specific foliage properties also determine how strongly deposited particles are stuck to the leaf and how easily they are resuspended into the air (Blanusa et al., 2015; Chen et al., 2017; Zhang W. et al., 2017).

However, deposition models such as i-Tree Eco (Hirabayashi et al., 2015) use one single value for deposition velocity and assume the same resuspension behavior for all tree types. The only difference that may be considered between deciduous and evergreen trees is related to the amount and duration of leaf area (Tiwary et al., 2016). This limitation is due to the uncertainty of quantification of leaf-property impacts, mostly

because of the absence of measurements for many species. Also, if measurements are available, they are not recorded under standardized environmental boundary conditions. Therefore, models generally cannot be run with species-specific parameters; instead, values may be selected rather arbitrarily (Peters and Eiden, 1992; Lovett, 1994).

To estimate the relative performance of coniferous and broadleaved trees (deciduous and evergreen), we investigated the sensitivity of calculated fine particle ( $\text{PM}_{2.5}$ ) removal to parameter settings in different environments along a latitudinal gradient that also represents a gradient in temperature and precipitation (Berlin, Munich, and Rome) during 2013–2015. The range of locations provides differences in precipitation, wind speed, and air pollution, which are likely to influence the extent of deposition and resuspension. We are therefore addressing the following objectives: (1) Investigating the dependence of mechanisms related to net pollution removal (deposition, washing, and resuspension) on climate. With this objective we are also investigating responses under potential climate changes which are likely to be accompanied with changes in rainfall patterns favoring long dry and warm periods (Giannakopoulos et al., 2009). (2) Assessing the impact of pollution levels and temporal dynamics on net particle removal by tree types which differ in basic foliage properties (Xiao et al., 2015). Based on the results, we will finally discuss how species selection can affect pollution removal performances in the three cities and suggest model modifications to improve the representation of deposition, resuspension, and removal of particulate matter.

## METHODS

### Model Description

We calculated the deposition flux of  $\text{PM}_{2.5}$  according to the method used in the i-Tree Eco model (Hirabayashi et al., 2015):

$$f_t = Vd_t \times C \times \text{LAI} \times 3600 \quad (1)$$

$$R_t = (A_{t-1} + f_t) \times \frac{rr_t}{100} \quad (2)$$

$$A_t = (A_{t-1} + f_t) - R_t \quad (3)$$

$$F_t = f_t - R_t \quad (4)$$

where  $f_t$  is the  $\text{PM}_{2.5}$  flux at time  $t$  ( $\text{g m}^{-2} \text{ h}^{-1}$ ),  $C$  is pollutant concentration ( $\text{g m}^{-3}$ ), and  $Vd_t$  is the deposition velocity at time  $t$  ( $\text{m s}^{-1}$ ) that is calculated from the wind speed (windSp) as  $vds \times \text{windSp}^\alpha$ , with  $vds$  being the “specific deposition velocity.” It should be noted that this model neglects the deposition on bark and branches for simplification reasons. The values are based on regression equations that are developed from the literature specifically for each tree type (see next paragraph).  $C$  is the  $\text{PM}_{2.5}$  air concentration ( $\text{g m}^{-3}$ ),  $\text{LAI}$  is the leaf-area index,  $R_t$  is the  $\text{PM}_{2.5}$  flux resuspended in the atmosphere at time  $t$  ( $\text{g m}^{-2} \text{ h}^{-1}$ ),  $A_{t-1}$  is the  $\text{PM}_{2.5}$  accumulated on leaves at time  $t$  ( $\text{g m}^{-2} \text{ h}^{-1}$ ) depending on previous deposition as well as precipitation,  $rr_t$  is the relative amount deposited  $\text{PM}_{2.5}$  that is resuspended at a specific wind speed at time  $t$  (%) which has been defined

**TABLE 1** | Deposition velocities for different wind-speed classes for deciduous broadleaved trees derived from published data.

Wind speed (m s <sup>-1</sup> )	1	3	6	8.5	10
<i>Quercus petraea</i> (Matt.) Liebl. <sup>1</sup>		0.831	1.757	3.134	
<i>Alnus glutinosa</i> (L.) Gaertner <sup>1</sup>		0.125	0.173	0.798	
<i>Fraxinus excelsior</i> (L.) <sup>1</sup>		0.178	0.383	0.725	
<i>Eucalyptus globulus</i> (Labill.) <sup>1</sup>		0.018	0.029	0.082	
<i>Ficus microcarpa</i> (L.) <sup>1</sup>		0.041	0.098	0.234	
<i>Acer campestre</i> (L.) <sup>2</sup>	0.03	0.08		0.46	0.57
<i>Sorbus intermedia</i> (Ehrh.) Pers. <sup>2</sup>	0.04	0.39		1.82	2.11
<i>Populus deltoides</i> × <i>trichocarpa</i> (Beaupré) <sup>2</sup>	0.03	0.12		1.05	1.18
Average	0.03	0.22	0.49	1.04	1.29

<sup>1</sup>Freer-Smith et al., 2004; <sup>2</sup>Beckett et al., 2000.

according to the i-tree model standards (see **Table S2** and next paragraph), and  $F_t$  is the net  $PM_{2.5}$  removal at time  $t$  after considering resuspension.

Deposition velocities are described as a function of wind speed, which we derived from prior-published measurements (Beckett et al., 2000; Freer-Smith et al., 2004; Pullman, 2009). First, we separated measurements into those carried out at conifers and those at broadleaf trees (**Tables 1, 2**). Then, we developed regression functions separately for the coniferous and broadleaf tree type, relating velocity and wind speed (**Figure 1**). For broadleaf evergreen trees (mostly species originating from southern Europe), we assumed the same deposition velocity as that of broadleaf deciduous trees because the deposition process seems to depend more on leaf shape (needle vs. flat leaf) than on other differences that might characterize evergreen vs. deciduous broadleaves. In any case, literature information is not sufficient to derive a separate function for evergreen broadleaves. With this differentiation, our model approach varies from the original i-Tree model which only uses one relation for all trees (and one that is similar to that of broadleaf trees). Resuspension also depends on wind speed. As in the i-Tree Eco model, a specific resuspension rate is assumed for each of 13 specific wind speed classes ( $rr_i$ ). This stepwise dependency function has first been described in the i-Tree Eco documentation (Hirabayashi et al., 2015). Finally, washing from the leaves (and thus final deposition) is calculated when precipitation events are higher than the maximum water storage capacity of the canopy, which is defined by potential leaf water storage  $plws$  ( $mm\ m^{-2}$ ) (leaf water storage =  $plws \times LAI$ ). If such an event occurs, all  $PM_{2.5}$  accumulated on leaves is assumed to be washed off and  $A_{t-1}$  is set to 0 (Hirabayashi et al., 2015).

### Site-Specific Parameterization

Apart from general parameterizations that are assumed valid for all tree types and sites, phenology parameters are set specifically for the investigated region. This includes the following parameters: (1) “maximum LAI” which is the LAI value achieved in the vegetation period when leaves are fully developed and not senescent; (2) leaf-on and leaf-off dates that indicate the start of flushing or leaf senescence, respectively; and

**TABLE 2** | Deposition velocities for different wind-speed classes for coniferous trees derived from published data.

Wind speed (m s <sup>-1</sup> )	1	3	6	8.5	10
<i>Pseudotsuga menziesii</i> (Mirb.) Franco <sup>1</sup>		1.269	1.604	6.04	
<i>Pinus nigra</i> (Arnold) <sup>2</sup>	0.13	1.15	19.24	28.05	
<i>Cupressocyparis</i> × <i>lexlandii</i> (Dellim.) <sup>2</sup>	0.08	0.76	8.24	12.2	
<i>Pinus strobus</i> (L.) <sup>3</sup>	0.0108				
<i>Tsuga canadensis</i> (L.) Carrière <sup>3</sup>	0.0193				
<i>Pseudotsuga japonica</i> (Shiras.) Beissn. <sup>3</sup>	0.0058				
<i>Picea abies</i> (L.) Karst. <sup>5</sup>	0.0189–0.038				
Average	0.04	1.06	1.60	11.1	20.1

<sup>1</sup>Freer-Smith et al., 2004; <sup>2</sup>Beckett et al., 2000; <sup>3</sup>Pullman, 2009.

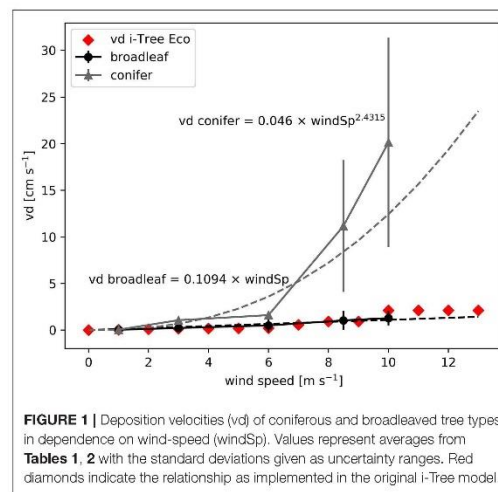


**FIGURE 1** | Deposition velocities ( $vd$ ) of coniferous and broadleaved tree types in dependence on wind-speed ( $windSp$ ). Values represent averages from **Tables 1, 2** with the standard deviations given as uncertainty ranges. Red diamonds indicate the relationship as implemented in the original i-Tree model.

(3) the length of the transition periods. We parameterized leaf-on and leaf-off dates as the average of the dates of first and last frost events ([www.weatheronline.co.uk](http://www.weatheronline.co.uk)). For Berlin, the day-of-year (doy) leaf-on and leaf-off dates are April 2nd (doy 92) and November 1st (doy 305); for Munich, April 5th (doy 95) and November 4th (doy 308); and for Rome, February 27th (doy 58) and December 2nd (doy 336). Furthermore, we assumed a maximum LAI of 3 and a 30-days transition period in the spring and fall, during which trees gradually produce or lose foliage. The maximum LAI has been set equal to all tree types despite conifers are usually considered to have a higher LAI (more than 6) than broadleaf trees (around 3–5) (Teske and Thistle, 2004; Peters et al., 2010). However, LAI in urban areas has been determined as considerably lower than in closed woodlands (Klingberg et al., 2017) with air pollution being a possible reason (Gratani and Varone, 2007). In fact, values for deciduous trees are commonly reported to be around 3 (Gratani and Varone, 2007; Öztürk

**TABLE 3** | Seasonal and yearly PM<sub>2.5</sub> average concentration.

PM <sub>2.5</sub> ( $\mu\text{g m}^{-3}$ )	2013					2014					2015				
	Winter	Spring	Summer	Autumn	Year	Winter	Spring	Summer	Autumn	Year	Winter	Spring	Summer	Autumn	Year
Berlin	24.7	16.1	10.9	14.9	16.7	28.7	15.4	14.0	25.4	20.9	21.7	13.5	13.2	19.4	16.9
Munich	20.5	17.0	11.0	14.8	15.8	16.8	12.4	11.2	12.9	13.3	16.1	11.9	11.6	13.0	13.2
Rome	21.4	12.3	12.8	20.0	16.6	19.7	11.9	11.3	19.5	15.6	19.6	12.5	12.8	22.0	16.7

**TABLE 4** | Seasonal and yearly cumulative precipitation.

Rain (mm)	2013					2014					2015				
	Winter	Spring	Summer	Autumn	Year	Winter	Spring	Summer	Autumn	Year	Winter	Spring	Summer	Autumn	Year
Berlin	98	154	168	143	564	54	137	158	69	418	88	81	132	158	458
Munich	114	276	213	134	737	59	158	306	164	688	88	319	119	136	662
Rome	285	123	27	270	706	343	108	128	315	893	212	110	86	154	562

**TABLE 5** | Seasonal and yearly average wind speed.

Wind speed ( $\text{m s}^{-1}$ )	2013					2014					2015				
	Winter	Spring	Summer	Autumn	Year	Winter	Spring	Summer	Autumn	Year	Winter	Spring	Summer	Autumn	Year
Berlin	3.4	3.2	2.9	3.5	3.3	3.8	3.1	2.9	3.4	3.3	4.0	3.6	3.6	3.7	3.7
Munich	3.1	2.9	2.4	2.6	2.7	2.6	2.7	2.6	2.9	2.7	3.5	3.1	2.5	3.1	3.1
Rome	2.6	2.3	2.0	2.0	2.2	2.3	2.1	2.1	2.0	2.1	2.2	2.1	1.9	1.8	2.0

et al., 2015; Massetti et al., 2019). On the other hand, pines, which are the most abundant conifers in the Mediterranean region (Grote et al., 2016) as well as in the forests around Berlin (Tigges et al., 2017) are also assumed to have a leaf area around 3 (Bréda, 2003). The same holds for evergreen oaks, which are representative for Mediterranean broadleaf evergreen trees (Escudero and Mediavilla, 2003). For this reason, we set LAI to 3 for all tree types although we acknowledge that regional and species-specific variation is relatively large.

### Driving Variable Derivation

PM<sub>2.5</sub>-concentration data were taken from the i-Tree Eco database, which contains pollution data from the European Environmental Agency. The pollution level is similar in all three cities, with Berlin having slightly higher concentrations, particularly in 2014 (Table 3). Seasonality of PM<sub>2.5</sub> concentration is not very expressed in either of the sites, but the pollution minimum is in the summer, while the highest PM<sub>2.5</sub> concentrations occur in the winter (except in 2015 in Rome, which had the highest concentrations in autumn). The reason for the maximum in winter is the increased residential heating and the longer lifetime of PM precursors. Hourly precipitation and wind-speed data were selected from airport-station records in Berlin (Tegel) and Munich (München-Flughafen) and from the weather station in Castelporziano for Rome. These weather stations are all located at the city border, some distance from the city centers. We assume that a similar relative position is better suited for our purpose to compare the different locations,

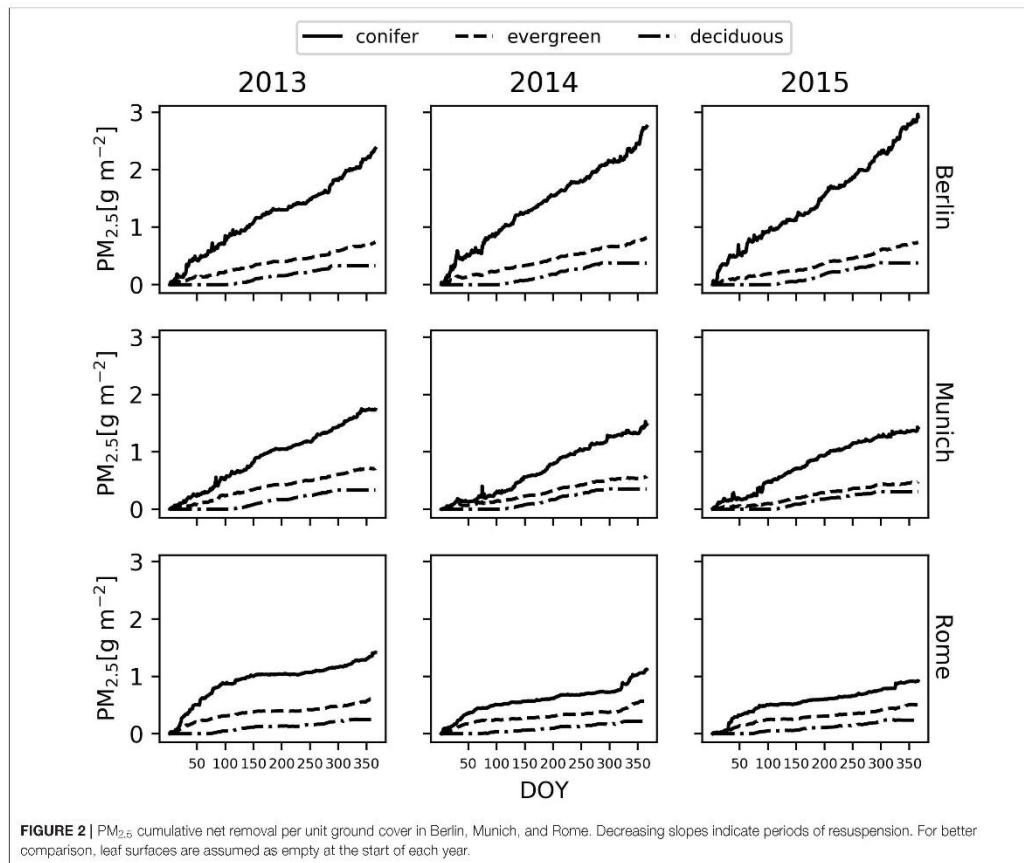
since wind speed is considerably heterogeneous within a city (Levy and Hanna, 2011; Drew et al., 2013). In Rome, spring, and summer precipitation is considerably lower than that in the winter and autumn, while the situation is almost the opposite in Munich, where the highest rainfalls occur in the spring. The overall precipitation in Berlin is about a third less than that at the other two sites (Table 4). Also, there is a clear gradient in wind speed from Berlin to Munich and Rome, with the highest air movements mostly in the autumn and winter and the lowest in the summer. In Rome, there is hardly any seasonal variation, unlike at the German sites, which show some growing-season variation (Table 5). Modeling simulations were performed for the years 2013–2015.

### RESULTS

We found that the highest PM<sub>2.5</sub> deposition was in Berlin, followed by Munich and Rome. The difference is particularly large for conifers, which remove seven times more air pollutants than the broadleaf deciduous trees in Berlin, and about five times more than in Munich and Rome, respectively (Table 6). In relative terms, the broadleaf evergreen trees remove twice as much air pollutants as broadleaf deciduous trees. The difference is smallest in Munich (factor 1.8) and largest in Rome (factor 2.5) with Berlin close to Munich (factor 2.1). Also, the data show inter-annual differences of  $\pm 24\%$  over the 3 years for conifers,  $\pm 7\%$  broadleaf evergreens, and  $\pm 2\%$  broadleaf deciduous, indicating that not only species properties but also air-pollution

**TABLE 6** | Annual  $PM_{2.5}$  removal by different tree types in three cities.

$PM_{2.5}$ ( $g\ m^{-2}\ yr^{-1}$ )	Berlin			Munich			Rome		
	Conifer	Evergreen	Deciduous	Conifer	Evergreen	Deciduous	Conifer	Evergreen	Deciduous
2013	2.4	0.7	0.3	1.7	0.7	0.3	1.4	0.6	0.2
2014	2.8	0.8	0.4	1.5	0.6	0.4	1.1	0.6	0.2
2015	2.9	0.7	0.4	1.4	0.5	0.3	0.9	0.5	0.2
Average	2.7	0.8	0.4	1.5	0.6	0.3	1.2	0.6	0.2



distribution and seasonal weather conditions are influencing PM removal (Table 6, Figure 2).

Since bark and branch deposition is not considered, deciduous trees do not deposit particles outside the vegetation period, i.e., in the winter (the deposition in Rome during this time occurs because the vegetation period here prolongs into the winter period). For the other two tree types, the seasonal pattern is similar for Berlin and Rome, with the highest deposition rates

in the autumn and winter, but different for Munich, where these months are often those with the lowest deposition rates (with some exceptions, e.g., high removal rate for Berlin in summer 2015, for Rome in spring 2013, and for Munich in autumn 2015) (Figure 3). A closer look at the daily net removal rates shows that it is in a range between  $-0.01$  and  $0.02\ g\ m^{-2}\ h^{-1}$  for conifers which perform maximum deposition rates of up to  $0.04\ g\ m^{-2}\ h^{-1}$  obtained in Munich, summer 2014 (as shown in



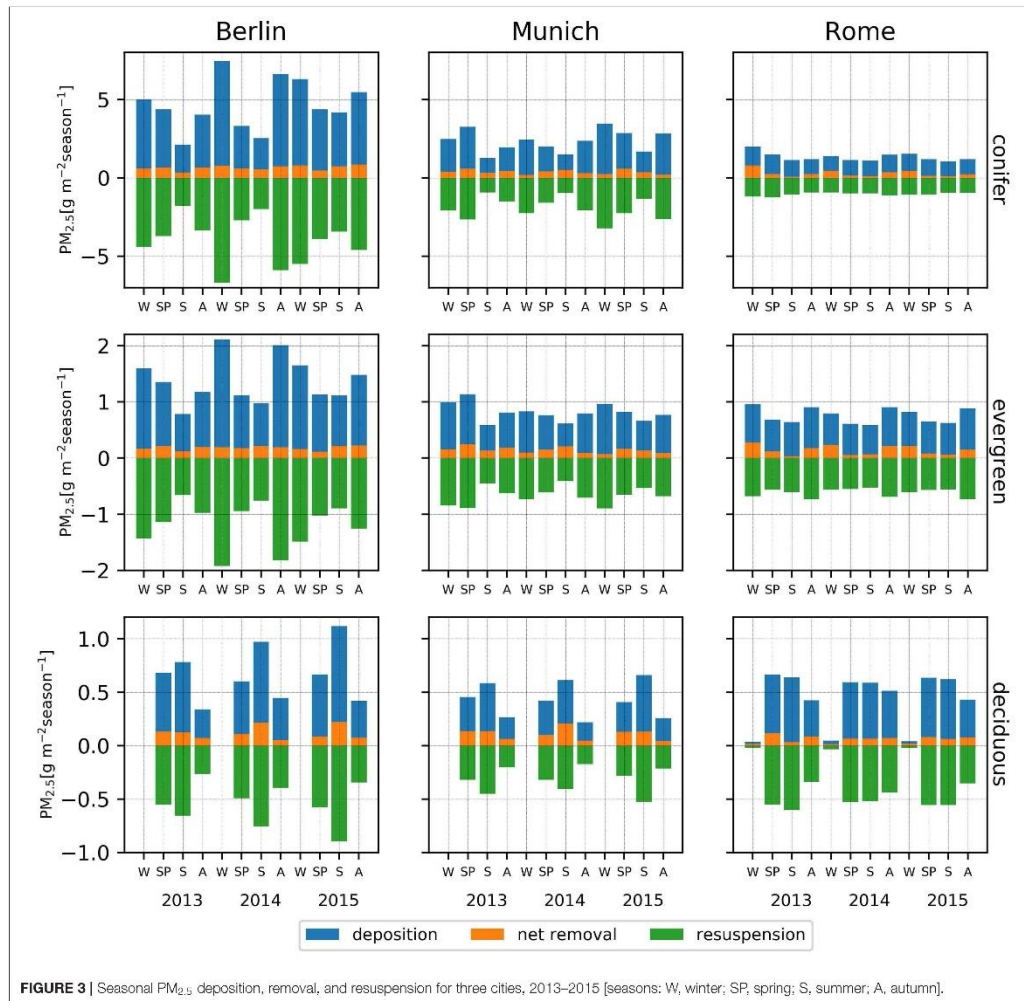
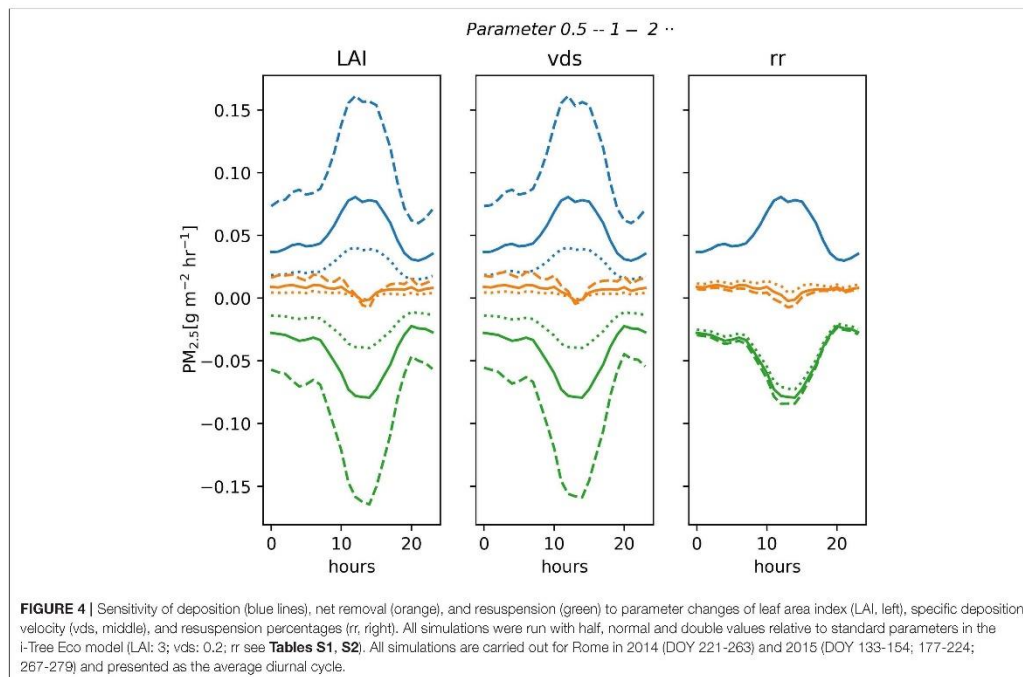


**Figure S1).** For evergreen broadleaf trees the net removal only varies between  $-0.002$  and  $+0.002 \text{ g m}^{-2} \text{ h}^{-1}$  and is even smaller for deciduous broadleaf trees ( $-0.001$  and  $+0.001 \text{ g m}^{-2} \text{ h}^{-1}$ ) (see **Figures S1–S3**).

There are only very few measurements that can serve to evaluate the calculations presented here. Fares et al. (2016) carried out an eddy-flux investigation of deposition in Rome on a Holm oak (*Quercus ilex* L.) forest during 2 years that are also part of our analysis (2014 and 2015). The averaged data from the measurements during the whole vegetation period are thus shown together with the calculated mean diurnal flux of  $PM_{2.5}$  into and from the canopy (see **Figure S4**).

The calculated deposition increases during the day with a peak at mid-day, closely following the development of wind speed. In parallel also resuspension rises because it depends on deposition. In the absence of rainfall, as in the case of Rome in summer, particulate matter is not washed off from leaves which leads to large accumulation, increased resuspension, and thus to negative values of net removal in particular during the middle hours of the day since it is more sensitive to higher wind speeds than deposition. A brief sensitivity analysis of the major influencing factors in Rome is shown in **Figure 4**: Both, deposition and resuspension fluxes are very sensitive to changes in LAI and deposition velocity, which had been modified



by varying  $vds$  as demonstrated in **Table S1**. Changing the resuspension sensitivity to wind speed does not affect deposition at all and has only a relatively small effect on resuspension. This is because a larger flux rate leads to a new equilibrium with smaller amounts of deposited matter and thus to smaller absolute resuspension rates (and vice versa). A comparison between sites with corresponding simulations is shown in **Figures S5–S7**. The influence of assuming different thresholds at which the particulates are washed off is demonstrated in **Figure 5** for different  $plws$  values: The results show again a relatively low sensitivity of overall results but subtle differences between the sites, indicating that the efficacy of a specific threshold is higher at sites with a more even precipitation pattern (Munich) than at sites with more heterogeneous rainfall distribution (Rome).

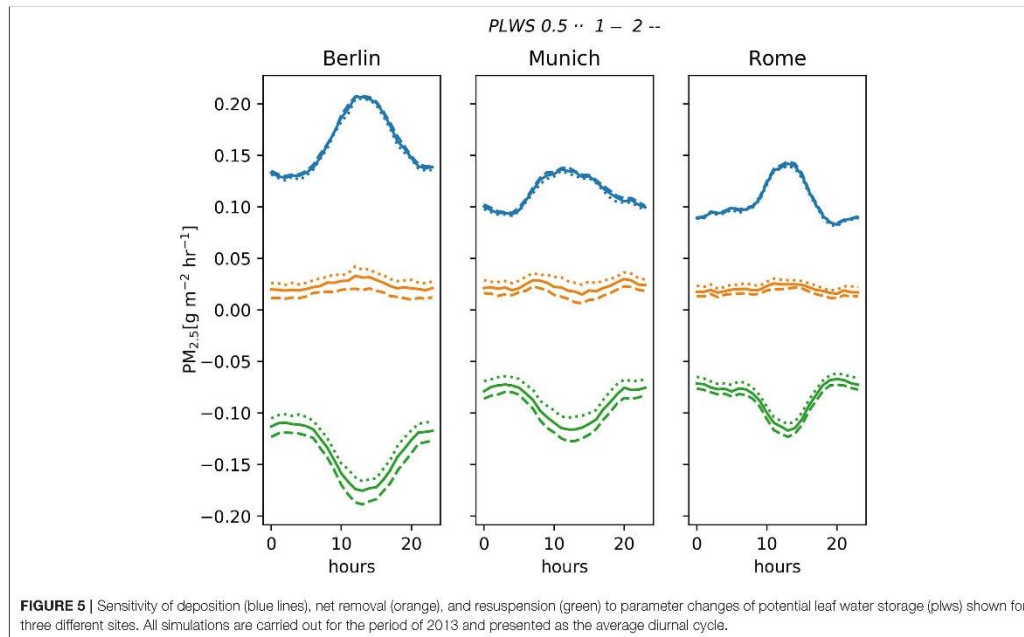
The higher  $PM_{2.5}$  concentration and wind speed promote a larger dry deposition in Berlin compared to the other cities. The effect is particularly expressed in winter and autumn, when repeated rainfall events also provide a regular washing of the leaves, increasing the overall effectiveness of conifers. Thus, the highest seasonal net removal rates calculated was for conifers in Berlin during the winter of 2014/2015. Although pollution and wind speed are somewhat smaller, the overall net removal for broadleaf deciduous trees in Munich is almost as high in Berlin. Here, the reason is that summer precipitation in Munich is much higher and thus resuspension in summer is smaller. In Rome, resuspension during summer is particularly high and wind speed is

relatively low, both resulting a smaller  $PM_{2.5}$  removal compared to that in the other cities. In addition, the vegetation period in Rome is longer, starting early in spring and sometimes reaching into the winter period. Therefore, the spring removal rates in Rome are more similar for broadleaf deciduous and evergreen trees than those in the other two cities where leaves were not fully developed at the time.

## DISCUSSION AND CONCLUSIONS

### Particulate-Matter Deposition and Comparison With Literature Data

The  $PM_{2.5}$ -deposition difference that we obtained from the model for leaves from conifers and broadleaf trees is quite similar to that reported by Chen et al. (2017), who found an accumulation of particles on conifers that was up to six times the amount of that on broadleaf trees measured in summer through autumn (with no distinction between evergreen and deciduous broadleaves). This result is related to leaf size, with smaller leaves being more effective per m<sup>2</sup> leaf surface (Xu et al., 2017; Weerakkody et al., 2018b), and surface properties such as roughness (Shao et al., 2019) as well as the occurrence of hairs (trichomes) (Chen et al., 2017; Muhammad et al., 2019) and waxes (Wang et al., 2015). Findings are, however, not always homogeneous as for example Leonard et al. (2016) found less PM accumulation on small and needle-like leaves,



which might be related to the specific trait combination in the investigated species. In particular the occurrence of waxes, which are prominent in conifers, increases the deposition capacity due to their lipophilic properties that are able to bind particles composed of organic pollutants (Dzierzanowski et al., 2011). Since some broadleaved trees also develop waxes and particularly hairy trichomes such as for example *Platanus acerifolia* (Aiton) Willd. (Li et al., 2019), a large variation can be found in the literature. Chen et al. (2017) indicate that the accumulated  $PM_{2.5}$  for conifers is in the range of  $10\text{--}30 \mu\text{g cm}^{-2}$  and for broadleaf trees,  $3\text{--}17 \mu\text{g cm}^{-2}$ . Similar values are also found for the broadleaf-evergreen Holm oak (*Quercus ilex* L.) (Sgrigna et al., 2015), which accumulated 4, 13, and  $2 \mu\text{g cm}^{-2}$  in January, August, and October, respectively.

On a site scale, the eddy-flux based particle exchange measurement carried out in Rome during a period that falls within the time period investigated here, were similar in range and pattern compared with our model results (Fares et al., 2013) although resuspension is calculated to be lower (see Figure S4). Since the net removal as indicated by the measurements is considerably negative, particles may not only originate from previous plant deposition but also from other surfaces in the vicinity (Yang et al., 2016).

In comparison with other model approaches, the differentiated parametrization also seems to be appropriate. For example,  $PM_{2.5}$  deposition in Leicester, UK, estimated with a Computational Fluid Dynamics model required a deposition velocity of  $0.64 \text{ cm s}^{-1}$  which is about 3-fold the

value used in i-Tree for the same wind speed as indicated in the study (Jeanjean et al., 2016). This indicates that the i-Tree underestimates deposition due to its too coarse parameterization (although other influences such as the differentiation of tree types have not been tested in this study).

### Effect of Weather Conditions on Dry Deposition and Resuspension

The deposition of particles on tree leaves changes during the year because not only PM concentration but also weather conditions such as precipitation and wind speed affect the deposition and resuspension of particles on and from leaves (Mori et al., 2015). Thus, although the PM concentration is higher in all cities in the winter and autumn, the deposition does not always follow the same pattern. The models assume that sufficient rainfall resets the potential deposition storage to zero, and thus precipitation events are a precondition to enable particle removal over a prolonged period. For example, the effect dominated the simulations for the summer 2014 in Munich, as high precipitation continuously increased cumulative deposition. In contrast, long dry periods such as those that frequently occur in Rome lead to a high resuspension rate, decreasing the actual net PM removal. This is more evident when LAI is higher and rain events are not able to wash off particles from foliage, leaving a larger amount that can be resuspended. Another aspect that needs to be considered is that wind speed and PM concentration are generally negatively correlated diurnally, which may even lead to a net emission during mid-day when wind speed is highest [as visible for



some parameter combinations for Rome (Figure 4) and Munich (Figure 5, Figures S5–S7).

This highlights the importance of including more mechanistic processes into the PM removal calculation that account for species-specific and rainfall-intensity dependent variation. For example, it might be favorable to consider that rainfall intensities differ within a canopy, with upper-canopy layers wetted first and lower layers affected only after prolonged precipitation. For example, Xu et al. (2017) found that PM wash-off rates increase with cumulative rainfall up to a maximum amount of 12.5 mm of rain removing 51 to 70% of PM accumulation, with a small amount of particles still retained on the leaf surface. Also, the removal of deposited PM from leaves depends on species-specific properties, as trichomes, or rough surfaces hold PM much more tightly, requiring more water for washing off (Hofman et al., 2014; Blanusa et al., 2015; Xu et al., 2017).

### Structural and Seasonal Influences on Particle Deposition

Conifers are well-known to remove more airborne PM than evergreen or deciduous broadleaved species (Sun et al., 2014; Khan and Perlinger, 2017; Zhang Z. et al., 2017). This is partly due to their crown shape, as cone-shaped conifers are commonly more exposed to turbulent air movements than spherical broadleaved trees (Beckett et al., 2000). Additionally, narrow conifer needles are more efficient capturing particles compared to flat leaves as expressed by the Stoke number, which describes the ability of stopping a particle in relation to the leaf characteristics (Beckett et al., 2000). Other leaf characteristics affect deposition and are specific to species rather than specific to coarsely lumped tree types. Such properties include in particular surface roughness and trichome as well as wax abundance (Sæbø et al., 2012; Räsänen et al., 2013; Chen et al., 2017; Muhammad et al., 2019). Another leaf characteristic that is mostly not considered in models is that deciduous-tree species differ in their leafing behavior, with most species establishing their leaves at the beginning of the vegetation period while some produce new leaves continuously. The latter type will thus also continuously refresh its deposition capacity.

### Model Limits and Potential Improvements

Given the arguments for species- and size-specific differences, we can now define a number of uncertainties in the model approach. In particular, parameters could be selected specifically by tree type or species that are not currently differentiated (i.e., species-specific deposition velocities, resuspension, and washing threshold according to leaf characteristics). The importance of this issue, the connected uncertainty, as well as the potentially large impacts have been demonstrated before (Pace et al., 2018). For the most sensitive parameter which is PM-deposition velocity, it is important to distinguish at least between deciduous, broadleaf evergreen, and conifer trees (Khan and Perlinger, 2017). It should be noted, however, that a functional relation between velocity and wind speed that considers species level leaf traits would be preferable (Chiam et al., 2019). Other parts of the deposition process might also be improved although the overall effect seems to be relatively

small (judged on the environmental conditions simulated). For example, the dependence of resuspension rates on wind speed might better be defined on a species level considering various foliage traits (Pullman, 2009; Buccolieri et al., 2018). Also, washing of deposited PM from leaves should principally depend on leaf properties in addition to amount, frequency, and intensity of rain and should not be represented by a single threshold value of rainfall per day (Weerakkody et al., 2018a). Finally, the calculation of deposition and net pollutant removal could be improved, considering a vertically distributed leaf area (e.g., Grote and Reiter, 2004), which could enable a differentiation into fractions of leaves subjected to specific wind speeds and intercepted precipitation (Teske and Thistle, 2004).

The suggested modifications can be easily introduced into existing approaches such as the i-Tree Eco model. Considering a differentiation of velocity functions by tree groups is likely to increase the accuracy of deposition results, which is particularly important if it is coupled to regional climate/air chemistry models (Cabaraban et al., 2013). If not coupled to a separate vegetation model, such air chemistry models simulate deposition velocity by estimating a number of resistances that do not depend on tree species properties (Khan and Perlinger, 2017). Thus, the uncertainty related to these simplified assumptions is very high, which has recently been criticized (Saylor et al., 2019). The results presented here may help to mend this problem by providing at least type specific dependencies as has been suggested by Hicks et al. (2016).

Another line of improvement should also be noted, which is the neglectation of branch and bark surfaces in estimates of pollutant removal. While the deposition at these surfaces may be indeed negligible for conifers with needles that densely cover twigs and a canopy that shields stems from pollutants, it has been shown to be considerable at least for some deciduous trees (Xu et al., 2019). Neglecting this effect might lead to serious biases during winter. In principle, however, separately accounting for different surfaces and velocities in Equation (1) (that also need to be species- or tree-type specific) could serve to consider this term.

### Tree-Type Distribution in Europe and Species-Selection Criteria

The efficiency of particle removal depends not only on species-specific properties but also on weather and air-pollution boundary conditions, which interact with vegetation period length. Judging different species regarding their ability to remove PM<sub>2.5</sub> therefore requires evaluation of species-specific or tree-type-specific properties in their particular growing conditions. Also, other ecosystem services such as the mitigation of air temperature extremes, and restriction from site conditions as for example shade tolerance and resistance against pollution may restrict the freedom of decisions and need to be considered. In this respect, it should be noted that evergreen trees are more abundant in Mediterranean cities than in northern regions, where deciduous trees are much more prominent (Grote et al., 2016). Deciduous trees are preferred along the roads because



their shading effect is limited to the summer period while in the winter, higher radiation input is welcomed. Nevertheless, in order to increase the ecosystem service of air-pollution removal, conifers, and other evergreen trees might be planted more often in parks. With the simulations presented here, we provide some evidence that conifer trees would be particularly effective in cities with higher precipitation and wind speed such as Berlin, while long dry periods such as those that are frequently observed in Rome decrease the deposition capacity, particularly for conifers. This does not mean that conifers are not preferable in Rome too, if PM<sub>2.5</sub> deposition would be the decisive criteria because they still remove at least about two times more particles than broadleaf evergreen and more than four times as much as broadleaf deciduous trees. However, since the modeled difference is not as large particularly during summer, other ecosystem services such as a higher transpiration rate and thus more cooling might be more decisive. The case study of Munich additionally demonstrates that conifers and other evergreens have limited advantages if the winter period is relatively dry and windy as in the simulated example years. In this case (similar to Rome in the summer), the deposition outside the vegetation period is low because of a high resuspension rate. Since shading in winter might also be a disadvantage, deciduous trees might thus be preferable at places where the pollution removal effect is not so urgently needed.

### Future Perspectives on Modeling PM Removal by Urban Trees

Analysis of past published studies and current model calculations have demonstrated that the uncertainties in calculating PM deposition are particularly high with regard to deposition velocities and degree to which particles are stuck on leaf surfaces. For the first issue, it is recommended to determine species-specific deposition velocities by direct measurements at the leaf or canopy scale, e.g., by the eddy-covariance technique. To improve the second issue, experimental studies are needed that relate removal efficiency to the amount of water that hits the leaf surfaces. The precision of models can be further improved by using stratified canopies that provide layer-specific wind speed and precipitation.

Finally, we would like to point out that not only particles but also dangerous gases such as O<sub>3</sub>, NO<sub>2</sub>, and SO<sub>2</sub> are deposited on or taken up by trees. Since uptake requires the consideration of stomatal conductance, the processes need to be connected

to photosynthesis and water-use efficiency, which would then also allow estimation of the effects of other ecosystem services such as shading and evaporative cooling. Such a model, as has been recently suggested by Fares et al. (2019), can be coupled with meteorological and soil–water balance models in order to consider the effect of future climate changes (windstorms, intense precipitation, prolonged drought) on urban-trees performance.

### DATA AVAILABILITY STATEMENT

Publicly available datasets were analyzed in this study. This data can be found here: <https://www.sciencedirect.com/science/article/pii/S0269749116310685?via%3DIihub>.

### AUTHOR CONTRIBUTIONS

RP has designed and carried out the research, implemented the model code, and written major parts of the text. RG contributed significantly to the design, discussion and writing of the text and supervised the research.

### FUNDING

This research was supported by the Graduate School for Climate and Environment (GRACE). We also acknowledge support by the Deutsche Forschungsgemeinschaft and Open Access Publishing Fund of Karlsruhe Institute of Technology.

### ACKNOWLEDGMENTS

We thank the i-Tree support team and in particular David Nowak for assisting the model implementation, Silvano Fares for providing evaluation data, Francesco De Pino for his help in writing the code, Shade Amini, Gabriele Guidolotti, Chiara Baldacchini for the fruitful discussion on the methodology, Zhenyou Zhang for his help with the graphs, and the Graduiertenzentrum Weihenstephan of Technical University of Munich as well as the ENAGO company for the English editing.

### SUPPLEMENTARY MATERIAL

The Supplementary Material for this article can be found online at: <https://www.frontiersin.org/articles/10.3389/ffgc.2020.00026/full#supplementary-material>

### REFERENCES

- Badeck, F. W., Bondeau, A., Böttcher, K., Doktor, D., Lucht, W., Schaber, J., et al. (2004). Responses of spring phenology to climate change. *New Phytol.* 162, 295–309. doi: 10.1111/j.1469-8137.2004.01059.x
- Beckett, K. P., Freer-Smith, P. H., and Taylor, G. (1998). Urban woodlands: their role in reducing the effects of particulate pollution. *Environ. Pollut.* 99, 347–360. doi: 10.1016/S0269-7491(98)00016-5
- Beckett, K. P., Freer-Smith, P. H., and Taylor, G. (2000). Particulate pollution capture by urban trees: effect of species and windspeed. *Glob. Chang. Biol.* 6, 995–1003. doi: 10.1046/j.1365-2456.2000.00376.x
- Blanusa, T., Fantozzi, F., Monaci, F., and Bargagli, R. (2015). Leaf trapping and retention of particles by holm oak and other common tree species in Mediterranean urban environments. *Urban For. Urban Green* 14, 1095–1101. doi: 10.1016/j.ufug.2015.10.004
- Breda, N. J. J. (2003). Ground-based measurements of leaf area index: a review of methods, instruments and current controversies. *J. Exp. Bot.* 54, 2403–2417. doi: 10.1093/jxb/erg263
- Buccolieri, R., Santiago, J.-L., Rivas, E., and Sanchez, B. (2018). Review on urban tree modelling in CFD simulations: aerodynamic, deposition and thermal effects. *Urban For. Urban Green* 31, 212–220. doi: 10.1016/j.ufug.2018.03.003
- Cabaraban, M. T. I., Kroll, C. N., Hirabayashi, S., and Nowak, D. J. (2013). Modeling of air pollutant removal by dry deposition to urban trees using a WRF/CMAQ/i-Tree Eco coupled system. *Environ. Pollut.* 176, 123–133. doi: 10.1016/j.envpol.2013.01.006

- Cai, M., Xin, Z., and Yu, X. (2017). Spatio-temporal variations in PM leaf deposition: a meta-analysis. *Environ. Pollut.* 231, 207–218. doi: 10.1016/j.envpol.2017.07.105
- Calafapietra, C., and Cherubini, L. (2019). Green infrastructure: nature-based solutions for sustainable and resilient cities. *Urban For. Urban Green* 37, 1–2. doi: 10.1016/j.ufug.2018.09.012
- Chen, L., Liu, C., Zhang, L., Zou, R., and Zhang, Z. (2017). Variation in tree species ability to capture and retain airborne fine particulate matter (PM<sub>2.5</sub>). *Sci. Rep.* 7, 1–11. doi: 10.1038/s41598-017-03360-1
- Chiam, Z., Song, X. P., Lai, H. R., and Tan, H. T. W. (2019). Particulate matter mitigation via plants: understanding complex relationships with leaf traits. *Sci. Tot. Environ.* 688, 398–408. doi: 10.1016/j.scitotenv.2019.06.263
- Drew, D. R., Barlow, J. F., and Cockerill, T. T. (2013). Estimating the potential yield of small wind turbines in urban areas: a case study for greater London, UK. *J. Wind Eng. Ind. Aerod.* 115, 104–111. doi: 10.1016/j.jweia.2013.01.007
- Dzierzanowski, K., Popek, R., Gawronska, H., Saebø, A., and Gawronski, S. W. (2011). Deposition of particulate matter of different size fractions on leaf surfaces and in waxes of urban forest species. *Int. J. Phytoremed.* 13, 1037–1046. doi: 10.1080/15226514.2011.552929
- Escudero, A., and Mediavilla, S. (2003). Decline in photosynthetic nitrogen use efficiency with leaf age and nitrogen resorption as determinants of leaf life span. *J. Ecol.* 91, 880–889. doi: 10.1046/j.1365-2745.2003.00818.x
- European Commission (2008). *Directive 2008/50/EC on Ambient Air Quality and Cleaner Air for Europe*.
- European Commission (2015). *Nature-Based Solutions & Re-Naturing Cities*. Luxembourg.
- European Environment Agency (2018). *Air Quality in Europe - 2018 Report*. Luxembourg: European Environment Agency.
- Fares, S., Alivernini, A., Conte, A., and Maggi, F. (2019). Ozone and particle fluxes in a Mediterranean forest predicted by the AIRTREE model. *Sci. Tot. Environ.* 682, 494–504. doi: 10.1016/j.scitotenv.2019.05.109
- Fares, S., Matteucci, G., Scarascia Mugnozza, G., Morani, A., Calafapietra, C., Salvatori, E., et al. (2013). Testing of models of stomatal ozone fluxes with field measurements in a mixed Mediterranean forest. *Atmos. Environ.* 67, 242–251. doi: 10.1016/j.atmosenv.2012.11.007
- Fares, S., Savi, F., Fusaro, L., Conte, A., Salvatori, E., Aromolo, R., et al. (2016). Particle deposition in a peri-urban Mediterranean forest. *Environ. Pollut.* 218, 1278–1286. doi: 10.1016/j.envpol.2016.08.086
- Forrest, J., and Miller-Rushing, A. J. (2010). Toward a synthetic understanding of the role of phenology in ecology and evolution. *Philos. Trans. R. Soc. B. Biol. Sci.* 365, 3101–3112. doi: 10.1098/rstb.2010.0145
- Freer-Smith, P. H., El-Khatib, A. A., and Taylor, G. (2004). Capture of particulate pollution by trees: a comparison of species typical of semi-arid areas and North American species. *Water, Air, Soil Pollut.* 155, 173–187. doi: 10.1023/B:WATE.0000026521.99552.f0
- Giannakopoulos, C., Le Sager, P., Bindi, M., Moriondo, M., Kostopoulou, E., and Goodess, C. M. (2009). Climatic changes and associated impacts in the Mediterranean resulting from a 2°C global warming. *Glob. Planet. Change* 68, 209–224. doi: 10.1016/j.gloplacha.2009.06.001
- Gratani, L., and Varone, L. (2007). Plant crown traits and carbon sequestration capability by *Platanus hybrida* brot. in Rome. *Landscape Urban Plan.* 81, 282–286. doi: 10.1016/j.landurbplan.2007.01.006
- Grote, R., and Reiter, I. M. (2004). Competition-dependent modelling of foliage biomass in forest stands. *Trees Struct. Funct.* 18, 596–607. doi: 10.1007/s00468-004-0352-9
- Grote, R., Samson, R., Alonso, R., Amorim, J. H., Cariñanos, P., Churkina, G., et al. (2016). Functional traits of urban trees: air pollution mitigation potential. *Front. Ecol. Environ.* 14:1426. doi: 10.1002/fee.1426
- Hansen, R., Olafsson, A. S., van der Jagt, A. P. N., Rall, E., and Pauleit, S. (2019). Planning multifunctional green infrastructure for compact cities: What is the state of practice? *Ecol. Indic.* 96, 99–110. doi: 10.1016/j.ecolind.2017.09.042
- Hicks, B. B., Saylor, R. D., and Baker, B. D. (2016). Dry deposition of particles to canopies—a look back and the road forward. *J. Geophys. Res. Atmosph.* 121, 691–707. doi: 10.1002/2015JD024742
- Hirabayashi, S., Kroll, C. N., and Nowak, D. J. (2015). *i-Tree Eco Dry Deposition Model Descriptions*. Available online at: [http://www.itreetools.org/eco/resources/iTree\\_Eco\\_Dry\\_Deposition\\_Model\\_Descriptions.pdf](http://www.itreetools.org/eco/resources/iTree_Eco_Dry_Deposition_Model_Descriptions.pdf) (accessed April 4, 2019).
- Hofman, J., Wuyts, K., Van Wittenberghe, S., and Samson, R. (2014). On the temporal variation of leaf magnetic parameters: seasonal accumulation of leaf-deposited and leaf-encapsulated particles of a roadside tree crown. *Sci. Total Environ.* 493, 766–772. doi: 10.1016/j.scitotenv.2014.06.074
- Janhäll, S. (2015). Review on urban vegetation and particle air pollution – deposition and dispersion. *Atmos. Environ.* 105, 130–137. doi: 10.1016/j.atmosenv.2015.01.052
- Jeanjean, A. P. R., Monks, P. S., and Leigh, R. J. (2016). Modelling the effectiveness of urban trees and grass on PM<sub>2.5</sub> reduction via dispersion and deposition at a city scale. *Atmos. Environ.* 147, 1–10. doi: 10.1016/j.atmosenv.2016.09.033
- Khan, T. R., and Perlinger, J. A. (2017). Evaluation of five dry particle deposition parameterizations for incorporation into atmospheric transport models. *Geosci. Model Dev.* 10, 3861–3888. doi: 10.5194/gmd-10-3861-2017
- Klingberg, J., Konarska, J., Lindberg, F., Johansson, L., and Thorsson, S. (2017). Mapping leaf area of urban greenery using aerial LiDAR and ground-based measurements in Gothenburg, Sweden. *Urban For. Urban Green* 26, 31–40. doi: 10.1016/j.ufug.2017.05.011
- Leonard, R. J., McArthur, C., and Hochuli, D. F. (2016). Particulate matter deposition on roadside plants and the importance of leaf trait combinations. *Urban For. Urban Green* 20, 249–253. doi: 10.1016/j.ufug.2016.09.008
- Levy, J. I., and Hanna, S. R. (2011). Spatial and temporal variability in urban fine particulate matter concentrations. *Environ. Pollut.* 159, 2009–2015. doi: 10.1016/j.envpol.2010.11.013
- Li, Y., Wang, S., and Chen, Q. (2019). Potential of thirteen urban greening plants to capture particulate matter on leaf surfaces across three levels of ambient atmospheric pollution. *Int. J. Environ. Res. Public Health* 16:402. doi: 10.3390/ijerph16030402
- Lovett, G. M. (1994). Atmospheric deposition of nutrients and pollutants in North America: an ecological perspective. *Ecol. Appl.* 4, 629–650. doi: 10.2307/1941997
- Lu, S., Yang, X., Li, S., Chen, B., Jiang, Y., Wang, D., et al. (2018). Effects of plant leaf surface and different pollution levels on PM<sub>2.5</sub> adsorption capacity. *Urban For. Urban Green* 34, 64–70. doi: 10.1016/j.ufug.2018.05.006
- Massetti, L., Petralli, M., Napoli, M., Brandani, G., Orlandini, S., and Pearlmutter, D. (2019). Effects of deciduous shade trees on surface temperature and pedestrian thermal stress during summer and autumn. *Int. J. Biometeorol.* 63, 467–479. doi: 10.1007/s00484-019-01678-1
- Mori, J., Saebø, A., Hanslin, H. M., Teani, A., Ferrini, F., Fini, A., et al. (2015). Deposition of traffic-related air pollutants on leaves of six evergreen shrub species during a Mediterranean summer season. *Urban For. Urban Green* 14, 264–273. doi: 10.1016/j.ufug.2015.02.008
- Muhammad, S., Wuyts, K., and Samson, R. (2019). Atmospheric net particle accumulation on 96 plant species with contrasting morphological and anatomical leaf characteristics in a common garden experiment. *Atmos. Environ.* 202, 328–344. doi: 10.1016/j.atmosenv.2019.01.015
- Öztürk, M., Bolat, I., and Ergün, A. (2015). Influence of air–soil temperature on leaf expansion and LAI of *Carpinus betulus* trees in a temperate urban forest patch. *Agric. Forest Meteorol.* 200, 185–191. doi: 10.1016/j.agrformet.2014.09.014
- Pace, R., Biber, P., Pretzsch, H., and Grote, R. (2018). Modeling ecosystem services for park trees: sensitivity of i-Tree eco simulations to light exposure and tree species classification. *Forests* 9:89. doi: 10.3390/f9020089
- Peters, E. B., McFadden, J. P., and Montgomery, R. A. (2010). Biological and environmental controls on tree transpiration in a suburban landscape. *J. Geophys. Res. Biogeosci.* 115, 1–13. doi: 10.1029/2009JG001266
- Peters, K., and Eiden, R. (1992). Modelling the dry deposition velocity of aerosol particles to a spruce forest. *Atmos. Environ. Part A. Gen. Top.* 26, 2555–2564. doi: 10.1016/0960-1686(92)90108-W
- Pullman, M. R. (2009). *Conifer PM<sub>2.5</sub> deposition and re-suspension in wind and rain events* (Master thesis). Cornell University, Ithaca, NY, United States.
- Räsänen, J. V., Holopainen, T., Joutsensaari, J., Ndam, C., Pasanen, P., Rinnan, A., et al. (2013). Effects of species-specific leaf characteristics and reduced water availability on fine particle capture efficiency of trees. *Environ. Pollut.* 183, 64–70. doi: 10.1016/j.envpol.2013.05.015
- Saebø, A., Popek, R., Nawrot, B., Hanslin, H. M., Gawronska, H., and Gawronski, S. W. (2012). Plant species differences in particulate matter

- accumulation on leaf surfaces. *Sci. Total Environ.* 427–428, 347–354. doi: 10.1016/j.scitotenv.2012.03.084
- Saylor, R. D., Baker, B. D., Lee, P., Tong, D., Pan, L., and Hicks, B. B. (2019). The particle dry deposition component of total deposition from air quality models: right, wrong or uncertain? *Tellus B: Chem. Phys. Meteorol.* 71, 1–22. doi: 10.1080/16000889.2018.1550324
- Schaubroeck, T., Deckmyn, G., Neiryck, J., Staelens, J., Adriaenssens, S., Dewulf, J., et al. (2014). Multilayered modeling of particulate matter removal by a growing forest over time, from plant surface deposition to washoff via rainfall. *Environ. Sci. Technol.* 48, 10785–10794. doi: 10.1021/es5019724
- Sgrigna, G., Sæbø, A., Gawronski, S., Popek, R., and Calfapietra, C. (2015). Particulate matter deposition on quercus ilex leaves in an industrial city of central Italy. *Environ. Pollut.* 197, 187–194. doi: 10.1016/j.envpol.2014.11.030
- Shao, F., Wang, L., Sun, F., Li, G., Yu, L., Wang, Y., et al. (2019). Study on different particulate matter retention capacities of the leaf surfaces of eight common garden plants in Hangzhou, China. *Sci. Tot. Environ.* 652, 939–951. doi: 10.1016/j.scitotenv.2018.10.182
- Sun, F., Yin, Z., Lun, X., Zhao, Y., Li, R., Shi, F., et al. (2014). Deposition velocity of PM<sub>2.5</sub> in the winter and spring above deciduous and coniferous forests in Beijing, China. *PLoS ONE* 9:e97723. doi: 10.1371/journal.pone.0097723
- Teske, M. E., and Thistle, H. W. (2004). A library of forest canopy structure for use in interception modeling. *For. Ecol. Manage.* 198, 341–350. doi: 10.1016/j.foreco.2004.05.031
- Tigges, J., Churkina, G., and Lakes, T. (2017). Modeling above-ground carbon storage: a remote sensing approach to derive individual tree species information in urban settings. *Urban Ecosyst.* 20, 97–111. doi: 10.1007/s11252-016-0585-6
- Tiwary, A., Williams, I. D., Heidrich, O., Namdeo, A., Bandaru, V., and Calfapietra, C. (2016). Development of multi-functional streetscape green infrastructure using a performance index approach. *Environ. Pollut.* 208, 209–220. doi: 10.1016/j.envpol.2015.09.003
- Wang, L., Gong, H., Liao, W., and Wang, Z. (2015). Accumulation of particles on the surface of leaves during leaf expansion. *Sci. Total Environ.* 532, 420–434. doi: 10.1016/j.scitotenv.2015.06.014
- Weerakkody, U., Dover, J. W., Mitchell, P., and Reiling, K. (2018a). The impact of rainfall in remobilising particulate matter accumulated on leaves of four evergreen species grown on a green screen and a living wall. *Urban For. Urban Green* 35, 21–31. doi: 10.1016/j.ufug.2018.07.018
- Weerakkody, U., Dover, J. W., Mitchell, P., and Reiling, K. (2018b). Quantification of the traffic-generated particulate matter capture by plant species in a living wall and evaluation of the important leaf characteristics. *Sci. Tot. Environ.* 635, 1012–1024. doi: 10.1016/j.scitotenv.2018.04.106
- World Health Organization (2006). *Health Risks of Particulate Matter From Long-Range Transboundary Air Pollution*. Copenhagen: World Health Organization, Regional Office for Europe.
- World Health Organization (2013). *Health Effects of Particulate Matter. Policy Implications for Countries in Eastern Europe, Caucasus and Central Asia*. Copenhagen: World Health Organization, Regional Office for Europe.
- Xiao, Q., Ma, Z., Li, S., and Liu, Y. (2015). The impact of winter heating on air pollution in China. *PLoS ONE* 10:e0117311. doi: 10.1371/journal.pone.0117311
- Xu, X., Yu, X., Mo, L., Xu, Y., Bao, L., and Lun, X. (2019). Atmospheric particulate matter accumulation on trees: a comparison of boles, branches and leaves. *J. Clean. Prod.* 226, 349–356. doi: 10.1016/j.jclepro.2019.04.072
- Xu, X., Zhang, Z., Bao, L., Mo, L., Yu, X., Fan, D., et al. (2017). Influence of rainfall duration and intensity on particulate matter removal from plant leaves. *Sci. Tot. Environ.* 609, 11–16. doi: 10.1016/j.scitotenv.2017.07.141
- Yang, Y., Vance, M., Tou, F., Tiwari, A., Liu, M., and Hochella, M. F. (2016). Nanoparticles in road dust from impervious urban surfaces: distribution, identification, and environmental implications. *Environ. Sci. Nano* 3, 534–544. doi: 10.1039/C6EN00056H
- Zhang, W., Wang, B., and Niu, X. (2017). Relationship between leaf surface characteristics and particle capturing capacities of different tree species in Beijing. *Forests* 8, 1–12. doi: 10.3390/f8030092
- Zhang, Z., Liu, J., Wu, Y., Yan, G., Zhu, L., and Yu, X. (2017). Multi-scale comparison of the fine particle removal capacity of urban forests and wetlands. *Sci. Rep.* 7, 1–13. doi: 10.1038/srep46214

**Conflict of Interest:** The authors declare that the research was conducted in the absence of any commercial or financial relationships that could be construed as a potential conflict of interest.

Copyright © 2020 Pace and Grote. This is an open-access article distributed under the terms of the Creative Commons Attribution License (CC BY). The use, distribution or reproduction in other forums is permitted, provided the original author(s) and the copyright owner(s) are credited and that the original publication in this journal is cited, in accordance with accepted academic practice. No use, distribution or reproduction is permitted which does not comply with these terms.

### 3. Paper III

Pace, R; De Fino, F.; Rahman M. A.; Pauleit, S; Nowak, D; Grote, R. (2020): A single tree model to consistently simulate cooling, shading, and pollution uptake of urban trees. International Journal of Biometeorology, submitted.

© [2020] IJB Springer. Reprinted preliminary manuscript. Copyright in case of final acceptance retains with IJB.

1     **A single tree model to consistently simulate cooling, shading, and pollution**  
 2                                   **uptake of urban trees**

3     Rocco Pace<sup>1</sup>, Francesco De Fino<sup>2</sup>, Mohammad A. Rahman<sup>3</sup>, Stephan Pauleit<sup>3</sup>, David Nowak<sup>4</sup>, Rüdiger  
 4     Grote<sup>1</sup>

5     1) Institute of Meteorology and Climate Research–Atmospheric Environmental Research (IMK-IFU),  
 6         Karlsruhe Institute of Technology (KIT), Germany

7     2) Department of Informatics, Bioengineering, Robotics and Systems Engineering (DIBRIS), University  
 8         of Genoa, Italy

9     3) Chair for Strategic Landscape Planning and Management, School of Life Sciences Weihenstephan,  
 10        Technische Universität München, Germany

11    4) USDA Forest Service, Northern Research Station, Syracuse, NY, USA

12    **ABSTRACT**

13    Extremely high temperatures, which negatively affect the human health and plant performances, are  
 14    becoming more frequent in cities. Urban green infrastructure, particularly trees, can mitigate this issue  
 15    through cooling due to transpiration, and shading. Temperature regulation by trees depends on  
 16    feedbacks among the climate, water supply, and plant physiology. However, most current models still  
 17    lack basic processes, such as the consideration of soil water limitation, or have not been evaluated  
 18    sufficiently. In this study, we present a new model that couples the soil water balance with energy  
 19    calculations to assess the physiological responses and microclimate effects of a common urban street-  
 20    tree species (*Tilia cordata* Mill.) on temperature regulation. We contrast two urban sites in Munich,  
 21    Germany with different degree of surface sealing at which micro-climate and transpiration had been  
 22    measured. Simulations indicate that differences in wind speed and soil water supply can be made  
 23    responsible for the differences in transpiration. Nevertheless, the calculation of the overall energy  
 24    balance showed that the shading effect, which depends on the leaf area index and canopy cover,  
 25    contribute the most to the temperature reduction at midday. Finally, we demonstrate that the  
 26    consideration of soil water availability for stomatal conductance improves the calculation of gaseous  
 27    pollutant uptake (e.g., ozone). In conclusion, the presented model has demonstrated its ability to  
 28    quantify two major ecosystem services (temperature mitigation and air pollution removal) consistently  
 29    in dependence on meteorological and site conditions.

30    **Keywords:** microclimate model; transpiration; shading; stomatal conductance; soil water availability;  
 31    urban green spaces

**32 INTRODUCTION**

33 The increasing occurrence of heatwaves due to global warming (Perkins et al. 2012; Baldwin et al.  
34 2019) presents a serious threat to human health (Watts et al. 2019). For example, the 2003 heatwave  
35 in Europe caused more than 70,000 deaths (Robine et al. 2008) and the heatwave-related premature  
36 mortality is expected to increase at the global scale (Guo et al. 2018). Extreme high temperatures are  
37 prevalent in cities, where the high percentage of sealed surfaces contributes to the so-called heat  
38 island effect (Oke 2002; Wilby 2003). Therefore, measures to mitigate the temperature stress are  
39 intensively discussed. The implementation of green infrastructure is the most prominent suggestion  
40 to mitigate air temperature in cities (Norton et al. 2015) because the associated cooling effect has been  
41 demonstrated in many studies (Bowler et al. 2010). In particular, increasing the number of urban trees  
42 is suggested to have a large cooling effect (Zölch et al. 2016).

43 Trees reduce the air temperature in two ways: by preventing solar radiation from heating up surfaces  
44 below the canopy (shading) and by transpiring water through the stomata of leaves, which has  
45 previously been absorbed by roots in the soil (in the following termed cooling; Rahman et al. 2020).  
46 However, these effects strongly depend on the tree dimensions and physiology and thus the climatic  
47 conditions (Rahman et al. 2018). In particular, low relative humidity (or high vapor pressure deficit)  
48 triggered by high temperature reflects a high transpiration demand. However, the actual transpiration  
49 is limited by the soil water availability. Insufficient water supply causes stomata closure and decreases  
50 the water uptake and thus the cooling effect of evaporation (Rötzer et al. 2019). Other meteorological  
51 factors that are positively related to evaporation are solar radiation, because stomata tend to open if  
52 the radiation is high, and the wind speed, which reduces the boundary layer thickness and thus the  
53 resistance to water transport from the canopy (Kramer 1983).

54 Several approaches have been considered to simulate the effect of vegetation on the  
55 micrometeorology in urban environments. The most prominent ones are computational fluid dynamics  
56 models that are built on fundamental fluid mechanics and thermodynamics laws and are used to  
57 calculate the interactions between trees and their surroundings (Buccolieri et al. 2018). Urban canopy  
58 models based on which the energy budget is determined with a simplified consideration of the flows  
59 represent a simpler approach (e.g., Lee and Park 2008; Krayenhoff et al. 2014; Zeng and Gao 2017).  
60 Recently, the use of large-eddy simulation models has been suggested for the estimation of the  
61 mitigating effect of vegetation on urban heat, although they currently do not fully consider the impact  
62 of evaporation (Li and Wang 2018). However, all these model types are computational demanding,  
63 difficult to parameterize, and very sensitive to the initial boundary conditions. Therefore, it is difficult

64 to consider different species or individual properties, which diminishes their value as decision support  
65 tools for urban planning.

66 Urban forest-specific models represent a different group of models, most prominent in urban  
67 ecosystem research (Lin et al. 2019). These models focus less on the interactions between vegetation  
68 and the environment but more on the physical and physiological properties and processes of plants,  
69 that is, trees. A prominent example is the i-Tree model that can be used to estimate a broad range of  
70 ecosystem functions such as the air pollution removal, carbon sequestration, as well as building energy  
71 conservation (Nowak et al. 2008; Endreny et al. 2017). Among these services, energy estimates are  
72 related to the cooling function of trees (Scholz et al. 2018), but are mainly related to tree shade  
73 (Mcpherson and Simpson 1999). Because cooling is arguably the most important ecosystem service  
74 regarding the mitigation of future climate change effects in cities, this function must be calculated  
75 explicitly, that is, the effects of stomatal conductance and water limitation must be clarified. The  
76 combination of shading and leaf area or crown coverage or cooling and evapotranspiration has only  
77 been attempted in a few studies (Yang et al. 2013; Rötzer et al. 2019).

78 If evapotranspiration is calculated based on the stomatal conductance, another ecosystem service,  
79 that is, the gaseous pollutant uptake, can be physically considered. In contrast to particle deposition,  
80 gaseous pollutants, such as ozone, are primarily taken up through the stomata (Hosker and Lindberg  
81 1982). Therefore, the uptake rates differ depending on the assimilation conditions or water supply of  
82 the plants. Among the various models that calculate stomatal uptake, few consider the soil water  
83 limitation, for example, the ozone deposition DO3SE model (Emberson et al. 2000; Büker et al. 2012).  
84 This type of model is primarily used to evaluate the effect on plants rather than on the environment  
85 because it was designed for the evaluation of trade-off between drought stress and ozone stress  
86 (Sicard et al. 2016). However, until very recently, we were not aware of any model that jointly considers  
87 the effects of limited water supply on both the cooling function and air pollutant removal of trees.

88 In this study, we introduce a single-tree model coupled to a one-dimensional soil water model to  
89 consider the effect of drought stress on stomatal conductance. The model is independent of regional  
90 hydraulic information but can be initialized with specific on-site information. Stomatal closure reduces  
91 the cooling function of trees as well as their capacity to remove gaseous pollutants (e.g., ozone). We  
92 evaluated the model results on transpiration and shading using data on common street-tree species  
93 (*Tilia cordata*) growing in two differently sealed urban public spaces in the center of Munich, Germany.  
94 By using the coupled model, we determine the effects of the tree size, soil water availability, and  
95 climate on the temperature mitigation capability of urban trees as well as the uptake of ozone.

96 **METHODS**97 **Study area and local data**

98 The study areas are located in Munich (Germany) and have different topographical features: Bordeaux  
 99 Platz is an open green square and Pariser Platz is a circular paved square. Five trees of *T. cordata* with  
 100 different morphological characteristics have been measured in each location (Table 1). Trees at  
 101 Bordeaux Platz were typically smaller than those at Pariser Platz.

102 **Table 1.** Average morphological characteristics of trees at the two study sites (DBH: diameter at 1.3  
 103 m height, LAI: leaf area index).

Sites	DBH (cm)	Height (m)	Canopy cover (m <sup>2</sup> )	LAI
Bordeaux Platz	29.18 ± 0.52	15.12 ± 0.21	67.12 ± 3.37	2.41 ± 0.19
Pariser Platz	44.68 ± 1.27	16.78 ± 0.29	81.7 ± 3.97	2.54 ± 0.18

104

105 Sap flux density measurements carried out from July 29 to August 31, 2015, were used to estimate the  
 106 tree transpiration. Tree core samples were used to normalize the diameter at breast height (DBH) and  
 107 sapwood area of trees (to an age of 40 years) to facilitate the direct comparison of the water use.

108 The soil moisture potential was measured throughout the soil profile to a depth of 30 cm and local  
 109 data, including the air temperature, pressure, relative humidity, and wind speed, were measured at  
 110 the two study sites. Furthermore, the global radiation was measured at Bordeaux Platz; all data were  
 111 continuously recorded at resolution of 15 min. Precipitation data were derived from the  
 112 *Theresienstrasse* weather station in Munich. Missing values on August 5<sup>th</sup> are due to vandalism-related  
 113 measurement problems. For more details on the methodology, please see Rahman et al. (2017).

114 **Model calculations**115 **Transpiration, stomatal conductance, and O<sub>3</sub> deposition velocity**

116 The transpiration flux ( $T_f$ , g m<sup>-2</sup> hr<sup>-1</sup>) was calculated using the i-Tree Eco model methodology  
 117 (Hirabayashi et al. 2015). The amount of water evaporating through stomata is controlled by the leaf  
 118 and boundary layer resistances (Kramer 1983):

$$119 \quad T_f = \frac{C_{leaf} - C_{air}}{\frac{1}{g_s} + R_a} \cdot \frac{3600}{LAI}, \quad (1)$$



120 where  $C_{leaf}$  is the water vapor concentration of evaporating surfaces within the leaf ( $\text{g m}^{-3}$ ),  $C_{air}$  is the  
 121 water vapor concentration in the air ( $\text{g m}^{-3}$ ),  $1/g_s$  is the stomatal resistance ( $\text{s m}^{-1}$ ,  $g_s$  = stomatal  
 122 conductance),  $R_a$  is the aerodynamic resistance ( $\text{s m}^{-1}$ ), and LAI is the leaf area index.

123 The parameters  $C_{leaf}$  and  $C_{air}$  can be calculated as follows (Monteith and Unsworth 2013):

$$124 \quad C_{leaf} = \frac{M_w e_s}{R T} \quad (2a)$$

$$125 \quad C_{air} = \frac{M_w e}{R T'} \quad (2b)$$

126 where  $M_w$  is the molecular weight of water ( $18 \text{ g mol}^{-1}$ ),  $R$  is the universal gas constant ( $8.314 \text{ J mol}^{-1}$   
 127  $\text{K}^{-1}$ ),  $e_s$  is the saturation vapor pressure (kPa),  $e$  is the vapor pressure (kPa), and  $T$  is the temperature  
 128 (K).

129 The stomatal conductance of each layer of the canopy can be calculated based on the methods  
 130 explained in Farquhar et al. (1980), Baldocchi (1994), and Harley et al. (1992):

$$131 \quad g_s = \frac{m A r h}{C_s} + g_m, \quad (3)$$

132 where  $m$  is the Ball–Berry coefficient,  $A$  is the photosynthetic carbon flux into the leaf,  $rh$  is the relative  
 133 humidity,  $C_s$  is the  $\text{CO}_2$  concentration at the leaf surface, and  $g_m$  is the minimum stomatal conductance  
 134 ( $0.02 \text{ mol m}^{-2} \text{ s}^{-1}$ ) when the stomata are closed ( $A = 0$ ) assuming a cuticular resistance of 0.

135 The aerodynamic resistance ( $R_a$ ) is calculated as follows:

$$136 \quad R_a = \frac{u(z)}{u_*^2}, \quad (4)$$

137 where  $u(z)$  is the mean wind speed at the height of the weather station  $z$  ( $\text{m s}^{-1}$ ) and  $u_*$  is the friction  
 138 velocity ( $\text{m s}^{-1}$ ).

139 The  $\text{O}_3$  deposition velocity ( $vd$ ) can be calculated as the inverse of the sum of the aerodynamic ( $R_a$ ),  
 140 quasi-laminar boundary layer ( $R_b$ ), and canopy ( $R_c$ ) resistances, expressed in  $\text{s m}^{-1}$  (Baldocchi et al.  
 141 1987):

$$142 \quad vd = \frac{1}{R_a + R_b + R_c} \quad (5)$$

143 The canopy resistance ( $R_c$ ) is calculated as:

$$144 \quad \frac{1}{R_c} = \frac{1}{r_s + r_m} + \frac{1}{r_{soil}} + \frac{1}{r_t}, \quad (6)$$

145 where  $r_s$  is the stomatal resistance ( $s\ m^{-1}$ ),  $r_m$  is the mesophyll resistance ( $s\ m^{-1}$ ),  $r_{soil}$  is the soil  
 146 resistance ( $2941\ s\ m^{-1}$ ), and  $r_c$  is the cuticular resistance ( $s\ m^{-1}$ ).

147 The quasi-laminar boundary layer ( $R_b$ ) is calculated as:

$$148 \quad R_b = 2(Sc)^{\frac{2}{3}} (Pr)^{-\frac{2}{3}} (ku_*)^{-1}, \quad (7)$$

149 where  $Sc$  is the Schmidt number (1),  $Pr$  is the Prandtl number (0.72),  $k$  is the von Karman constant  
 150 (0.41), and  $u_*$  is the friction velocity ( $m\ s^{-1}$ ).

### 151 **Water balance model**

152 The water balance is based on the DeNitrification and DeComposition (DNDC) model (Li et al. 1992)  
 153 modified for urban conditions and short-term calculations. The following water fluxes are considered:

$$154 \quad P = T + I + E + R + S, \quad (8)$$

155 where  $P$  is the precipitation,  $T$  is the transpiration,  $I$  is the interception,  $E$  is the evaporation,  $R$  is the  
 156 runoff, and  $S$  is the seepage (percolation below the last considered soil layer). The model determines  
 157 the daily potential evapotranspiration from the daily temperature based on a modified Thornthwaite  
 158 equation (Thornthwaite and Mather 1957) and considering the dependency on the latitude (Camargo  
 159 et al. 1999; Pereira and Pruitt 2004). The potential demand for hourly evaporation was determined by  
 160 dividing the daily evaporation by 24. The interception is assumed to be linearly related to the LAI and  
 161 retained water evaporates from leaves according to the evaporation demand. Water drawn from the  
 162 soil by evaporation and transpiration can be calculated as the minimum of either the remaining  
 163 potential evapotranspiration or water demand, which in turn depends on photosynthesis and the  
 164 species-specific water-use efficiency ( $3\ \mu\text{mol}\ \text{mmol}^{-1}$ ; Gillner et al. 2015a). The soil evaporation was  
 165 determined from the residual evaporation demand and soil water available below a predefined depth  
 166 (0.3 m). The water movement within the soil depends on the difference between the relative water  
 167 contents of the three adjacent soil layers and is regulated by the soil hydraulic conductivity (Table 2).  
 168 For Pariser Platz we assumed a runoff of 40% due to the impervious surface and lower soil depth (0.1,  
 169 0.2, and 0.4 m for the three layers, respectively, compared with 0.2, 0.3, and 0.5 m, respectively, at  
 170 Bordeaux Platz). A drought index (DI) was defined to limit the stomatal conductance and reduce the  
 171 Ball–Berry constant ( $m$ ) from 10 to 3 according to the soil water availability:

$$172 \quad DI = \frac{(water\ content - wilting\ point)}{(field\ capacity - wilting\ point)}, \quad (9)$$

173 where:

- 174 • if  $DI \leq 0.3 \rightarrow m = 3$   
 175 •  $0.3 < DI < 0.5 \rightarrow m = 3 + 35 \times (DI - 0.3)$   
 176 •  $DI \geq 0.5 \rightarrow m = 10$

177 **Energy balance model**

178 Energy reduction based on cooling and shading was evaluated at midday (12:00–15:00, CET). The  
 179 average hourly transpiration  $T$  ( $\text{ml hr}^{-1} \text{m}^{-2}$ ) was converted into energy loss ( $\text{W m}^{-2}$ ) by multiplication  
 180 with the latent heat of vaporization  $L_v$ , which is  $2450 \text{ J kg}^{-1}$  and division by 3600 s:

$$181 \quad E_{cooling} = \frac{T \times L_v}{3600} \quad (10)$$

182 The energy reduction based on concrete shading was assessed by determining the equilibrium  
 183 temperature of the pavement surface based on the heat transfer and energy balance (Solaimanian and  
 184 Kennedy 1993):

$$185 \quad q_a + q_s - q_c - q_k - q_r = 0, \quad (11)$$

186 where  $q_a$  is the absorbed energy,  $q_s$  is the Longwave radiation,  $q_c$  is the convection energy,  $q_k$  is the  
 187 conduction energy, and  $q_r$  is the surface emission.

$$188 \quad q_a = (1 - a) \times R, \quad (12)$$

189 where  $a$  is the albedo (0.3) and  $R$  is the direct radiation (determined from the global radiation as  
 190 described in Spitters et al. 1986).

$$191 \quad q_s = \varepsilon_a \sigma T_{air}^4 \quad (13)$$

$$192 \quad \varepsilon_a = 0.77 - 0.28 \times 10^{(-V_p \times 0.074)} \text{ (Geiger 1959)}$$

193  $V_p$  = vapor pressure (mmHg)

194  $\sigma$  = Stefan–Boltzmann constant ( $= 5.68 \times 10^{-8} \text{ W m}^{-2} \text{ K}^{-4}$ )

195  $T_{air}$  = air temperature (K)

$$196 \quad q_c = h_c (T_s - T_{air}) \quad (14)$$

197  $h_c$  = surface coefficient of heat transfer =  $698.24[0.00144 T_m^{0.3} U^{0.7} + 0.00097(T_s - T_{air})^{0.3}]$

198  $T_s$  = surface temperature (K)

199  $T_m$  = average of the surface and air temperature (K)

200  $U$  = average daily wind speed ( $\text{m s}^{-1}$ )

$$201 \quad q_k = -k \frac{T_d - T_s}{d} \quad (15)$$

202  $k$  = thermal conductivity ( $1.65 \text{ W m}^{-1} \text{ K}^{-1}$ )

203  $d$  = depth (0.5 m)

204  $T_d$  = temperature at depth  $d$  ( $20 \text{ }^\circ\text{C}$ )

$$205 \quad q_r = \varepsilon_b \sigma T_s^4 \quad (16)$$

206 with

$$207 \quad \varepsilon_b = 1.24 \times (10 \times V_p / T_{air})^{\frac{1}{2}} \text{ (Brutsaert 1982).}$$

208 The reduction of the direct radiation through the tree crown was calculated using a modified Beer–  
209 Lambert law considering a uniform leaf arrangement in the canopy:

$$210 \quad R_{in} = R \times e^{-k \times LAI}, \quad (17)$$

211 where  $R_{in}$  is the irradiance under the tree canopy ( $\text{W m}^{-2}$ ) and  $k$  is the extinction coefficient (0.7 for  
212 deciduous forest).

213 The energy reduction by shading ( $E_{shading}$ ;  $\text{W m}^{-2}$ ) was calculated as the absolute difference between  
214 the energy balance outside and inside the tree canopy:

$$215 \quad E_{shading} = |q_{a,out} - q_{a,in}| + |q_{s,out} - q_{s,in}| + |q_{c,out} - q_{c,in}| + |q_{k,out} - q_{k,in}| + |q_{r,out} - q_{r,in}|$$

216 (18)

217 The total energy reduction  $E$  ( $\text{W m}^{-2}$ ) was calculated as the sum of  $E_{shading}$  ( $\text{W m}^{-2}$ ) and  $E_{cooling}$  ( $\text{W m}^{-2}$ ).

## 218 RESULTS

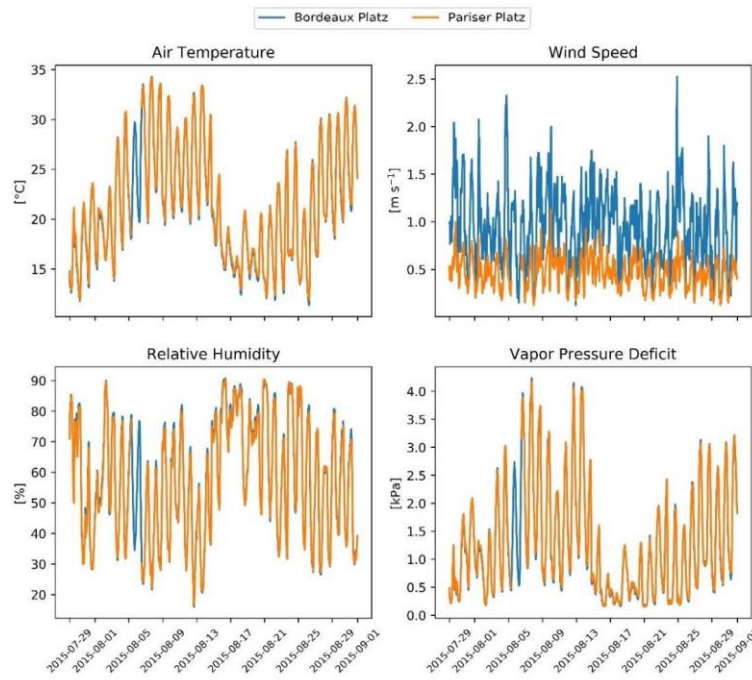
219 The two sites are not show significantly different in terms of the air temperature, relative humidity,  
220 and vapor pressure deficit. However, the wind speed at Bordeaux Platz (mean =  $0.9 \text{ m s}^{-1}$ ) is much  
221 higher than that at Pariser Platz (mean =  $0.5 \text{ m s}^{-1}$ ; Fig. 1). Consequently, the resistances of the  
222 aerodynamic and quasi-laminar boundary layer were considerably lower at Bordeaux Platz (on average

223 105.9 and  $60 \text{ s m}^{-1}$ , respectively) than at Pariser Platz ( $222.4$  and  $125.9 \text{ s m}^{-1}$ , respectively; Fig. 2), which  
224 explains the higher transpiration demand at the former location.

225 During the observation period, the negative soil water potential increased until mid-August when  
226 several precipitation events occurred, leading to the replenishment of the soil layers with water and  
227 increase in the soil moisture potential. This trend could be represented with the simulation of the soil  
228 water content, verifying the assumed differences in the soil depth and surface sealing. However, the  
229 recovery of the relative water content at Pariser Platz is lower than that at Bordeaux Platz (Fig. 3)  
230 because the water supply is reduced due to larger runoff. Therefore, the impact of drought on the  
231 stomatal conductance adds to the differences between the study sites, especially in the investigated  
232 period (Fig. 4), leading to a lower transpiration at Pariser Platz than at Bordeaux Platz. The modeled  
233 and measured transpiration values at the two sites overall agree, highlighting the ability of the model  
234 to cope with the differences between the two sites (Fig. 5).

235 In a model experiment, we can estimate the temperature effect originating from the shading of the  
236 crown to illustrate the usefulness of the model approach. Therefore, we calculate the temperature of  
237 an unshaded and a shaded concrete surface based on the recorded weather conditions at the two  
238 investigated places. This shows that the simulated surface temperature would be a lot lower under the  
239 tree canopy at the hottest days (up to  $20.6 \text{ }^\circ\text{C}$  in Pariser Platz and  $17.2 \text{ }^\circ\text{C}$  in Bordeaux Platz; Fig. 6),  
240 while during the cool period without much direct radiation, the shading effect is negligible. The  
241 differences between the places originate again from the lower wind speed at Pariser Platz, which limits  
242 the heat flow by convection to the surrounding air and thus leads to higher temperatures in the sun.  
243 On the other side, the surface temperature under shaded conditions at this site is slightly lower  
244 because of its slightly higher leaf area index.

245 The transpiration performance particularly influences the cooling effect at Pariser Platz (mean =  $0.03$ ;  
246 max =  $0.04 \text{ kW/m}^2$ ) compared with Bordeaux Platz (mean =  $0.05$ ; max =  $0.075 \text{ kW/m}^2$ ). Instead, the  
247 energy reduction by shading is similar at the two locations (mean =  $0.3$ ; max =  $0.6 \text{ kW/m}^2$ ), indicating  
248 that the largest energy reduction occurs at midday (Fig. 7). The differences in the stomatal  
249 conductance result in remarkable differences in  $vd$ , as indicated in Fig. 8. Thus, it can be assumed that  
250 the conditions at Bordeaux Platz lead to a higher removal of gaseous pollutants than at Pariser Platz.  
251 For sites with comparable ozone formation and transport, this may ultimately lead to a relatively better  
252 air quality.

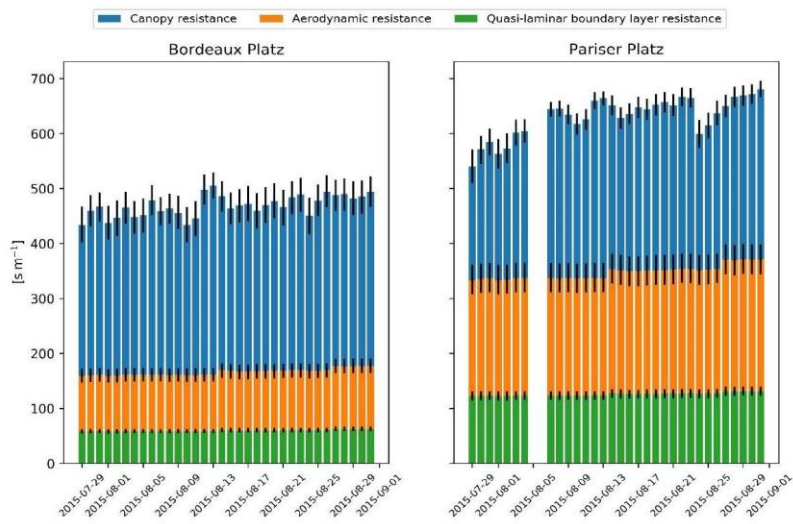


253

254

255

Figure 1. Meteorological conditions at the two study sites.

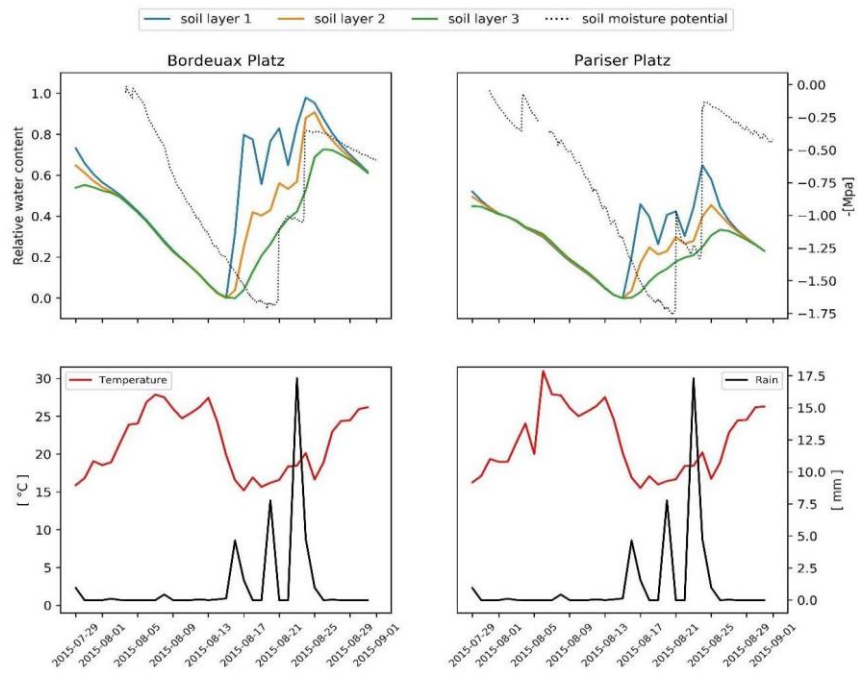


256

257

258

Figure 2. Model resistances at the two sites. The quasi-laminar boundary layer is referred to as  $O_3$ .



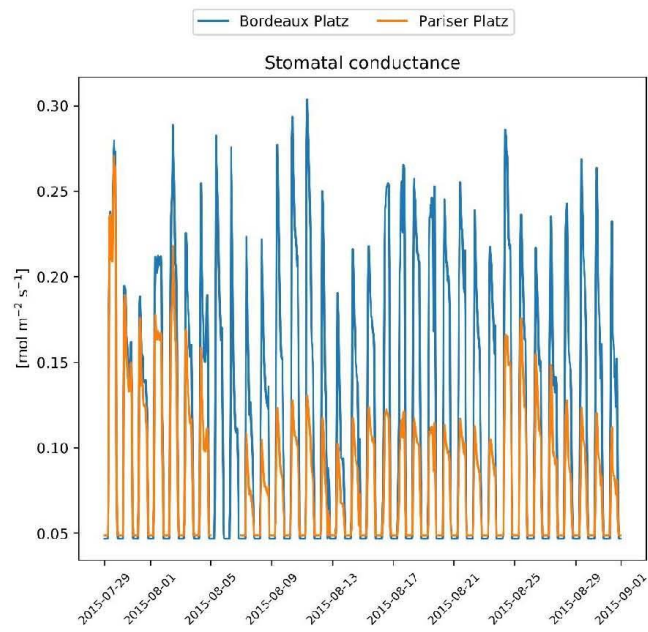
259

260

261

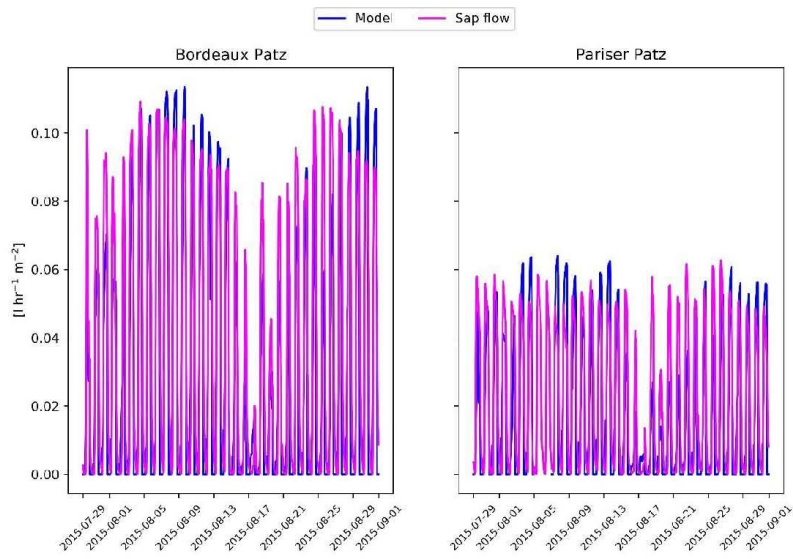
**Figure 3.** Upper panels: Relative water content in each soil layer and measured soil moisture potential. Lower panels: Average daily temperature and rain events in the study period.

262



263  
264  
265

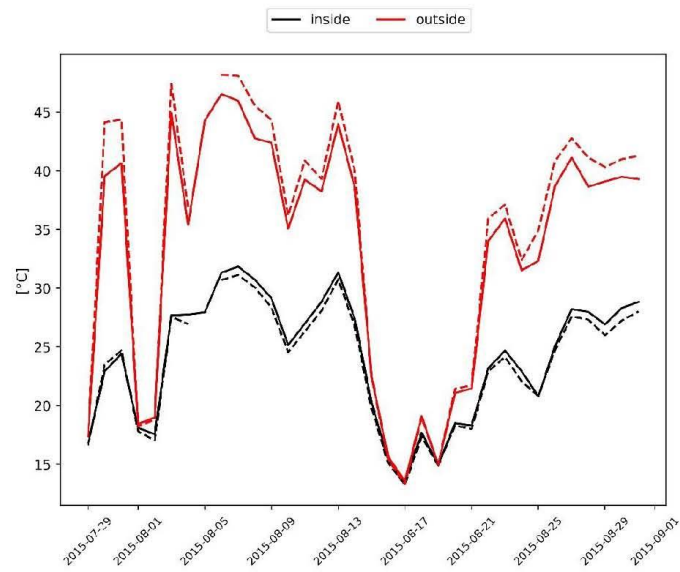
Figure 4. Stomatal conductance at the two sites.



266  
267  
268  
269

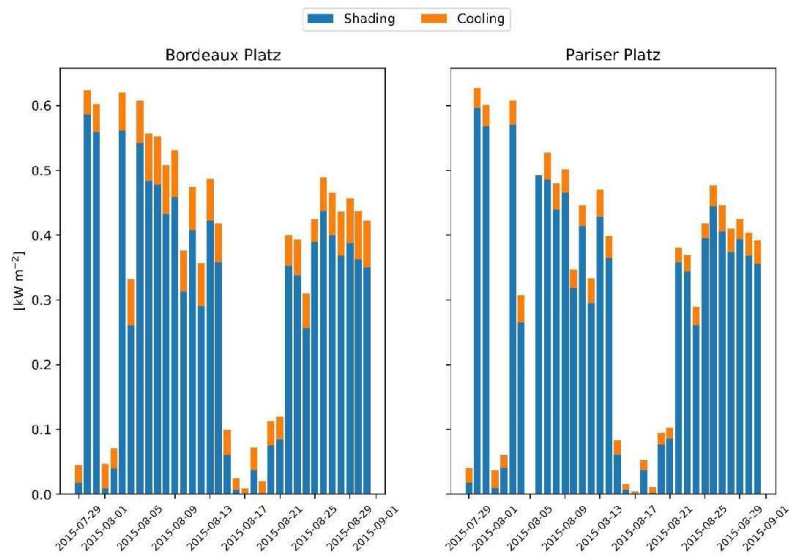
Figure 5. Comparison of modeled transpiration and values measured using the sap flow for the two sites.





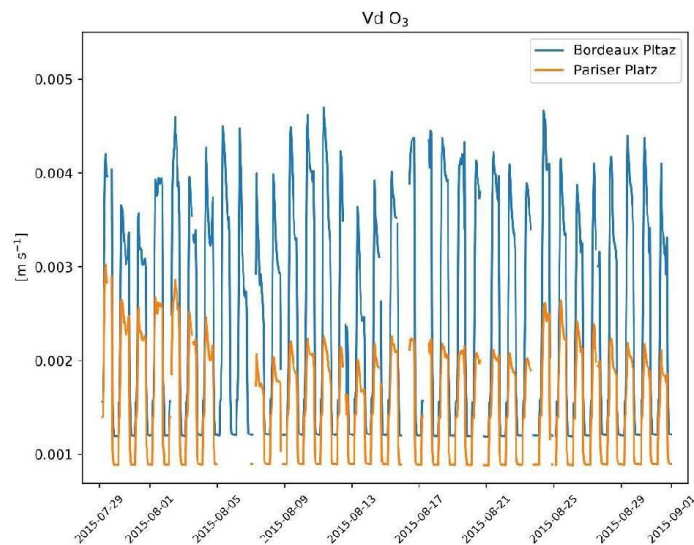
270

271 **Figure 6.** Simulated surface temperature (of an assumed concrete surface) outside and inside the tree  
 272 canopy. The solid line is the simulation for Bordeaux Platz and the dashed line for Pariser Platz.  
 273



274

275 **Figure 7.** Energy reduction by concrete shading and cooling by transpiration at the two sites at  
 276 midday.  
 277



278

279 **Figure 8.** Dry deposition velocity ( $vd$ ) of  $O_3$  at the two sites. Missing values correspond to hours with  
 280 precipitation.

281

## 282 DISCUSSION

283 Urban trees can help mitigate urban extreme temperature events, which are expected to be more  
 284 frequent and more severe in the future (Guerreiro et al. 2018). To better evaluate the efficiency of  
 285 increased tree abundance, models are required that can be used to determine ecosystem services  
 286 depending on both tree-specific properties and the (potentially changing) environment. Environmental  
 287 conditions include direct influences of immediate climate and indirect influences, particularly the soil  
 288 water availability (Livesley et al. 2016). Increased drought can be expected to affect the plant  
 289 properties and thus the ecosystem services that are related to water evaporation (cooling) and  
 290 pollution uptake (Stratópoulos et al. 2019b; Zhang et al. 2020). Consequently, water availability  
 291 impacts must be reflected in a model for decision support. Therefore, we implemented and tested a  
 292 model that cannot only be used to directly calculate heat mitigation in terms of energy reduction due  
 293 to cooling and shading but also considers the impact of drought stress on evaporation and the stomatal  
 294 uptake. A similar approach that link different ecosystem services based on physiological responses has  
 295 been very recently presented by Delaria and Cohen (2020) although not in the urban context.

296 The test simulations demonstrate that the energy reduction of urban trees is particularly high at  
 297 midday on sunny and warm days due to the shading provided by tree crowns. The effectiveness of this

298 process scales with LAI, crown depth, and width (Sanusi et al. 2017). For example, in a recent study in  
299 which a thermal camera was used to determine the surface temperature change of asphalt, porphyry,  
300 and grass based on shading of different tree species, median average cooling values of 16.4, 12.9, and  
301 8.5 °C were reported, respectively (Speak et al. 2020), which confirm the results of our simulation  
302 experiment (Fig. 6). In other studies, a maximum hourly cooling of 2.3 °C based on the shading of a  
303 single tree on the building facade (Zhao et al. 2018) and average cooling of the air temperature by  
304 trees in streets and courtyards of 2.5 °C (Shashua-Bar and Hoffman 2004) were determined.

305 The transpiration effect depends on the meteorological conditions (wind speed, vapor pressure deficit)  
306 and soil water availability (pervious or impervious surfaces) and represents on average 12% of the total  
307 energy reduction (15% at Bordeaux Platz and 9% at Pariser Platz). The simulated transpiration is in  
308 overall well accordance with the measurements although recovery after cool periods is delayed by a  
309 few days. This is despite the simulated restriction by soil water limitation is less severe than indicated  
310 by measurements of soil water potential during the respective period. A possible explanation is that  
311 foliage and thus transpiration demand might increase faster in reality than assumed in the model which  
312 would call for a more comprehensive determination of surface temperature. Also, some differences  
313 are apparent between the development of soil water potential and the simulated soil water content,  
314 indicating either a very inhomogeneous precipitation distribution within the city or a non-linear  
315 relation between runoff and percolation that might need to consider ponding or channeling effects  
316 from gutters (Meili et al. 2020). The very scattered distribution of sensors, the scarce information  
317 about the soil properties as well as the assumption of homogeneous soil sealing, however, demand for  
318 further evaluation studies in order to determine the importance of different foliage, surface, and soil  
319 properties to improve the respective parameterization.

320 Despite these uncertainties, the differences between the investigated sites have highlighted the  
321 importance of considering impervious surfaces, which characterize the urban fabric, enhances the  
322 water runoff and reduces soil water infiltration (Wang et al. 2008). A limited water availability reduces  
323 the potential for evaporative cooling, in particular because of transpiration reduction (Gillner et al.  
324 2015a). This effect might significantly affect the immediate environment. For example, the results of  
325 experimental studies showed that evaporative cooling alone contributes to an air temperature  
326 reduction up to 3° within the canopies (Rahman et al. 2017b, 2020a) and the canopy-to-air  
327 temperature difference depends on meteorological conditions, tree species and, urban site-specific  
328 characteristics (Meier and Scherer 2012). The cooling effect by transpiration depends to a large extent  
329 on stomatal conductance (Tan et al. 2018) and our results are in agreement with measured values at  
330 midday on *Tilia europaea* in Sweden ( $0.1 - 0.2 \text{ mol m}^{-2} \text{ s}^{-1}$ ) (Konarska et al. 2016). The energy loss due

331 to tree transpiration for commonly planted species in Central Europe including *T. cordata* range  
332 between 0.059 and 0.075 kW m<sup>-2</sup> (Rötzer et al. 2019) which are similar to our results in Bordeaux Platz.

333 We demonstrate that the new model introduced in this study can capture the effect of drought on  
334 gaseous pollution uptake, as previously suggested by Wang et al. (2017). This may be of particular  
335 importance for future studies in Mediterranean cities characterized by climate with pronounced  
336 drought events; neglecting the effects of stomatal conductance may result in a significant  
337 overestimation of gaseous pollutant deposition (Morani et al. 2014). However, long periods of heat  
338 and drought exacerbated by the high percentage of sealed surfaces have also been recorded in cities  
339 at higher latitudes, which affected transpiration and reduced cooling (Gillner et al. 2015b; Rahman et  
340 al. 2017a).

341 Note that only gaseous air pollution uptake was considered in this study because particle deposition is  
342 generally assumed to be independent of stomatal conductance. However, simple estimates based on  
343 the velocity and leaf area can easily be added. However, the stomatal conductance interacts with  
344 particle deposition, for example, the stomatal functionality decreases due to heavy particle absorption  
345 (Burkhardt and Pariyar 2014; Burkhardt et al. 2018). Species selection is essential to maximize  
346 ecosystem services of urban trees because their features or performances are related to the climate  
347 and environmental conditions of the locations in which they grow. For example, it is desirable to ensure  
348 a year-round canopy in Mediterranean cities by planting evergreen trees to mitigate high temperatures  
349 during autumn (Masseti et al. 2019) and to remove particulate matter from the air (Pace and Grote  
350 2020). Furthermore, tree species have different water-use strategies (anisohydric vs. isohydric), which  
351 should be considered to optimize the water transpiration and stomatal uptake of gaseous pollutants  
352 over long periods (Grote et al. 2016). Overall, we demonstrate that the new model can be used to  
353 consistently estimate different ecosystem services and is capable of considering a range of  
354 environmental conditions as well as different species based on the respective parameterization of  
355 factors such as the crown properties, conductance, water-use efficiency, and photosynthesis (Kagotani  
356 et al. 2016; Stratópoulos et al. 2019b).

357 We would like to highlight that several issues need to be considered in future research for further  
358 increases in the precision and usefulness of model-based assessment based on individual tree services.  
359 For example, the leaf area and related physiological processes depend on individual competition,  
360 which could be introduced to models to obtain a better individual performance estimate (Pace et al.  
361 2018). On the process level, the interaction between ozone and the stomatal conductance might be  
362 introduced, that is, the decrease of the stomatal control under high ozone concentrations (Hoshika et  
363 al. 2018, 2020). The introduction of such a feature would also provide the means for considering the  
364 potential positive effects of reduced ozone concentrations on the water balances. In addition, seasonal

365 responses of trees, such as leaf shedding, xylem embolism, and higher root turnover or the death of  
366 trees might be introduced in response to pollution or drought stress (Stratópoulos et al. 2019a; Zhang  
367 et al. 2019). Finally, not only direct temperature effects but also changes in the air humidity should be  
368 simulated based on evaporation, which also improves the human thermal comfort and thus may add  
369 to the benefit of urban tree abundance (Upreti et al. 2017; Wang et al. 2018).

## 370 **CONCLUSIONS**

371 Overall, it has been demonstrated that the newly introduced model can be used to calculate the  
372 temperature mitigation and pollutant deposition depending on environmental conditions and species-  
373 specific properties. The physiological basis facilitates the simultaneous and consistent consideration of  
374 direct shading by canopy coverage, cooling effects by transpiration, and uptake of gaseous pollutants.  
375 Based on the introduction of a simple water balance model, which is coupled to the stomatal  
376 conductance of trees, the effect of drought can be accounted for. The central role of stomatal  
377 conductance for cooling as well as air pollution removal also enables the consideration of pollution  
378 feedbacks on the physiology, although this remains to be implemented in the future. Already, the  
379 model might be applied for investigations covering longer time periods and regions.

## 380 **Funding**

381 This research was supported by the Graduate School for Climate and Environment (GRACE).

## 382 **Acknowledgments**

383 The authors would like to thank the Graduiertenzentrum Weihenstephan of Technical University of  
384 Munich and Enago ([www.enago.com](http://www.enago.com)) for the English language review.

## 385 **REFERENCES**

- 386 Baldocchi D (1994) An analytical solution for coupled leaf photosynthesis and stomatal conductance  
387 models. *Tree Physiol* 14:1069–1079 . doi: 10.1093/treephys/14.7-8-9.1069
- 388 Baldocchi DD, Hicks BB, Camara P (1987) A canopy stomatal resistance model for gaseous deposition

- 389 to vegetated surfaces. *Atmos Environ* 21:91–101 . doi: 10.1016/0004-6981(87)90274-5
- 390 Baldwin JW, Dessy JB, Vecchi GA, Oppenheimer M (2019) Temporally Compound Heat Wave Events  
391 and Global Warming: An Emerging Hazard. *Earth's Futur* 7:411–427 . doi:  
392 10.1029/2018EF000989
- 393 Bowler DE, Buyung-Ali L, Knight TM, Pullin AS (2010) Urban greening to cool towns and cities: A  
394 systematic review of the empirical evidence. *Landsc Urban Plan* 97:147–155 . doi:  
395 10.1016/j.landurbplan.2010.05.006
- 396 Brutsaert W (1982) *Evaporation into the atmosphere: theory, history, and applications*. D.Reidel,  
397 Hingham MA.
- 398 Buccolieri R, Santiago JL, Rivas E, Sanchez B (2018) Review on urban tree modelling in CFD  
399 simulations: Aerodynamic, deposition and thermal effects. *Urban For Urban Green* 31:212–220  
400 . doi: 10.1016/j.ufug.2018.03.003
- 401 Bükler P, Morrissey T, Briolat A, et al (2012) DO 3SE modelling of soil moisture to determine ozone  
402 flux to forest trees. *Atmos Chem Phys* 12:5537–5562 . doi: 10.5194/acp-12-5537-2012
- 403 Burkhardt J, Pariyar S (2014) Particulate pollutants are capable to “degrade” epicuticular waxes and  
404 to decrease the drought tolerance of Scots pine (*Pinus sylvestris* L.). *Environ Pollut* 184:659–667  
405 . doi: 10.1016/j.envpol.2013.04.041
- 406 Burkhardt J, Zinsmeister D, Grantz DA, et al (2018) Camouflaged as degraded wax: Hygroscopic  
407 aerosols contribute to leaf desiccation, tree mortality, and forest decline. *Environ Res Lett* 13: .  
408 doi: 10.1088/1748-9326/aad346
- 409 Camargo AP, Marin FR, Sentelhas PC, Picini AG (1999) Adjust of the Thornthwaite’s method to  
410 estimate the potential evapotranspiration for arid and superhumid climates, based on daily  
411 temperature amplitude. *Bras Agrometeorol* 251–257
- 412 Delaria ER, Cohen RC (2020) A model-based analysis of foliar NO<sub>x</sub> deposition. *Atmos Chem Phys*

- 413 20:2123–2141 . doi: 10.5194/acp-20-2123-2020
- 414 Emberson LD, Ashmore MR, Cambridge HM, et al (2000) Modelling stomatal ozone flux across  
415 Europe. *Environ Pollut* 109:403–413 . doi: [https://doi.org/10.1016/S0269-7491\(00\)00043-9](https://doi.org/10.1016/S0269-7491(00)00043-9)
- 416 Endreny T, Santagata R, Perna A, et al (2017) Implementing and managing urban forests: A much  
417 needed conservation strategy to increase ecosystem services and urban wellbeing. *Ecol Modell*  
418 360:328–335 . doi: 10.1016/j.ecolmodel.2017.07.016
- 419 Farquhar GD, Caemmerer S Von, Berry J a. (1980) A biochemical model of photosynthesis CO<sub>2</sub>  
420 fixation in leaves of C<sub>3</sub> species. *Planta* 149:78–90
- 421 Geiger R (1959) *The Climate Near the Ground*. Harvard University Press, Cambridge
- 422 Gillner S, Korn S, Roloff A (2015a) Leaf-gas exchange of five tree species at urban street sites. *Arboric  
423 Urban For* 41:113–124
- 424 Gillner S, Vogt J, Tharang A, et al (2015b) Role of street trees in mitigating effects of heat and drought  
425 at highly sealed urban sites. *Landsc Urban Plan* 143:33–42 . doi:  
426 10.1016/j.landurbplan.2015.06.005
- 427 Grote R, Samson R, Alonso R, et al (2016) Functional traits of urban trees: air pollution mitigation  
428 potential. *Front Ecol Environ* 14:543–550 . doi: 10.1002/fee.1426
- 429 Guerreiro SB, Dawson RJ, Kilsby C, et al (2018) Future heat-waves, droughts and floods in 571  
430 European cities. *Environ Res Lett* 13: . doi: 10.1088/1748-9326/aaaad3
- 431 Guo Y, Gasparrini A, Li S, et al (2018) Quantifying excess deaths related to heatwaves under climate  
432 change scenarios: A multicountry time series modelling study. *PLoS Med* 15:1–17 . doi:  
433 10.1371/journal.pmed.1002629
- 434 Harley PC, Thomas RB, Reynolds JF, Strain BR (1992) Modelling photosynthesis of cotton grown in  
435 elevated CO<sub>2</sub>. *Plant Cell Environ* 15:271–282 . doi: 10.1111/j.1365-3040.1992.tb00974.x

- 436 Hirabayashi S, Kroll CN, Nowak DJ (2015) i-Tree Eco Dry Deposition Model Descriptions
- 437 Hoshika Y, Fares S, Pellegrini E, et al (2020) Water use strategy affects avoidance of ozone stress by  
 438 stomatal closure in Mediterranean trees—A modelling analysis. *Plant Cell Environ* 43:611–623 .  
 439 doi: 10.1111/pce.13700
- 440 Hoshika Y, Watanabe M, Carrari E, et al (2018) Ozone-induced stomatal sluggishness changes  
 441 stomatal parameters of Jarvis-type model in white birch and deciduous oak. *Plant Biol* 20:20–28  
 442 . doi: 10.1111/plb.12632
- 443 Hosker RP, Lindberg SE (1982) Review: Atmospheric deposition and plant assimilation of gases and  
 444 particles. *Atmos Environ* 16:889–910 . doi: 10.1016/0004-6981(82)90175-5
- 445 Kagotani Y, Nishida K, Kiyomizu T, et al (2016) Photosynthetic responses to soil water stress in  
 446 summer in two Japanese urban landscape tree species (*Ginkgo biloba* and *Prunus yedoensis*):  
 447 effects of pruning mulch and irrigation management. *Trees - Struct Funct* 30:697–708 . doi:  
 448 10.1007/s00468-015-1312-2
- 449 Konarska J, Uddling J, Holmer B, et al (2016) Transpiration of urban trees and its cooling effect in a  
 450 high latitude city. *Int J Biometeorol* 60:159–172 . doi: 10.1007/s00484-015-1014-x
- 451 Kramer JP (1983) *Water relations of plants*. Academic Press
- 452 Krayenhoff ES, Christen A, Martilli A, Oke TR (2014) A Multi-layer Radiation Model for Urban  
 453 Neighbourhoods with Trees. *Boundary-Layer Meteorol* 151:139–178 . doi: 10.1007/s10546-013-  
 454 9883-1
- 455 Lee SH, Park SU (2008) A vegetated urban canopy model for meteorological and environmental  
 456 modelling. *Boundary-Layer Meteorol* 126:73–102 . doi: 10.1007/s10546-007-9221-6
- 457 Li C, Frolking S, Frolking TA (1992) A model of nitrous oxide evolution from soil driven by rainfall  
 458 events: 2. Model applications. *J Geophys Res* 97:9777–9783 . doi: 10.1029/92jd00510



- 459 Li Q, Wang ZH (2018) Large-eddy simulation of the impact of urban trees on momentum and heat  
460 fluxes. *Agric For Meteorol* 255:44–56 . doi: 10.1016/j.agrformet.2017.07.011
- 461 Lin J, Kroll CN, Nowak DJ, Greenfield EJ (2019) A review of urban forest modeling: Implications for  
462 management and future research. *Urban For Urban Green* 43: . doi:  
463 10.1016/j.ufug.2019.126366
- 464 Livesley SJ, McPherson EG, Calafapietra C (2016) The Urban Forest and Ecosystem Services: Impacts on  
465 Urban Water, Heat, and Pollution Cycles at the Tree, Street, and City Scale. *J Environ Qual*  
466 45:119–124 . doi: 10.2134/jeq2015.11.0567
- 467 Massetti L, Petralli M, Napoli M, et al (2019) Effects of deciduous shade trees on surface temperature  
468 and pedestrian thermal stress during summer and autumn. *Int J Biometeorol* 63:467–479 . doi:  
469 10.1007/s00484-019-01678-1
- 470 Mcpherson EG, Simpson JR (1999) Carbon dioxide reduction through urban forestry: Guidelines for  
471 professional and volunteer tree planters. Albany, CA
- 472 Meier F, Scherer D (2012) Spatial and temporal variability of urban tree canopy temperature during  
473 summer 2010 in Berlin, Germany. *Theor Appl Climatol* 110:373–384 . doi: 10.1007/s00704-012-  
474 0631-0
- 475 Meili N, Manoli G, Burlando P, et al (2020) An urban ecohydrological model to quantify the effect of  
476 vegetation on urban climate and hydrology (UT&C v1.0). *Geosci Model Dev* 13:335–362 . doi:  
477 10.5194/gmd-13-335-2020
- 478 Monteith JL, Unsworth MH (2013) *Principles of Environmental Physics*, Fourth Edi. Academic Press
- 479 Morani A, Nowak D, Hirabayashi S, et al (2014) Comparing i-Tree modeled ozone deposition with  
480 field measurements in a periurban Mediterranean forest. *Environ Pollut* 195:202–209 . doi:  
481 10.1016/j.envpol.2014.08.031
- 482 Norton BA, Coutts AM, Livesley SJ, et al (2015) Planning for cooler cities: A framework to prioritise

- 483 green infrastructure to mitigate high temperatures in urban landscapes. *Landsc Urban Plan*  
 484 134:127–138 . doi: 10.1016/j.landurbplan.2014.10.018
- 485 Nowak DJ, Crane DE, Stevens JC, et al (2008) A Ground-Based Method of Assessing Urban Forest  
 486 Structure and Ecosystem Services. *Arboric Urban For* 34:347–358
- 487 Oke TR (2002) *Boundary Layer Climates*
- 488 Pace R, Biber P, Pretzsch H, Grote R (2018) Modeling ecosystem services for park trees: Sensitivity of  
 489 i-tree eco simulations to light exposure and tree species classification. *Forests* 9:1–18 . doi:  
 490 10.3390/f9020089
- 491 Pace R, Grote R (2020) Deposition and Resuspension Mechanisms Into and From Tree Canopies: A  
 492 Study Modeling Particle Removal of Conifers and Broadleaves in Different Cities. *Front For Glob*  
 493 *Chang* 3:26 . doi: 10.3389/ffgc.2020.00026
- 494 Pereira AR, Pruitt WO (2004) Adaptation of the Thornthwaite scheme for estimating daily reference  
 495 evapotranspiration. *Agric Water Manag* 66:251–257 . doi: 10.1016/j.agwat.2003.11.003
- 496 Perkins SE, Alexander L V., Nairn JR (2012) Increasing frequency, intensity and duration of observed  
 497 global heatwaves and warm spells. *Geophys Res Lett* 39:1–5 . doi: 10.1029/2012GL053361
- 498 Rahman MA, Hartmann C, Moser-Reischl A, et al (2020a) Tree cooling effects and human thermal  
 499 comfort under contrasting species and sites. *Agric For Meteorol* 287:107947 . doi:  
 500 10.1016/j.agrformet.2020.107947
- 501 Rahman MA, Moser A, Gold A, et al (2018) Vertical air temperature gradients under the shade of two  
 502 contrasting urban tree species during different types of summer days. *Sci Total Environ*  
 503 633:100–111 . doi: 10.1016/j.scitotenv.2018.03.168
- 504 Rahman MA, Moser A, Rötzer T, Pauleit S (2017a) Microclimatic differences and their influence on  
 505 transpirational cooling of *Tilia cordata* in two contrasting street canyons in Munich, Germany.  
 506 *Agric For Meteorol* 232:443–456 . doi: 10.1016/j.agrformet.2016.10.006

- 507 Rahman MA, Moser A, Rötzer T, Pauleit S (2017b) Within canopy temperature differences and  
 508 cooling ability of *Tilia cordata* trees grown in urban conditions. *Build Environ* 114:118–128 . doi:  
 509 10.1016/j.buildenv.2016.12.013
- 510 Rahman MA, Stratopoulos LMF, Moser-Reischl A, et al (2020b) Traits of trees for cooling urban heat  
 511 islands: A meta-analysis. *Build Environ* 170: . doi: 10.1016/j.buildenv.2019.106606
- 512 Robine JM, Cheung SLK, Le Roy S, et al (2008) Death toll exceeded 70,000 in Europe during the  
 513 summer of 2003. *Comptes Rendus - Biol* 331:171–178 . doi: 10.1016/j.crvi.2007.12.001
- 514 Rötzer T, Rahman MA, Moser-Reischl A, et al (2019) Process based simulation of tree growth and  
 515 ecosystem services of urban trees under present and future climate conditions. *Sci Total*  
 516 *Environ* 676:651–664 . doi: 10.1016/j.scitotenv.2019.04.235
- 517 Sanusi R, Johnstone D, May P, Livesley SJ (2017) Microclimate benefits that different street tree  
 518 species provide to sidewalk pedestrians relate to differences in Plant Area Index. *Landsc Urban*  
 519 *Plan* 157:502–511 . doi: 10.1016/j.landurbplan.2016.08.010
- 520 Scholz T, Hof A, Schmitt T (2018) Cooling effects and regulating ecosystem services provided by urban  
 521 trees—Novel analysis approaches using urban tree cadastre data. *Sustain* 10: . doi:  
 522 10.3390/su10030712
- 523 Shashua-Bar L, Hoffman ME (2004) Quantitative evaluation of passive cooling of the UCL  
 524 microclimate in hot regions in summer, case study: Urban streets and courtyards with trees.  
 525 *Build Environ* 39:1087–1099 . doi: 10.1016/j.buildenv.2003.11.007
- 526 Sicard P, De Marco A, Dalstein-Richier L, et al (2016) An epidemiological assessment of stomatal  
 527 ozone flux-based critical levels for visible ozone injury in Southern European forests. *Sci Total*  
 528 *Environ* 541:729–741 . doi: 10.1016/j.scitotenv.2015.09.113
- 529 Solaimanian M, Kennedy TW (1993) Predicting Maximum Pavement Surface Temperature Using  
 530 Maximum Air Temperature and Hourly Solar Radiation. *Transp Res Rec* 1–11

- 531 Speak A, Montagnani L, Wellstein C, Zerbe S (2020) The influence of tree traits on urban ground  
532 surface shade cooling. *Landsc Urban Plan* 197: . doi: 10.1016/j.landurbplan.2020.103748
- 533 Spitters CJT, Toussaint HAJM, Goudriaan J (1986) Separating the diffuse and direct component of  
534 global radiation and its implications for modeling canopy photosynthesis Part I. Components of  
535 incoming radiation. *Agric For Meteorol* 38:217–229 . doi: 10.1016/0168-1923(86)90060-2
- 536 Stratópoulos LMF, Zhang C, Duthweiler S, et al (2019a) Tree species from two contrasting habitats for  
537 use in harsh urban environments respond differently to extreme drought. *Int J Biometeorol*  
538 63:197–208 . doi: 10.1007/s00484-018-1653-9
- 539 Stratópoulos LMF, Zhang C, Häberle KH, et al (2019b) Effects of drought on the phenology, growth,  
540 and morphological development of three urban tree species and cultivars. *Sustain* 11:1–15 . doi:  
541 10.3390/su11185117
- 542 Tan PY, Wong NH, Tan CL, et al (2018) A method to partition the relative effects of evaporative  
543 cooling and shading on air temperature within vegetation canopy. *J Urban Ecol* 4:1–11 . doi:  
544 10.1093/jue/juy012
- 545 Thornthwaite CW, Mather JR (1957) Instructions and tables for computing potential  
546 evapotranspiration and the water balance. *Publ Climatol* 183–311
- 547 Upreti R, Wang ZH, Yang J (2017) Radiative shading effect of urban trees on cooling the regional built  
548 environment. *Urban For Urban Green* 26:18–24 . doi: 10.1016/j.ufug.2017.05.008
- 549 Wang J, Endreny TA, Nowak DJ (2008) Mechanistic simulation of tree effects in an urban water  
550 balance model. *J Am Water Resour Assoc* 44:75–85 . doi: 10.1111/j.1752-1688.2007.00139.x
- 551 Wang W, Wang H, Xiao L, et al (2018) Microclimate regulating functions of urban forests in  
552 changchun city (North-east China) and their associations with different factors. *IForest* 11:140–  
553 147 . doi: 10.3832/ifor2466-010
- 554 Wang Y, Xie Y, Dong W, et al (2017) Adverse effects of increasing drought on air quality via natural

- 555 processes. *Atmos Chem Phys* 17:12827–12843 . doi: 10.5194/acp-17-12827-2017
- 556 Watts N, Amann M, Arnell N, et al (2019) The 2019 report of The Lancet Countdown on health and  
 557 climate change: ensuring that the health of a child born today is not defined by a changing  
 558 climate. *Lancet* 394:1836–1878 . doi: 10.1016/S0140-6736(19)32596-6
- 559 Wilby RL (2003) Past and projected trends in London’s Urban heat island. *Weather* 58:251–260 . doi:  
 560 10.1256/wea.183.02
- 561 Yang Y, Endreny TA, Nowak DJ (2013) A physically based analytical spatial air temperature and  
 562 humidity model. *J Geophys Res Atmos* 118:10449–10463 . doi: 10.1002/jgrd.50803
- 563 Zeng F, Gao N (2017) Use of an Energy Balance Model for Studying Urban Surface Temperature at  
 564 Microscale. *Procedia Eng* 205:2956–2966 . doi: 10.1016/j.proeng.2017.10.113
- 565 Zhang C, Stratopoulos LMF, Pretzsch H, Rötzer T (2019) How do *Tilia cordata* Greenspire trees cope  
 566 with drought stress regarding their biomass allocation and ecosystem services? *Forests* 10:1–14  
 567 . doi: 10.3390/f10080676
- 568 Zhang C, Stratopoulos LMF, Xu C, et al (2020) Article Development of fine root biomass of two  
 569 contrasting urban tree cultivars in response to drought stress. *Forests* 11:1–14 . doi:  
 570 10.3390/f11010108
- 571 Zhao Q, Yang J, Wang Z-H, Wentz E (2018) Assessing the Cooling Benefits of Tree Shade by an  
 572 Outdoor Urban Physical Scale Model at Tempe, AZ. *Urban Sci* 2:4 . doi:  
 573 10.3390/urbansci2010004
- 574 Zölch T, Maderspacher J, Wamsler C, Pauleit S (2016) Using green infrastructure for urban climate-  
 575 proofing: An evaluation of heat mitigation measures at the micro-scale. *Urban For Urban Green*  
 576 20:305–316 . doi: 10.1016/j.ufug.2016.09.011
- 577